ENTEROCOCCUS FAECALIS AGGREGATION SUBSTANCE (ASC10) AS LIAISON BETWEEN BACTERIUM AND HEART VALVE IN ENDOCARDITIS

A DISSERTATION
SUBMITTED TO THE FACULTY OF THE GRADUATE SCHOOL
OF THE UNIVERSITY OF MINNESOTA
BY

OLIVIA NEWTON CHUANG-SMITH

IN PARTIAL FULFILLMENT OF THE REQUIREMENTS
FOR THE DEGREE OF
DOCTOR OF PHILOSOPHY

GARY M. DUNNY

AUGUST 2009

Acknowledgements

I want to thank God for bringing me through graduate school; without Him, I would not be at this point in my life today. He is the one who brought so many supportive and encouraging people into my life, providing me with a community to lean upon especially during the many trials of graduate school. I thank Him for bringing my husband, Tony, into my life—he has been a great source of strength and encouragement, and always makes me laugh despite all the stress. My family, Ming, I-Min, Kelley, and Julia Chuang, have been there to support me through the highs and lows of graduate school; they're always willing to listen to me and offer words of encouragement.

To my advisor, Gary Dunny, I am thankful for all of the guidance, patience, and wisdom he has provided for me. He has given me a boost of confidence when I needed it most, and I am grateful for his fatherly concern about my graduate career and beyond. I have always enjoyed our conversations about martial arts, sharing what we've learned in class, and about music, an interest we both share. I have always appreciated that he has many interests besides science.

Thanks also to Pat Schlievert, who has been a co-mentor to me through the years. He has been a continued source of humor and fun, particularly during all the hours spent with the rabbits in endocarditis experiments. I am grateful for the encouragement and guidance he has offered me through my graduate career. I feel lucky to have two great mentors in Gary and Pat, both of whom are understanding and patient with their students.

To the graduate students of the "old" Dunny lab, Josie Chandler, Briana Kozlowicz, and Yuqing Chen, I have appreciated the fun that we've had together. Thanks for encouraging me through all the steps of graduate school, and providing so much good advice. Josie, I will always remember you for the times I found you staring at me, only to realize that you were only deep in thought. I will remember you, Briana, for your spunkiness, and how you reversed everything on my desk just for fun. Yuqing, thank you for being a great bench buddy!

And to the current and other past members of the Dunny lab, I am indebted to Dawn Manias for being so patient with all of my questions and training me into the lab. Thanks for all the encouraging and fun conversations over the years. I am thankful for the friendship that Vy Nguyen provided, and the bubble tea runs to break up the day. Thank you, Kristi Frank, for being my snack buddy in the hallway, and the many conversations we've shared over chips and fruit. Katie, you will never cease to amuse me, and I seem to find decapitated or hanging green toy soldiers in new places constantly around the lab! And to Laura Case, my new bench buddy, thanks for keeping things light and funny. Thank you to Tim Tripp, a member of the Schlievert lab who trained me in the catheterizing techniques of endocarditis. We had a lot of fun and laughs with the rabbits. To the Chrises of the lab (Kristich and Johnson), Aaron, Heather, Suzanne, and Thinh, thanks for all of your suggestions and conversation.
I am grateful for all of the suggestions and advice from my thesis committee—Gary Dunny, Pat Schlievert, Carol Wells, Sandra Armstrong, and Bruce Walcheck. Thanks to the MICaB program, and especially Louise Shand for always answering all of my questions about paperwork and other graduate school-related requirements. Thanks,

Louise, for all of our conversations—I am grateful for the breaks from work. I also want to thank the DGSs—Chris Pennell, Yoji Shimizu, and Sandra Armstrong for their hard work and help. My research was funded by the NIH and the MinnCResT training grant.

Abstract

Aggregation Substance proteins encoded by sex pheromone plasmids increase virulence of *Enterococcus faecalis* in experimental pathogenesis models, including infectious endocarditis. These large surface proteins may contain multiple functional domains involved in various interactions with other bacterial cells and with the mammalian host. Aggregation Substance Asc10, encoded by the plasmid pCF10, is induced during growth in the mammalian bloodstream, and pCF10 carriage gives *E. faecalis* a significant selective advantage in this environment. We employed a rabbit model to investigate the role of various functional domains of Asc10 in endocarditis. The data suggested that the bacterial load of the vegetation was the best indicator of virulence. Previously identified aggregation domains contributed to the virulence associated with the wild-type protein, and a strain expressing an Asc10 derivative where glycine residues in two RGD motifs were changed to alanines showed the greatest reduction in virulence. Remarkably this strain, and the strain carrying the pCF10 derivative with the in-frame deletion of *prgB* were both significantly less virulent than an isogenic plasmid-free strain. In addition, mutants carrying Tn*917* insertions in the *prgB* gene demonstrated that secreted N-terminal Asc10 fragments possess activity promoting endocarditis virulence. The data demonstrate that multiple functional domains are important in Asc10-mediated interactions with the host during the course of experimental endocarditis, and that in the absence of a functional *prgB* gene, pCF10 carriage is actually disadvantageous *in vivo*.

Since Asc10 is important as a virulence factor in *E. faecalis* endocarditis pathogenesis, developing immunization approaches against this surface protein will be

useful in combating endocarditis disease. Use of Fab fragment antibodies against Asc10 was found to decrease vegetation size and bacterial load in the rabbit endocarditis model. In addition, microarray and histological studies revealed two routes of infection in vegetation formation; one in the absence of Asc10, characterized by a robust inflammatory response, and the second in which the presence of Asc10 dampens this response, possibly impeding the influx of immune cells into the vegetation.

We also employed an *ex vivo* porcine heart valve adherence model to study the initial interactions between Asc10$^+$ *E. faecalis* and valve tissue, and to examine formation of biofilms. We found that the aggregation domains contribute most to Asc10-mediated *E. faecalis* valve adherence, whereas the RGD motifs have importance in later stages of valve colonization. Again, an N-terminal Asc10 fragment expressed from a *prgB* Tn*917* insertion mutant mediated adherence of *E. faecalis* cells, emphasizing the importance of the aggregation domains in valve attachment. Most of the Asc10 mutants examined showed some defects in valve adherence at 4 h, corroborating results from our rabbit endocarditis model, and implying that Asc10 contributes mainly to persistence of *E. faecalis* during endocarditis infection. Extracellular matrix (ECM) protein studies to determine the eukaryotic Asc10 ligand in valve tissue found that full-length Asc10 protein did not mediate *E. faecalis* binding to vitronectin, fibronectin, fibrinogen, von Willebrand factor, heparan sulfate, or chondroitin sulfate. In scanning electron microscopy analysis of the infected valve tissue, we found evidence of biofilm formation, including growing aggregates of bacteria, and the increasing presence of exopolymeric matrix over time. Additionally, *E. faecalis* cells preferentially bound to damaged tissue, though it was difficult to determine whether the bacteria caused the

damage, or if it was due to deterioration of the tissue over time. This porcine heart valve tissue colonization model will serve as a useful tool in future studies of biofilm formation.

Table of Contents

List of Tables

List of Figures

Foreward

This thesis is divided into five sections: (1) Multiple functional domains of *Enterococcus faecalis* aggregation substance Asc10 contribute to endocarditis virulence, (2) Passive immunization with fab fragments of anti-Asc10 antibodies diminishes *Enterococcus faecalis* endocarditis, (3) Use of porcine cardiac valve tissue in an *ex vivo* study of Asc10-mediated adherence of *Enterococcus faecalis* and biofilm formation, (4) Characterization of Asc10 Tn*917* insertion *Enterococcus faecalis* mutants, and (5) Asc10-expressing *Enterococcus faecalis* survive in whole blood and in a rabbit abscess model.

The first section is based on results published in *Infection and Immunity* and is reprinted with their permission:

> **Chuang, O. N., Patrick M. Schlievert, Carol L. Wells, Dawn A. Manias, Timothy J. Tripp and Gary M. Dunny. 2009. Multiple functional domains of *Enterococcus faecalis* aggregation substance Asc10 contribute to endocarditis virulence. *Infection and Immunity* 77: 539-548.**

All endocarditis experiments were conducted by Dr. Pat Schlievert and I, and several of the initial studies were done with the help of Timothy Tripp. In addition, Laura Case, John Mleziva, and Kristi Frank assisted with the surgical procedure. Dawn Manias and Dr. Chris Waters constructed the Asc10 mutant derivative strains. The statistical analysis and CHO cell studies were performed by Dr. Carol Wells; the remaining experiments were conducted by me. I wrote the manuscript, with revisions from the rest of the authors.

The second section is based on a manuscript that has been submitted for publication:

Schlievert, P. M., O. N. Chuang-Smith, Marnie L. Peterson, Suzanne M. Grindle, Laura C. Case, and Gary M. Dunny. Reduction of *Enterococcus faecalis* endocarditis with IgG fabs that interfere with aggregation substance. Submitted to *Journal of Immunology*.

All endocarditis studies involving passive immunization with Fab fragments were carried out by Dr. Patrick Schlievert and I; all other endocarditis studies, RNA extraction and preparation for microarray chip hybiridization for the microarray analysis was done by Drs. Patrick Schlievert and Marnie Peterson. Bioinformatic analysis of microarray data was performed by Suzanne Grindle, and statistical analysis by Dr. Patrick Schlievert. Purification and verification of anti-Asc10 Fab fragments was done by Laura Case. The manuscript was written by Dr. Patrick Schlievert, with revisions by me and other authors.

The third section is based on a manuscript that is in preparation:

Chuang-Smith, O. N., Carol L. Wells, Michelle J. Henry-Stanley, and Gary M. Dunny. Use of porcine cardiac valve tissue in an *ex vivo* study of aggregation substance-mediated adherence of *Enterococcus faecalis* and biofilm formation. *Manuscript in preparation.*

Porcine hearts were obtained from Drs. David Brown and Gregory Beilman, and the Experimental Surgical Services department at the University of Minnesota. Timothy Tripp performed the initial adherence study with the cardiac valve tissue, but all other adherence assays were done by me. Drs. Carol Wells and Michelle Henry-Stanley

obtained images of infected valves using SEM, and Melody Shepard prepared valve samples for SEM analysis. Statistical analysis was done with assistance by Dr. Carol Wells; I wrote the manuscript.

The final section on the Tn*917* insertion mutants is not published; the studies with the Tn*917* mutant strains were done by me, though the endocarditis study again was done by Dr. Patrick Schlievert and I. For the whole blood bacterial killing assay in the appendix, protocols and advice were obtained from Drs. Pat Cleary, Beinan Wang, and Bruce Walcheck, but the experiments were done by me.

INTRODUCTION

Enterococcal infectious endocarditis

Enterococcus faecalis has gained notoriety due to increasing cases of enterococcal nosocomial infections, which are complicated by the inherent and acquired antibiotic resistance of this bacterium. It is a naturally tenacious organism that survives at temperatures as high as 60°C and in tap water (57), making it an organism that is difficult to eliminate. In addition, it lives naturally as a commensal organism in the human gastrointestinal tract; its prevalence in the hospital environment is likely due to easy transmission from the intestinal tract through feces to surfaces, hospital workers, and patients (22). Infectious endocarditis, urinary tract and wound infections, and bacteremia are all associated with *E. faecalis* (41, 57). Its high propensity to transfer antibiotic resistance elements also leads to transfer of these determinants to more virulent bacteria such as *Staphylococcus aureus* (72).

Enterococci account for 20% of all bacterial endocarditis cases, and are the third leading cause of this disease (36, 39). Ultimately, this infection leads to congestive heart failure, then death. This is due to the focal lesion of this disease, the vegetation, which is comprised of platelets, fibrin, other pro-coagulant factors, recruited phagocytes, and bacterial cells, typically attached to a valve leaflet. As the vegetation grows in size, it has the potential to block blood flow around the valve area.

Two routes of vegetation formation have been proposed: (1) non-bacterial thrombotic vegetation formation, and (2) vegetation formation on previously undamaged, healthy valves. Formation of the non-bacterial thrombotic (NBT) vegetation involves damage on the valve (typically the aortic valve), which can occur

through processes such as irregular blood flow as caused by valve regurgitation or also through intravenous drug use (42). Platelets and fibrin are recruited to the damaged site, which composes the NBT vegetation (**Fig. 1**). Surgical procedures and increased bacterial translocation due to antibiotic-induced bacterial overgrowth (36), can enable enterococci or other bacteria to gain entrance to the bloodstream. These bacteria can adhere to the NBT vegetation, forming the septic vegetation (16). Phagocytes are then recruited to fight off the infection, and often these immune cells are found engulfing bacteria while walled inside of layers of fibrin (15). Although the majority of enterococcal endocarditis infections probably result from opportunistic infection of previously damaged tissue, as described above, it is possible that endocardiac infections of healthy tissues occurs in some cases (51).

In the cases where no previous valve aberrancies are noted in the patient, some types of bacteria, once in the bloodstream, can inflict damage on the endothelial cell layer of the valve tissue (17, 51). This route of vegetation formation has been hypothesized for *Staphylococcus aureus*, where it is endocytosed by valve endothelial cells, and can trigger initiation of the coagulation cascade. Eventually, the *S. aureus* cells lyse the endothelial cells, which amplifies the coagulation cascade, bringing more platelets and fibrin to bind to the damaged site (66). *E. faecalis* has been noted in some cases to cause endocarditis in patients who have no past history of valve aberrancies, so this route of vegetation formation could be applicable to *E. faecalis* (51).

The vegetation itself is considered a biofilm; bacteria are encased inside layers of fibrin and platelets, and other pro-coagulant factors, which are effective in impeding the effectiveness of antibiotic and immune mediator bacterial killing (46).

Figure 1. (A) Non-bacterial thrombotic vegetation formation, demonstrating interactions between Asc10^{+} *E. faecalis* and host cells during formation of the septic vegetation in endocarditis. Platelets, fibrin and other clotting proteins may comprise a part of the vegetation, enabling blood-borne *E. faecalis* to bind to the growing clot. **(B)** Vegetation formation on undamaged valve tissue. Bacteria are internalized by endothelial cells, triggering coagulation cascade, and this is amplified once the bacteria lyse the endothelial cells. This recruits fibrin and platelets, and other bacteria are then able to bind to form the vegetation.

Figure 1.

A.

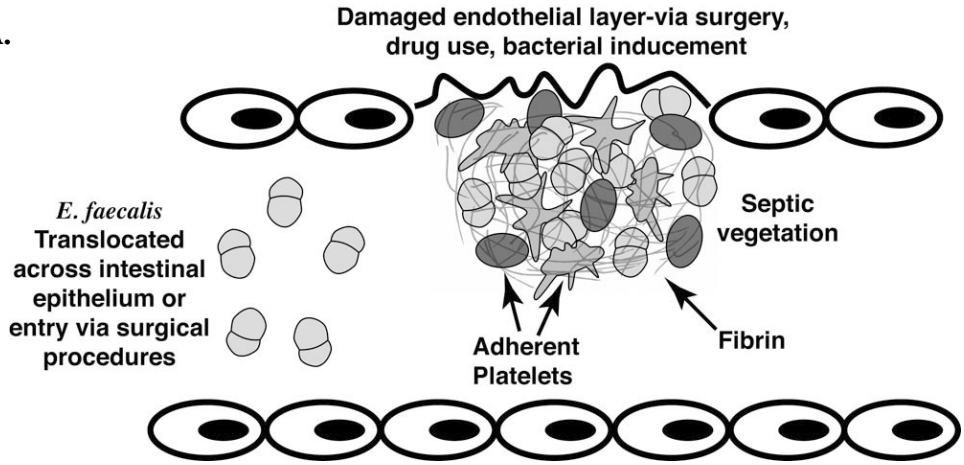
Damaged endothelial layer-via surgery, drug use, bacterial inducement
E. faecalis
Translocated across intestinal epithelium or entry via surgical procedures
Septic vegetation
Adherent Platelets
Fibrin

B.

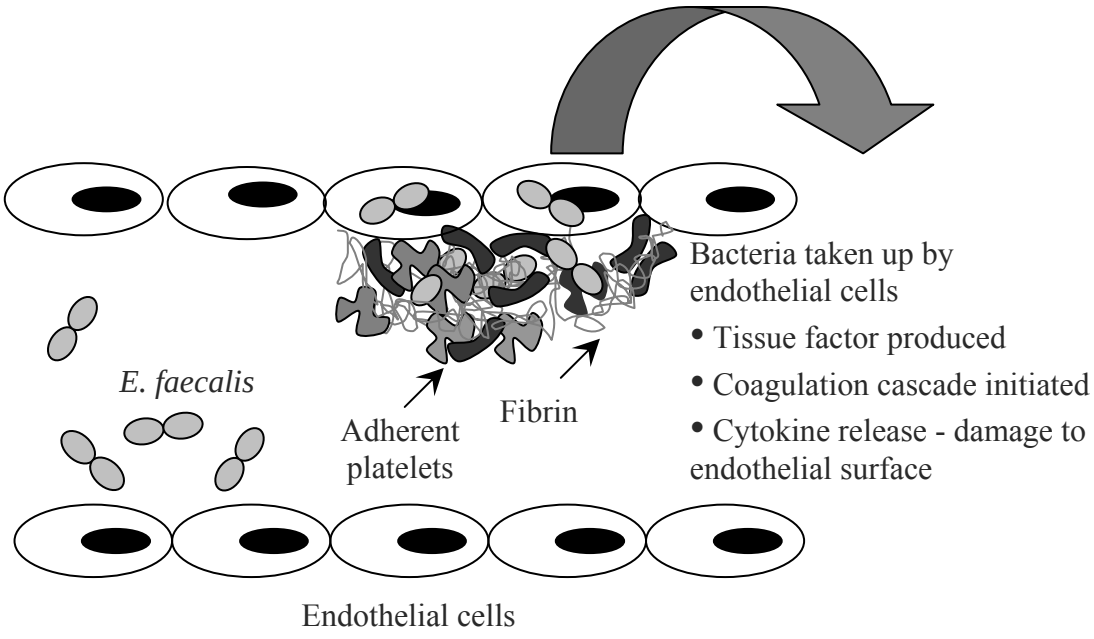
Bacteria taken up by endothelial cells
• Tissue factor produced
• Coagulation cascade initiated
• Cytokine release - damage to endothelial surface
E. faecalis
Adherent platelets
Fibrin
Endothelial cells

Though antibiotics are able to enter the vegetation, the physiological state of the bacteria in the biofilm could prevent the antibiotics from damaging the bacteria (9). Durack *et al.* demonstrated that unless bacteria are unprotected by fibrin layers, macrophages were not able to phagocytose the exposed bacteria (15). In addition, antibodies against a major *E. faecalis* surface protein, aggregation substance, were unable to penetrate the established vegetation to opsonize the *E. faecalis* cells (38). Fragments of the vegetation can break off, allowing for dissemination of the invading microorganisms to other organs, and leading to reseeding of the vegetation.

Aggregation substance (Asc10)

The focus of this thesis is on the role of an *E. faecalis* surface protein, Aggregation Substance (Asc10), in mediating *E. faecalis*-host tissue interactions in the context of endocarditis. Since many difficulties are faced in eliminating the bacteria once they adhere to the sterile vegetation and become encased in layers of platelets and fibrin, it is ideal that the bacterial infection is halted at the step of initial bacterial adherence to the vegetation. For *Enterococcus faecalis,* Asc10 is one of several known adhesins that could be targeted for treatment against infectious endocarditis. Asc10 has two major functions that have been characterized: (1) aggregation between donor and recipient cells during conjugation to allow for plasmid transfer, and (2) adherence to host tissues. Asc10 contributes to formation of larger vegetations (4), and mediates adherence to neutrophils (PMNs) (50, 65), renal tubular cells (30), and intestinal epithelial cells (28, 43, 56, 71, 73). Asc10 is a 137-kDa Aggregation Substance protein encoded by the *prgB* gene of the conjugative plasmid pCF10; its expression is triggered

by the presence of a peptide pheromone cCF10 that is produced by plasmid-free cells and induces transfer of pCF10 by conjugation (12, 13).

Importantly, Asc10 expression is also induced by a host factor during *in vivo* growth; pCF10 carriage has a strong selective advantage for enterococci in their hosts under these conditions (3, 25). Chandler *et al.* demonstrated that a factor present in serum is responsible for sequestering the inhibitor peptide, iCF10, which is secreted by the donor cell along with the pheromone cCF10 peptide to prevent self-induction. Donor cells need to be able to sense the cCF10 pheromone produced by recipient cells without reacting to the pheromone that they produce themselves. By binding iCF10, the serum factor (possibly albumin) disrupts the balance between iCF10 and cCF10, and expression of Asc10 is triggered on the donor cell (3).

The plasmid pCF10 is a member of the family of pheromone-responsive plasmids that encompasses approximately 20 plasmids, all of which carry genes involved in conjugative functions; gene expression is triggered by small 7-8 aa peptide pheromones. This family also includes pAD1 and pPD1**,** both of which encode their own Aggregation Substance proteins (Asa1 and Asp1, respectively; (70). These proteins share greater than 90% identity throughout most of the protein, except for a centrally located variable region where the identity is 30-40% (Asc10 variable region shown in **Fig. 2B**; (20, 21, 29).

Sequence analysis found a signal sequence at the N-terminus, and an LPXTG motif at the C-terminus; both are commonly found in Gram-positive surface proteins.

Figure 2. Donor-recipient interactions during conjugation, and a schematic map of the wild-type Asc10 protein to highlight functional domains. **(A)** The recipient cell produces a pheromone peptide, cCF10, which is sensed and internalized by the donor cell. Asc10 is expressed on the surface of the donor cell as a consequence, followed by expression of the conjugation machinery. Plasmid transfer can thus take place, and ultimately the recipient cell becomes another donor cell once it receives the plasmid. (**B)** Wild-type full-length Asc10 (pCF10). SS = signal sequence. Adapted from Waters *et al.* 2001 (69)**.** The right-hand portion of the figure indicates whether expression of each Asc10 variant resulted in visible clumping of the host *E. faecalis* strain. The amino acid positions of the two RGD motifs are indicated.

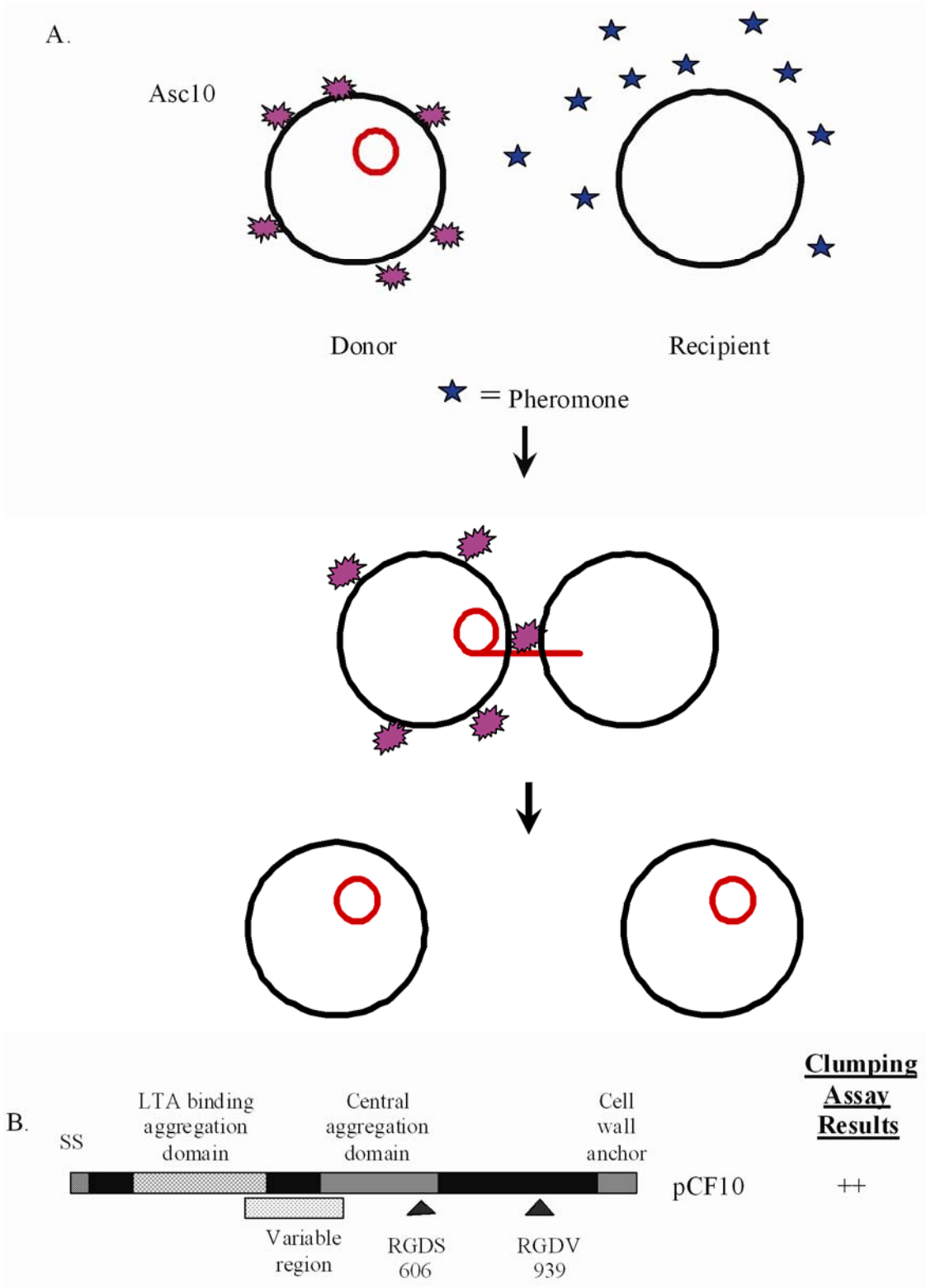
A.
Asc10
Donor
Recipient
= Pheromone
B.
SS
LTA binding aggregation domain
Central aggregation domain
Cell wall anchor
Variable region
RGDS 606
RGDV 939
pCF10
Clumping Assay Results
++

Figure 2.

The N-terminal signal sequence signifies that the protein will be translocated across the cell membrane, but the signal sequence itself is cleaved after this translocation. The sortase enzyme, located in the plasma membrane, cleaves the LPXTG motif between the threonine and glycine residues, then catalyzes a transpeptidase reaction to link the surface protein to peptidoglycan in the cell wall (35). Several functional domains of the Asc10 protein have been previously identified (**Fig. 2B**). Since problems were initially encountered in purifying stable full-length Asc10 protein, a Tn*lacZ/*in and Tn*phoA/*in transposon screen was conducted to identify functional domains of Asc10 (69). Two aggregation domains are required for binding to occur between a donor and recipient pair during conjugation. The more N-terminal aggregation domain is also known to bind lipoteichoic acid (LTA) (70), while a distinct central domain is also important for aggregation. LTA, a major component of the Gram positive cell wall, has been found to comprise a part of the cognate receptor for Asc10. A set of genes (*ebs*, enterococcal binding substance) that are required for this receptor encode products that are involved in LTA biosynthesis (1, 64). A Tn*916* transposon insertion mutant, INY3000, expresses LTA that is shortened in the polyglycerol phosphate chain length, and is increased in unsaturated fatty acids. With these altered LTA molecules expressed on the surface of the *E. faecalis* cell, this INY3000 strain is no longer able to bind Asc10 and mediate aggregation (1, 64).

Two RGD motifs have been identified in Asc10; these motifs in eukaryotic systems are known to mediate binding to integrins, and are involved in other adhesion events, such

as those pertaining to the extracellular matrix (55). In *E. faecalis*, evidence suggests that the RGD motifs may mediate interactions with polymorphonuclear (PMN) leukocytes (61, 65). Exogenously added RGD peptides were able to reduce Asc10$^+$ *E. faecalis* binding to PMNs; it has been suggested that the presence of Asc10 on the cell surface may interfere with phagosome maturation once the bacterium is engulfed by the phagocyte. Rakita *et al.* (50) demonstrated that *E. faecalis* cells expressing Asc10 were found in phagosomes that were larger and had a higher pH than phagosomes containing Asc10$^-$ *E. faecalis*. The interaction between Asc10$^+$ *E. faecalis* and PMNs was shown to be mediated by an opsonin-independent mechanism, involving the complement receptor type 3 (CR3) and the $\alpha_5\beta_3$ integrin/integrin-associated protein (IAP) complex. This $\alpha_5\beta_3$/IAP complex expressed on PMNs is important for binding RGD motifs, while CR3 is needed for opsonin-independent uptake of pathogens into the phagocyte. Often this opsonin-independent pathway through the CR3 receptor is utilized by bacteria to evade the respiratory burst response that is typically used by phagocytes to kill their prey (75). Thus, it is possible that Asc10 is used by *E. faecalis* to promote intracellular survival in the phagocyte until a later time when the bacteria can lyse the host cell and migrate to other sites in the host.

Other evidence that Asc10 promotes immune evasion leading to persistence of *E. faecalis* in the host during endocarditis is presented in a study conducted by Schlievert *et al*. (58). They administered Asc10$^+$ EBS$^+$ and Asc10$^-$ EBS$^+$ strains directly into the left ventricle of rabbits and during a 2-day period, they monitored the rabbits for disease symptoms. They found that pericardial inflammation was absent in rabbits infected with Asc10$^+$ EBS$^+$ strains, though all animals infected with this strain

died by the end of the 2-day period. In addition, tissue destruction was evident in myocardial and lung tissues. In contrast, only one of the animals infected with the Asc10$^-$ EBS$^+$ strain died, and their examination of their hearts found significant amounts of pericardial inflammation, with PMNs observed in the pericardial fluid. The authors suggest that the Asc10$^+$ EBS$^+$ strain produces a factor that is capable of inhibiting phagocyte recruitment, or that this strain is able to destroy incoming phagocytes.

Immunization Strategies Against Aggregation Substance (Asc10)

Since aggregation substance promotes binding to PMNs, renal tubular cells, and intestinal epithelial cells, and increases the size of vegetations in endocarditis, it is an attractive candidate for immunization strategies in diseases such as endocarditis. However, McCormick *et al.* (37) demonstrated that antibodies against an N-terminal fragment of Asc10 (encompassing aa 44-331) were not protective in the rabbit model of endocarditis. This N-terminal region of Asc10 was determined by flow cytometry analysis to be surface-exposed. It was postulated that whole antibodies against Asc10 promote increased aggregation between Asc10-expressing cells. The *E. faecalis* cells are more easily aggregated, and large masses are caught in the vegetation, accelerating formation of the vegetation. Larger masses of bacteria could disseminate from the vegetation and more quickly establish infection sites in other organs. The authors also suggest that Asc10 might not have a major role in the initial establishment of the vegetation, but that its importance lies in immune evasion. This could also be an explanation for the ineffectiveness of the anti-N-terminal Asc10 antibodies as a vaccine, because of the known contributions of Asc10 to binding to PMNs and interference in phagosomal maturation.

Rabbit Endocarditis and *Ex Vivo* Porcine Cardiac Valve Models

The rabbit endocarditis model is a well-established model used by our laboratory to study the pathogenesis of endocarditis disease (7, 25, 37, 38, 58). This model allows us to examine virulence of bacterial strains in the context of the entire disease process. We have also sought to dissect the process of vegetation formation, and thus we developed the *ex vivo* porcine cardiac valve model to investigate the initial interactions between *E. faecalis* and the valve tissue. The initial adherence of bacteria to the damaged valve tissue is most crucial in preventing formation of the septic vegetation, in which the bacteria are more difficult to eliminate. In combination, both models will give us a better understanding of how Asc10-expressing *E. faecalis* are able to form vegetations during endocarditis infection.

We have developed an *ex vivo* porcine heart valve adherence assay to study this role, where studying the initial events in vegetation formation are simpler without the complications of an animal model. The domains of Asc10 are further characterized in bacterial-valve tissue interactions in this model. Also, because biofilm growth is relevant to endocarditis and for many other types of infections, we have developed this porcine valve tissue system as a model to study biofilm formation. The porcine valve surface is more physiologically relevant than glass or plastic, and will allow us to examine the structure of *E. faecalis* biofilms in the context of living tissue.

Cardiac Valve Structure

The heart valves are tissues that are built to withstand a great amount of shear forces and turbulence, as our hearts are constantly pumping blood to deliver oxygen to the tissues and bring back carbon dioxide waste. For such strong forces, the valve

tissue must be flexible and maintain elasticity to accommodate the numerous times the valve must open and close for entry of blood. The valve is composed of a single outer layer of endothelial cells, and inside of this layer is the extracellular matrix (ECM) with a scattering of interstitial cells (62). These interstitial cells include fibroblasts, which are responsible for remodeling the ECM to maintain levels of elastin, collagen, proteoglycans, fibronectin, and growth factors. These materials are necessary for durability of the valve over its lifetime. Other types of interstitial cells found in the valve tissue are smooth muscle cells and myofibroblasts, both of which may assist in contractile properties of the valve (63). However, over the lifetime of a human, the number of interstitial cells present in the valve tissue diminishes, which leads to loss of elasticity and increased incidence of heart valve disease (63).

MATERIALS AND METHODS

Bacterial strains and growth conditions

Strains used are listed in **Table 1**. For protein expression and virulence studies, the plasmids listed in the second part of **Table 1** were mated into OG1SSp *E. faecalis* (13), as this was the strain used in past studies. *E. faecalis* strains were grown in beef heart dialyzable medium plus 5% glucose-phosphate for all endocarditis experiments and in Todd-Hewitt (TH; Becton Dickinson, Franklin Lakes, NJ) broth otherwise for approximately 16 h at 37°C. For *Streptococcus pyogenes*, strains were grown in TH broth plus 1% yeast extract (TH-Y; Becton Dickinson, Sparks, MD) for 12-15 h at 37°C in 7% CO_2. Overnight cultures were diluted 1:20 in fresh TH-Y and grown for 2-3 h to an OD_{600} of 0.3. Stock cultures were frozen and maintained at -80°C; these were used for inoculation of overnight cultures.

Construction of Asc10 mutant derivative-expressing *E. faecalis* strains

In previous work (69, 70), a series of in-frame insertion and deletion mutations in the *prgB* gene encoding Asc10 was generated using a Tn*lacZ*/in Tn*phoA*/in transposon system, and oligonucleotide-directed mutagenesis was used to change the two RGD sequences to RAD (singly and in combination). Physical maps of these constructs are shown in **Fig. 4**. The *prgB* gene was expressed from the nisin-inducible vector pMSP3535 (69). For the present study, we used a recently developed allelic exchange system (32) to insert the mutant *prgB* derivatives into the native context in pCF10. Plasmids used for this protocol are listed in **Table 1**. The pCJK2 plasmid (32) was used to transfer *prgB* mutations to pCF10 by markerless allelic exchange. pCJK1, pCJK2-2,

Table 1. Strain and plasmids used in these studies.

Strain or plasmid	Description	Source or reference
Bacteria		
Enterococcus faecalis		
OG1SSp	Streptomycin and spectinomycin-resistant strain	(13)
OG1RF	Rifampicin and fusidic acid-resistant strain	(14)
TX5128	OG1RF derivative *gelE*$^{-}$*sprE*$^{-}$	(59)
Streptococcus pyogenes		
90-226	Serotype M1 wild-type strain of cultured from blood of patient with sepsis	(11)
90-226 Δ*emm*	Markerless in-frame deletion of *emm* gene, M protein-deficient strain	(77)
Plasmids		
pCF10	Pheromone-inducible conjugative plasmid	(12)
pCF121	pCF10 derivative with Tn*917* insertion in *prgB* gene at nucleotide 1409, deficient in cell surface Asc10, but instead is secreted	(6)
pCF175	pCF10 derivative with Tn*917* insertion in *prgB* gene at nucleotide 1784; deficient in cell surface Asc10, but instead is secreted	(5)
pMSP7517	pMSP3535 derivative, expression of *prgB* from nisin-inducible promoter	(24)
pMSP3535	Cloning shuttle vector with nisin-inducible promoter	(2)
pCWΩ3599	Derived from pMSP3535 shuttle vector; contains *prgB* gene cloned under a nisin-inducible promoter; secreted full-length Asc10 protein lacking cell wall	(69)

	anchor motif LPXTG	
pMSP3609	Double RGD → RAD in *prgB* inserted in pMSP3535 vector	(71)
pCF10-1	Asc10 mutant derivative; 31-amino acid insertion in central aggregation domain at nucleotide 1638	(32)
pCF10-2	Asc10 mutant derivative; double RGD mutant with single amino acid substitutions RGD → RAD	(7)
pCF10-3	Asc10 mutant derivative; N-terminal single RGD mutant RGDS → RADS	(7)
pCF10-4	Asc10 mutant derivative; N-terminal aggregation domain deletion (nucleotides 468-1074)	(7)
pCF10-5	Asc10 mutant derivative; double aggregation domain mutant – 31-amino acid insertion in central aggregation domain, deletion in N-terminal aggregation domain	(7)
pCF10-6	Asc10 mutant derivative; C-terminal domain deletion (nucleotides 2064-3414)	(7)
pCF10-7	Asc10 mutant derivative; C-terminal single RGD mutant RGDV → RADV	(7)
pCF10-8	*prgB* deletion mutant retaining first three and last three codons, Asc10$^-$	(7)
pCWΔ468-1074	pMSP3535 carrying in-frame deletion of nucleotides 468-1074 in *prgB*	(70)
pCWΔ468-1074/Ω1638	pMSP3535 carrying double aggregation domain mutant	(70)
pCWΔ2064-3414	pMSP3535 carrying in frame deletion of nucleotides 2064-3414 in *prgB*	(70)

CK104	OG1RFΔ*upp*	(32)
pVE6007	Supplies RepA (temperature sensitive), Cm^r	(32)
pCJK2	P-*upp* expression cassette cloned into pORI280	(32)
pCJK47	Conjugative donor plasmid, carries $oriT_{pCF10}$ and P-*pheS**; pORI280 derivative; Erm^R	(31)
pCJK47Δ*prgB*	*prgB* deletion construct with first and last 9 nucleotides cloned into pCJK47	(7)
pCJK2-2	*prgB* double RGD mutant cloned into pCJK2	(7)
pCJK2-4	*prgB* in-frame deletion of nucleotides 468-1074 cloned into pCJK2	(7)
pCJK2-5	*prgB* double aggregation domain Δ468-1074/Ω1638 cloned into pCJK2	(7)
pCJK2-6	*prgB* in-frame deletion of nucleotides 2064-3414 cloned into pCJK2	(7)
pCJK2-7	*prgB* C-terminal single RGD mutant cloned into pCJK2	(7)
pWM401	Shuttle vector used as $Asc10^-$ $Sec10^-$ negative control for pINY1801, still maintains expression of Ebs	(74)
pINY1801	Constitutive expression of Asc10 and Sec10; expression of enterococcal binding substance (Ebs); fragment of pCF10 cloned into shuttle vector pWM401	(6, 45)

pCJK2-4 and pCJK2-5 were constructed by inserting the *Bsr*GI/*Bpl*I *prgB* fragment (blunt ended with T4 DNA polymerase) from pMSP3609, pCWΔ468-1074 and pCWΔ468-1074/Ω1638 and pCWΔ2064-3414, respectively, into pCJK2 digested with *Sma*I. pCJK2-7 was created by digesting pMSP3609 with *Pst*I and treating a 1.3 kb fragment with T4 DNA polymerase, prior to cloning into *Sma*I-digested pCJK2. Allelic exchange was carried out according to Kristich *et al.* (32) to create pCF10-2, pCF10-3, pCF10-4, pCF10-5, pCF10-6, and pCF10-7. Plasmids pCJK2-2, pCJK2-4, pCJK2-5, pCJK2-6 and pCJK2-7 were electroporated into *E. faecalis* strain CK104, carrying pVE6007/pCF10. The temperature was increased to 37ºC to induce the loss of plasmid pVE6007, making survival of the pCJK2 derivatives dependent on their insertion into pCF10 by homologous recombination. The strains were grown for approximately 20 generations at 37ºC and then plated on 5-fluorouracil to select for excision of the integrated plasmid. The strains were screened for the desired *prgB* mutation. An aggregation analysis (32) was used to screen mutations that abolished aggregation function (pCF10-4, pCF10-5 and pCF10-6). Other pCF10 mutants, pCF10-2, pCF10-3 and pCF10-7 were screened by sequencing *prgB* fragments amplified by PCR. Each variant *prgB* allele was either sequenced completely following its insertion into pCF10, or the junctions where homologous recombination occurred were sequenced to verify proper insertion of the *prgB* variant into pCF10.

Construction of a pCF10 derivative containing an in-frame *prgB* deletion *E. faecalis* mutant

Two-step PCR was utilized to create an in-frame deletion construct that contained only the first nine and last nine nucleotides of the *prgB* gene (first 3 and last 3 codons; **Fig. 3**). This fragment was then subcloned into the pGEMT-Easy plasmid (Promega; Madison, WI) to verify deletion of *prgB*; the fragment containing the deletion was digested with *Eco*RI and *Xba*I and cloned into pCJK47 (31). This pCJK47Δ*prgB* construct was electroporated into CK104, carrying pVE6007/pCF10, as described in the previous section. A temperature increase to 37°C induced the loss of the temperature-sensitive pVE6007 plasmid, and pCJK47Δ*prgB* was then forced to integrate into the pCF10 plasmid, with excision of the pCJK47 plasmid upon growth on *p*-Cl-phenylalanine for approximately 30-40 generations. Colony PCR was used to confirm deletion of the *prgB* gene in the pCF10 background (pCF10-8), and the correct plasmid construct was transferred from CK104 (pCF10-8) into OG1SSp by conjugation. The deleted *prgB* gene and junction regions were sequenced in both the CK104 and OG1SSp backgrounds, with no spurious mutations found. Western blot and clumping assay analysis were performed to ensure that no surface Asc10 was expressed or secreted and that this strain was unable to aggregate.

Rabbit model of endocarditis

The left carotid artery of New Zealand white rabbits was isolated, and a catheter was inserted until the aortic valve was reached, as previously described (58). Young adult

Figure 3. Utilization of two-step PCR to create an in-frame *prgB* deletion construct for cloning into the plasmid pCJK47. One primer consisted of the first 9 nucleotides of *prgB* plus the upstream flanking sequence (total primer size was 1 kb) that encompassed the intergenic region and part of the 3' *prgA* sequence (blue arrow). The other primer was also a total size of 1 kb, with the last 9 nucleotides of *prgB*, intergenic region, *prgU*, and a portion of *prgC* (pink arrow). The resulting two step-PCR product was used in constructing the *E. faecalis prgB* deletion mutant OG1SSp (pCF10-8), where only the first nine and last nine nucleotides of *prgB* are left intact.

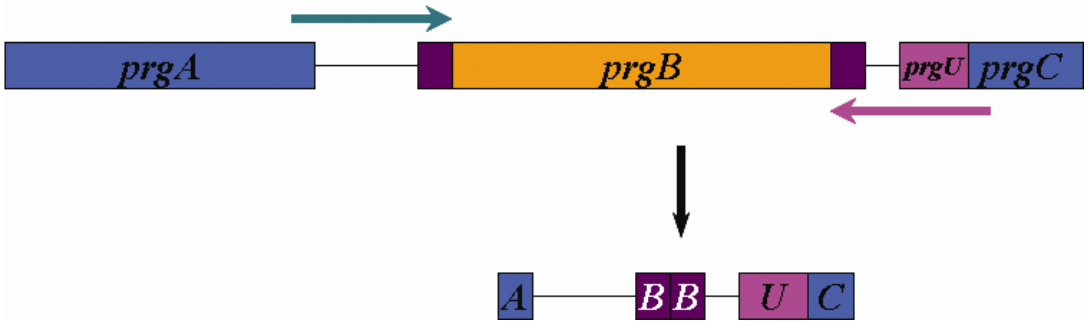

rabbits that weighed 2-3 kg were obtained from Bakkom Rabbitry (Red Wing, MN). The catheter remained in place for 2 h to induce damage to the valve and then was removed, whereupon the neck region was closed and approximately 2×10^9 colony-forming units (CFU) of *E. faecalis* were injected intravenously through the marginal ear vein. Four days post-procedure animals were sacrificed, hearts were removed and photographed, and vegetations were weighed and homogenized for bacterial count determination. Homogenates were plated onto TH agar with and without the appropriate antibiotics, to ensure that resistance markers were not lost during the infection period. Bacterial counts from antibiotic-containing and non-antibiotic plates were similar, indicating that the pCF10 derivatives were not cured during the course of infection. If no visible vegetations were found, then all of the aortic valve leaflets were removed and cultured to enumerate bacteria colonizing the valves in the absence of a visible lesion. The following antibiotics and concentrations were used: streptomycin at 1000 μg/ml (Cellgro; Herndon, VA), spectinomycin at 250 μg/ml (Sigma-Aldrich; St. Louis, MO), and erythromycin at 10 μg/ml (Sigma). All experiments were conducted under the established guidelines of the University of Minnesota Institutional Animal Care and Use Committee (IACUC).

Purification of cell wall and supernatant fractions for Asc10 mutant strain analysis

Cell wall fractions were purified from the plasmid-free Asc10$^-$ OG1SSp, Asc10$^+$ OG1SSp (pCF10), all of the Asc10 mutants (pCF10-1 through pCF10-8), Tn*917* insertion mutants OG1SSp (pCF121) and OG1SSp (pCF175), and TX5128 (pCWΩ3599). The TX5128 strain produces an almost full-length Asc10 protein that is

secreted, due to the absence of the LPXTG cell wall anchor. A protocol adapted from Kristich *et al.* (32) was used for this purification. Briefly, an overnight culture of the *E. faecalis* strains listed above was diluted 1:6 in TH broth containing the appropriate antibiotics. Pheromone (cCF10; 50 ng/ml) was added to the pCF10-carrying strains, to stimulate Asc10 expression. The diluted cultures were incubated at 37°C for 2.7 h with aeration and photographed to document the extent of clumping of the Asc10 mutant expressing strains. OD_{600} measurements were made to ensure use of equivalent amounts of cells for each culture.

Precipitation of protein from culture supernatant.

Cultures were pelleted, and the supernatant was filtered through a 0.22 μM syringe filter and precipitated with 15% trichloroacetic acid (TCA; Sigma-Aldrich). The supernatant-TCA mixture was centrifuged, and the pellet was washed twice with acetone. After drying the pellet, it was resuspended in wash buffer (50 mM Tris [Sigma-Aldrich] + 25 mM EDTA [Fisher; Pittsburgh, PA]). Volume of wash buffer that was used to resuspend the pellet was standardized to the OD_{600} of the $Asc10^{+}$ OG1SSp (pCF10) strain.

Isolation of cell wall fraction.

The pellet from a diluted overnight culture was washed with 0.5 ml wash buffer (1 M KCl; Fisher). Another wash was performed with 0.5 ml 50 mM wash buffer, followed by a final wash in protoplast buffer [wash buffer + 23% sucrose (Fisher)]. The pellet was then resuspended in protoplast buffer plus 10 mg/ml lysozyme (Sigma) and 250 U/ml mutanolysin (Sigma); this mixture was incubated at 37°C for 30 min. The

protoplasts were collected by centrifugation (16,060 × g, 1 min) and discarded, while the supernate was retained for Western blot analysis.

Western blot analysis of Asc10 mutant strain cell wall and supernatant fractions

Cell wall fractions were mixed with sodium dodecyl sulfate-polyacrylamide gel electrophoresis (SDS-PAGE) protein buffer, boiled for 5 min, electrophoresed in a 7.5% SDS-PAGE gel, and transferred to a 0.45 μm nitrocellulose membrane (Schleicher and Schuell; Dassel, Germany). A polyclonal anti-Asc10 antibody (1:5000) was used to blot for the presence of Asc10; 2 μl of this antibody was absorbed against 200 μl of a surface extract from TX5128 (pMSP3535) to eliminate non-specific antibodies. The blot was developed using the Pierce SuperSignal West Pico chemiluminescent protocol (Rockford, IL).

Purification of Fab fragment anti-Asc10 antibodies

Rabbits were immunized with full-length Asc10 protein purified from TX5128 (pCWΩ3599); this protein was emulsified in Freund's incomplete adjuvant (Sigma Aldrich). Asc10 antibody titers were determined by ELISA, and shown to be 2500/ml. To isolate the IgG fraction of the antiserum collected from the rabbits, precipitation in 34% ammonium sulfate was done. The resulting precipitate was resolubilized in PBS and dialyzed in PBS for 2 d to remove any remaining ammonium sulfate, whereupon papain digestion was used to cleave the antibody into Fab fragments. Purified Fab fragments were run on a non-reducing SDS-PAGE gel to determine whether digestion was complete. This was verified as the IgG fraction had disappeared, and a band at 50,000 MW was apparent. A volume of 2.5 ml of Fab fragments was delivered

intravenously to the rabbits, an equivalent of 125/ml titer if total volume of blood was assumed to be about 50 ml per rabbit.

To confirm that whole anti-Asc10 antibodies were causing increased aggregation of Asc10$^+$ *E. faecalis* cells, 0.5 ml of anti-Asc10 IgG antibodies (purified by ammonium sulfate precipitation) and 0.5 ml of Fab fragments against Asc10 were added to 0.5 ml of Asc10$^+$ OG1SSp (pINY1801) stationary phase culture. This was incubated for 30 min at room temperature and visually examined for aggregation.

Active immunization of rabbits with whole *E. faecalis* cells

Overnight cultures Asc10$^+$ OG1SSp (pINY1801) and Asc10$^-$ OG1SSp (pWM401) were grown in beef heart medium to stationary phase, with a subsequent wash in PBS and brought to an OD_{600} of 1.0. Bacteria were heat killed at 65°C for 10 min and then killed with 100 μg/ml gentamicin for 1 h at 37°C. Volumes of 0.5 ml of each strain were mixed with equal volumes of Freund's incomplete adjuvant and injected subcutaneously into the nape of the neck of New Zealand white rabbits, at a concentration of 2×10^9 CFU bacteria. Nine to 10 rabbits were immunized with each strain. Injections were done 3 times per 2 weeks, with antibody titers of greater than 10,000 verified by ELISA. Rabbits were then challenged with Asc10$^+$ OG1SSp (pINY1801) to test the effectiveness of the immunization regime against endocarditis.

Microarray studies

Three rabbits were infected with Asc10$^+$ OG1SSp (pINY1801) and another three with Asc10$^-$ OG1SSp (pWM401). Vegetations from each individual rabbit were pooled

together and frozen in liquid nitrogen for RNA isolation; however, vegetations from different rabbits were not mixed for RNA extraction. Aortic valve and arterial tissue was extracted from 3 catheterized but uninfected rabbits for RNA isolation, which served as the control. RNA was labeled and hybridized to U133A Affymetrix GeneChip (Affymetrix, Santa Clara, CA) at the University of Minnesota Biomedical Genomics Center, which compared the rabbit RNA against 22,283 human genes. Using Affymetrix MAS5.0 algorithms, 5,264 transcripts cross hybridized to the chip, resulting in expression values. A low level of expression was observed due to the use of rabbit RNA to hybridize to human transcripts. The analysis performed compared $Asc10^+$-infected vegetations to uninfected, and $Asc10^-$-infected to uninfected. A two group Student's *t* test was used to select gene groups with a p-value of 0.05 or lower, and a fold-change value of greater than 1.5. Because expression of a single gene could be modulated by efficiency of hybridization or chance, we used Ingenuity Pathway Analysis software to examine relationships between genes. Only gene pathways with more than one gene altered significantly in expression were examined.

Histological examination of $Asc10^+$- and $Asc10^-$-infected vegetations

Rabbits were infected with 2×10^9 CFU of either $Asc10^+$ OG1SSp (pINY1801) or $Asc10^-$ OG1SSp (pWM401) in the endocarditis infection model. Vegetations were removed after 4 days, frozen in liquid nitrogen, and preserved in O.C.T. (Sakura Finetek U.S.A., Inc.; Torrence, CA). The fixed vegetations were sectioned at 5 μm thickness and stained at the University of Minnesota Cancer Center with peroxidase-conjugated antibodies against $CD4^+$ T lymphocytes (KEN-4, BD Biosciences, San Jose, CA) and $CD8^+$ T lymphocytes (Clone 12.C7, Abcam, Cambridge, MA). We were unable to find

antibody conjugates that were effective in staining our samples for B cells and phagocytes. Light microscopy was used to document immune cell infiltration into the vegetation tissues, at 10x or 50x magnification.

Porcine heart valve bacterial adherence assay

Hearts were removed from sacrificed outbred Yorkshire-Landrace pigs (courtesy of Drs. David Brown and Gregory Beilman and the Experimental Surgical Services department at the University of Minnesota). The aortic, tricuspid, and mitral valves were removed aseptically using a skin biopsy punch tool (Acuderm; Fort Lauderdale, FL) to divide the valve tissue into 6-mm diameter round sections. Each valve section was placed into separate wells of a 6-well Costar 3516 tissue culture plate (Corning, Inc.). Based on the average weight of the valve sections, a ratio was calculated for each section; all volumes of medium, phosphate-buffered saline (PBS) washes, and bacterial inocula were calculated according to this ratio.

$$\frac{\text{Valve section weight}}{\text{Average valve weight}} = \text{ratio}$$

$$\text{Ratio} \times \begin{array}{c}\text{Standard volume of medium (4 ml),}\\ \text{PBS wash (4 ml), bacterial inoculum (10 µl),}\\ \text{or final homogenization (500 µl)}\end{array} = \begin{array}{c}\text{Volume used}\\ \text{for each condition}\end{array}$$

Each valve section was placed in approximately 4 ml endothelial cell medium (ECM; Lonza, Walkersville, MD) supplemented with 5% fetal bovine serum, 500 mg hydrocortisone, 6 mg bovine brain extract, 0.1% human recombinant epidermal growth factor. These valve sections were incubated in ECM plus 100 µg/ml gentamicin at 37°C in 7% CO_2 for the overnight period with rocking, to ensure lack of contamination. On the following day, the valve sections were washed three times with 4 ml PBS to

eliminate any residual gentamicin, with a final replacement by fresh ECM without antibiotics. Bacterial strains were grown overnight without aeration at 37°C in Todd-Hewitt (TH) broth (Becton-Dickinson); cells were washed twice and resuspended with PBS at an OD_{600} of 1.5. Approximately 10^6 CFU/ml of the appropriate bacterial suspension was added to each well, with subsequent incubation at 37°C in 7% CO_2 for 0.5, 1, 2, and 4 h, with rocking.

Valve sections were washed three times in approximately 4 ml PBS by flicking of tubes for removal of loosely associated bacteria, placed in about 500 μl PBS and treated with a motorized pestle (Fisher Scientific, Hanover Park, IL) for 2 min to remove adherent bacteria. To quantify bacteria, aliquots from all washes and media after incubation with bacteria were serially diluted and plated onto TH agar with the appropriate antibiotics (streptomycin 1000 μg/ml, spectinomycin 250 μg/ml, erythromycin 10 μg/ml).

Results are expressed as a compilation of the actual CFU/ml values from all experiments. Values for each strain's valve-adherent bacterial loads (CFU/ml) were averaged in generating each plot.

Scanning electron microscopy (SEM)

Tricuspid, aortic, and mitral valves were removed from porcine hearts as described in the previous section. Valve sections were infected with bacteria as described above, and at each timepoint (0.5, 1, 2, and 4 h), valves were washed as before. Each valve was placed in approximately 4 ml of SEM fixative (7% sucrose, 100 mM sodium cacodylate buffer, and 3% glutaraldehyde) with incubation at room temperature overnight to allow for fixing of bacteria-infected valve tissue. Valve tissue was stored

in fixative at 4°C for 2 days, then washed in 100 mM sodium cacodylate buffer and postfixed in 1% osmium tetroxide and 1.5% potassium ferricyanide in cacodylate buffer. All buffers and aldehyde solutions were obtained from Electron Microscopy Services (Hatfield, PA). The samples were rinsed, dehydrated through a graded ethanol series, with subsequent critical point drying with CO_2. A coating of 1 to 2 nm platinum was applied to the valve sections with an argon ion beam coater (Denton DV-502), and imaging was done on a Hitachi S-4700 field emission scanning electron microscope (FESEM) operated at 2 to 3 kV. Quartz PCI software was utilized to obtain images, where they were stored in a TIFF format.

Statistical analysis

Rabbit endocarditis experiments.

Microbial loads (total CFU and CFU/g) were converted to $\log_{10}$ values prior to statistical analysis using one-way analysis of variance followed by Fisher's post-hoc testing. Statistical significance was $p < 0.05$.

Porcine heart valve bacterial adherence assays.

Microbial loads (CFU/ml) were analyzed using an unpaired T-test; one-way analysis of variance followed by Fisher's post-hoc testing was utilized to analyze the aggregation domain mutant data in comparison to $Asc10^{+}$ OG1SSp (pCF10). Statistical significance was $p < 0.02$.

Extracellular matrix (ECM) protein binding by purified Asc10 protein in a microplate ELISA assay

Purification of wild-type and mutant Asc10 proteins through ethanol precipitation and isoelectric focusing was described previously (70). Derivatives of *E. faecalis* strain TX5128 were utilized, containing plasmids that expressed Asc10 variants (**Fig. 4**) under a nisin-inducible promoter. ECM binding by purified Asc10 protein was assayed according to a protocol found elsewhere (49), with some modifications. ECM proteins were resuspended in phosphate-buffered saline (PBS, 1.68 mM KH_2PO_4, 8.00 mM K_2HPO_4, pH 7.4, 0.15 M NaCl) or deionized water, depending on the manufacturer's instructions. Fibrinogen (Calbiochem; San Diego, CA), fibronectin (Roche; Switzerland), vitronectin (Promega; Madison, WI), and von Willebrand factor (Enzyme Research Laboratories; South Bend, IN) were coated onto 96-well 3590 CoStar plates (Corning, Inc.; Corning, NY). For fibrinogen, fibronectin, and von Willebrand factor, concentrations of 0, 200, 500, 700, 800, and 1000 ng/well were used; for vitronectin we used 0, 50, 200, 300, 500, and 800 ng/well. Plates were then incubated at 4°C overnight and washed with PBS-0.05% Tween 20 (Sigma). Purified Asc10 protein was layered on the ECM protein (100 μl of a 5 μg/ml solution) for 1 h at 37°C; adherent Asc10 protein was detected with a polyclonal rabbit antibody made against full-length purified Asc10 protein (70). A goat anti-rabbit IgG secondary antibody conjugated to horseradish peroxidase (Zymed Laboratories, Inc.; San Francisco, CA) was used to bind the adherent primary anti-Asc10 antibody**.** O-phenylenediamine (OPD) substrate (Zymed) containing H_2O_2 was added (100 μl), and the reaction was stopped with 2.5 M

H_2SO_4 (10 μl). Absorbance at 490 nm wavelength was read spectrophotometrically, to determine the quantity of Asc10 protein bound to the ECM protein.

Whole bacteria binding of ECM proteins

E. faecalis cells expressing the mutant Asc10 derivatives were tested for ECM binding using a crystal violet stain-based assay as previously described (48, 60). Bacteria were grown overnight, then washed in PBS twice and brought to an OD_{600} of 1.5. As in the ELISAs described in the previous section, the derivatives of TX5128 were used. ECM proteins were coated on 3590 CoStar plates, at the same concentrations as specified in the previous section. Two percent bovine serum albumin (BSA, Sigma) in PBS was used to block unbound sites on the plates for 1 h at 37°C. Plates were washed 4 times with PBS, and bacteria were added to each well (50 μl; approximately 5.0×10^7 CFU/well). Crystal violet (0.5%) solution (weight/volume in H_2O, 100 μl; Sigma) was added for 1 min after washing 4 times with PBS. Six washes with PBS were used to remove excess stain, and then 200 μl of citrate buffer pH 4.3 was added to suspend the bacteria and solubilize the stain. Absorbance at 562 nm wavelength was used to determine the relative amounts of stained bacteria adherent to the ECM proteins.

Chinese hamster ovary (CHO) cell bacterial uptake assays

As described previously (23), CHO cell lines expressing differing levels of glycosaminoglycans (GAGs) were utilized, which are listed in **Table 2** (53). Cell lines were purchased from ATCC (American Type Culture Collection; Rockville, MD) and seeded at 1×10^5 cells per well, after which they were grown at 37°C in 5% CO_2 for 2

Table 2. Chinese hamster ovary cell lines used in this study.

CHO Cell Line	Deficiency	Phenotype	References
K1	None	Wild-type cell line expressing GAGs containing ~70% heparan sulfate (HS), ~30% chondroitin-4-sulfate	(18, 19, 34, 76)
CRL-2242	Lacks xylotransferase I expression	Production of GAGs containing less than 1% of chondroitin sulfate or heparan sulfate as compared to K1 (wild-type CHO cell line)	(18, 19, 34, 76)
CRL-2244	Lacks N-acetylglucosaminyl-transferase and glucuronyl-transferase enzymes, both needed for HS synthesis	Express GAGs with approximately 3% heparan sulfate, and about three times amount of chondroitin sulfate (~97%) as compared to wild-type cell line	(18, 19, 34, 76)
CRL-2245	Deficiency in sulfate transport	Sulfate transport for incorporation into GAG chains impaired	(18, 19, 34, 76)

to 3 days. Ham's F-12 medium supplemented with 4 mM glutamine and 10% fetal bovine serum was used to cultivate the CHO cells in 24-well plastic dishes. Approximately 10^8 *E. faecalis* cells were incubated with ~ 10^6 CHO cells for 1 hour, in Hanks balanced salt solution (HBSS). *E. faecalis* strains were incubated with either nisin (25 ng/ml) or pheromone (1 ng/ml) for the entire overnight culturing period, or only for the final 2 hours, to induce the expression of Asc10. Cultures were grown at 35°C. Clumping was observed, confirming expression of Asc10, and the cultures were sonicated with 20 W for 10 s using a 40-W high-intensity ultrasonic processor (Sonics and Materials; Danbury, CT) to ensure single-cell suspensions (confirmed by light microscopy). A wash with HBSS was done with subsequent addition of tissue culture medium with 50 μg/ml gentamicin sulfate (Sigma-Aldrich) to eliminate extracellular bacteria. After a 1.5 h treatment with antibiotics, the CHO cells were washed with HBSS and then lysed 5 min. with 1% Triton X-100 (Sigma-Aldrich). Intracellular bacterial numbers were determined by serial dilution, followed by plating on agar and the appropriate antibiotics. The same bacterial inoculum was tested on multiple CHO cell lines simultaneously, and intracellular bacterial numbers were expressed as $\log_{10}$ per 10^5 CHO cells, to account for variation in CHO cells for each cell line.

Filter and broth matings for Tn*917* insertion mutants

Filter mating. Overnight cultures of *E. faecalis* donor strains (OG1SSp [pCF10], [pCF121], and [pCF175]) and recipient strain OG1RF were grown in TH broth (Becton-Dickinson). Polycarbonate filters (0.22 μm, Osmonics, Inc., Minnetonka, MN) were UV-sterilized for 15 min on each side, and then placed on a TH agar plate without antibiotics, matte-side facing up. From overnight cultures, 1 ml was removed and

washed twice with PBS. Dilutions of 1:10 in fresh TH broth without antibiotics were made and the diluted cultures were incubated at 37°C for 1 h. Fifty microliters of the following mixtures were spotted onto the filters: (1) 100 µl donor + 900 µl recipient, (2) 100 µl donor + 900 µl medium, (3) 100 µl recipient + 900 µl recipient. The last two pairs were used as negative controls, to ensure that the donor and recipient did not grow on 15 µl/ml tetracycline, since the pCF10 plasmid contains a tetracycline resistance marker. The spotted filter plates were incubated at 37°C for at least 4 h; filters were then removed and placed into 1 ml PBS. Vortexing was used to dislodge the bacteria off of the filter, and this homogenate was diluted and plated onto the appropriate antibiotics (pCF10, pCF121, or pCF175 transferred into OG1RF requires rifampicin 200 µl/ml, fusidic acid 25 µl/ml, and tetracycline 15 µl/ml; all antibiotics from Sigma).

Broth mating. Overnight cultures of the same strains as in the filter matings were grown for 13-15 h. Cultures also diluted 1:10 after washing with PBS, then grown for 1 to 1.5 h at 37°C with aeration. The same pairs of cultures (donor plus recipient) were mixed, but these liquid culture mixtures were incubated at 37°C for 30 min without aeration. Aliquots were removed, diluted, and plated onto the same antibiotics as described for the filter mating.

RESULTS

Multiple functional domains of *Enterococcus faecalis* aggregation substance Asc10 contribute to endocarditis virulence

Experimental rabbit endocarditis studies were performed to characterize the function of different domains in the Asc10 protein to mediate *E. faecalis* endocarditis pathogenesis. Previous studies of the functional domains of Asc10 involved expression of cloned mutant alleles of *prgB* in a nisin-inducible expression vector (69). While it is well established that Asc10 is expressed *in vivo* in the mammalian bloodstream and during endocarditis infections when the infecting strain carries wild type pCF10 (3), we were not confident that we could sustain nisin-induced expression from the cloned alleles of the gene during experimental endocarditis. Therefore, we used a recently developed allelic exchange system (32) to move mutant *prgB* alleles into the native context of pCF10, and confirmed that their pheromone-induced expression at the protein level mimicked that of the wild-type gene. In addition, we used allelic exchange to construct an in-frame deletion of *prgB* in the context of pCF10 background making it possible for the first time to test a true null allele of this gene. We then examined the behavior of isogenic strains carrying these pCF10 derivatives in experimental endocarditis. We found that a plasmid-containing strain carrying the *prgB* null allele was significantly less virulent than an isogenic plasmid-free strain, confirming that a functional *prgB* gene is required for the previously observed selective advantage of pCF10 carriage during endocarditis infections by *E. faecalis* (25). The differences in virulence of strains expressing different variants of Asc10 are consistent with the existence of multiple functional domains in the protein.

Generation of pCF10 derivatives carrying mutant alleles of *prgB*. We successfully generated pCF10 derivatives encoding production of all of the Asc10 variants depicted in **Fig. 4**, in addition to an in-frame *prgB* deletion mutant (containing only the first and last three codons), and used Western blot analysis to confirm that pheromone-inducible expression of the variant proteins was similar to that observed with wild-type Asc10 (**Fig. 5**). This gave us confidence that any differences observed between the virulence of mutant and Asc10$^+$ OG1SSp (pCF10) strains in experimental endocarditis would likely be due to functional differences among the proteins, rather than to differences in expression.

Mutations in *prgB* reduce the virulence of *E. faecalis*. In a previously published endocarditis study (25) we examined the effects of Asc10 expression on vegetation weights, and found that Asc10$^+$ strains (OG1SSp [pCF10]) produced larger vegetations than Asc10$^-$ (OG1SSp plasmid-free). In the present study, the surgical procedures, the genetic background of the bacterial host strain (OG1SSp), and the infecting doses of bacteria were essentially the same as those used previously, but smaller and younger rabbits were used because larger animals were not available. We determined both the vegetation weights (where distinct vegetations could be found) and the bacterial loads in the infected cardiac tissues as potential indicators of virulence. All data reported here were obtained from rabbits that survived the 4-day course of the experiment. We found that bacterial load was the most consistent and reproducible indicator of virulence, and that strains carrying pCF10 derivatives containing either the in-frame deletion of *prgB* or an allele encoding an Asc10 variant with glycine-to-alanine substitutions in both

Figure 4. Schematic maps of the Asc10 mutant proteins expressed by the strains used in the rabbit endocarditis model, highlighting the functional domains of the Asc10 protein. (**A)** Wild-type full-length Asc10 (pCF10). **(B)** C-terminal domain deletion variant (pCF10-6), with amino acids 688-1138 (nucleotides 2064-3414) missing. **(C)** N-terminal aggregation domain deletion (pCF10-4); amino acids 156-358 deleted (nucleotides 468-1074). **(D)** Central aggregation domain insertion (pCF10-1) with 31 amino acids inserted at amino acid 546 (nucleotide 1638). Past studies have determined amino acid residues 473-683 are an essential component of this central aggregation domain. **(E)** Double aggregation domain mutant (pCF10-5) with central aggregation domain insertion and N-terminal aggregation domain deletion combined. **(F)** N-terminal single RGDS → RADS substitution (pCF10-3). **(G)** C-terminal single RGDV → RADV substitution (pCF10-7). **(H)** Double RGD → RAD substitutions (pCF10-2). RGD motifs fall at amino acid residues 606 and 939, as shown in part A. **(I)** Tn*917* insertion at nucleotide 1409 (pCF121). Secreted fragment of Asc10 is produced, with no surface expression. **(J)** Tn*917* insertion at nucleotide 1784 (pCF175). Secreted fragment of Asc10 is produced, with no surface expression. SS = signal sequence. Adapted from Waters *et al.* 2001 (69)**.** The right-hand portion of the figure indicates whether expression of each Asc10 variant resulted in visible clumping of the host bacteria.

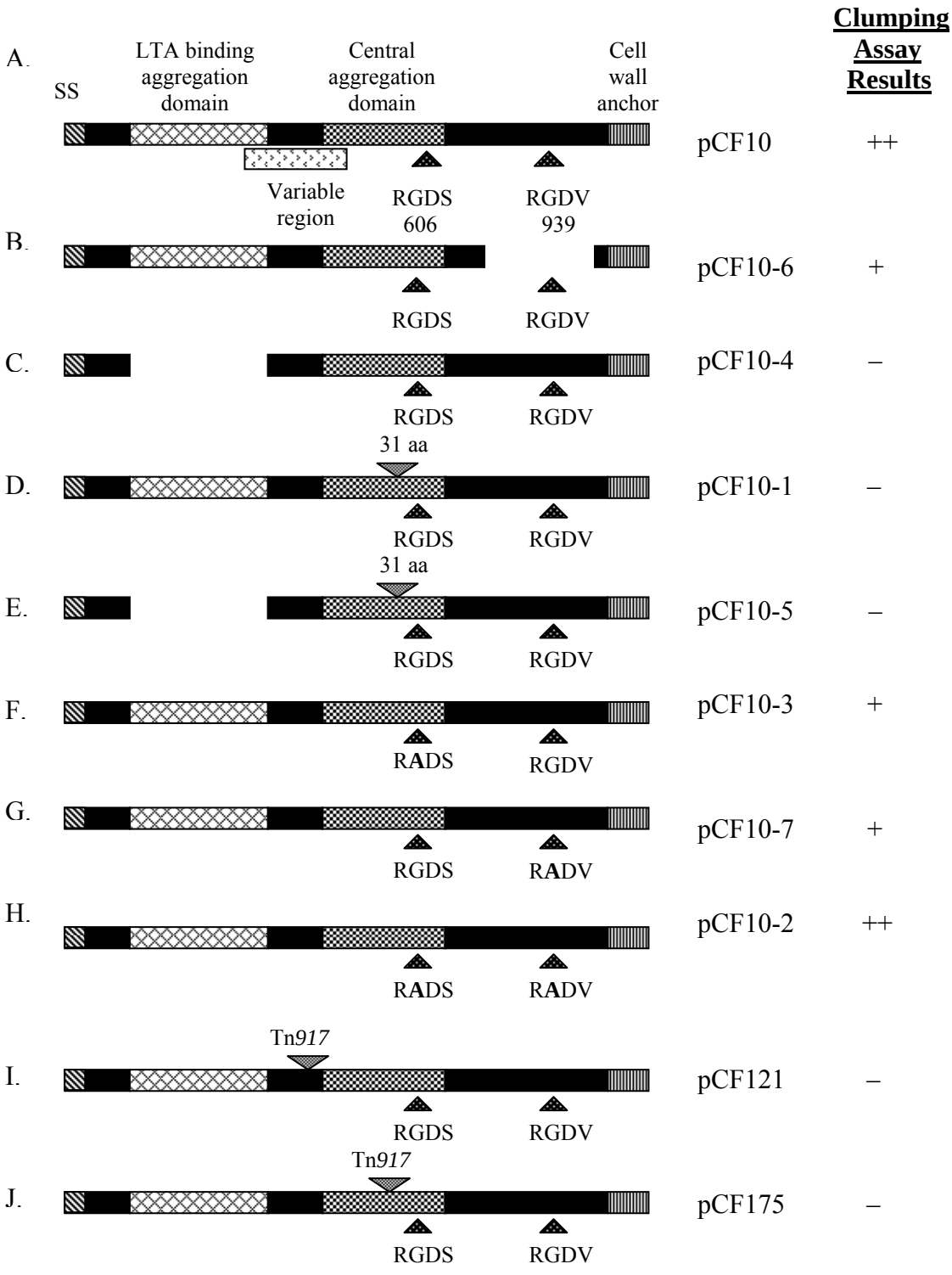
Clumping Assay Results
A.
SS
LTA binding aggregation domain
Central aggregation domain
Cell wall anchor
Variable region
RGDS 606
RGDV 939
pCF10
++
B.
RGDS
RGDV
pCF10-6
+
C.
RGDS
RGDV
pCF10-4
–
31 aa
D.
RGDS
RGDV
pCF10-1
–
31 aa
E.
RGDS
RGDV
pCF10-5
–
F.
RADS
RGDV
pCF10-3
+
G.
RGDS
RADV
pCF10-7
+
H.
RADS
RADV
pCF10-2
++
Tn917
I.
RGDS
RGDV
pCF121
–
Tn917
J.
RGDS
RGDV
pCF175
–

Figure 4.

Figure 5. Asc10 surface expression by the Asc10 mutant strains, analyzed by Western blot. Western blot analysis of purified cell wall fractions. All strains used in Western blot analyses were of an OG1SSp background. OG1SSp (pCF10) produces mainly an ~150-kDa band (indicated by blue arrow), which is larger than the predicted 137-kDa size for Asc10. This may be due to glycosylation or association of LTA with Asc10. The ~98-kDa band produced by OG1SSp (pCF10) corresponds to an N-terminal 78-kDa cleavage product (yellow arrow; 26). The electrophoretic patterns of these Asc10 derivatives including the multiple banding patterns have been observed previously (30, 69). The *prgB* deletion mutant OG1SSp (pCF10-8) was analyzed on a separate Western blot, and no Asc10 surface expression was detected. The smaller-sized bands observed for pCF10-4, pCF10-5, and pCF10-6 are due to large deletions in the *prgB* gene.

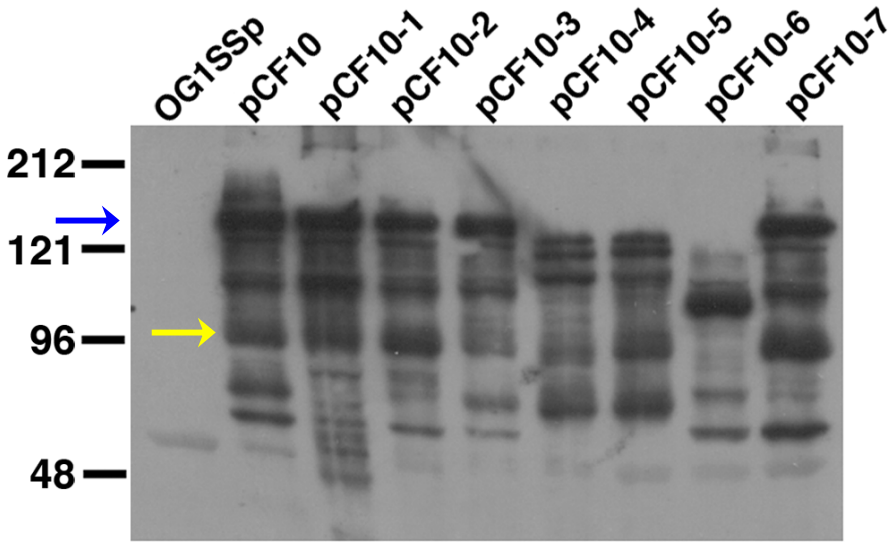

RGD motifs were much less virulent than all other strains, including an isogenic plasmid-free strain. Other *prgB* mutations affecting different regions of the protein each had distinct, more modest effects on virulence.

Fig. 6 displays representative photographs of dissected hearts from rabbits in these experiments. These specific images were selected to illustrate the appearance of vegetations of various sizes; also shown are infected tissues where no distinct vegetations could be observed. In **Fig. 7** a comparison of the bacterial load of the infected hearts is compared to the mass of the recovered vegetations for all of the infected animals used in these experiments. Although we generally found that large vegetations tended to have large numbers of bacteria, there was not a strong quantitative correlation in the pooled data for each bacterial strain between bacterial load in the infected tissue and the mass of the vegetation. Based on this result, we decided to use the total bacterial load as the primary indicator of the relative ability of each strain to colonize and proliferate within the infected heart tissue. In **Fig. 8**, the cumulative results of all experimental infections in terms of total bacterial loads are shown (the CFU/g of infected tissue from the same experiments are presented in **Fig. 9**). Of note was the Asc10$^-$ *prgB* deletion mutant (OG1SSp [pCF10-8]), whose bacterial load was significantly lower than the Asc10$^+$ OG1SSp (pCF10) and plasmid-free (OG1SSp) strains. The deletion mutant colonized the vegetations at levels approximately 1/100000th that of the strain carrying wild type pCF10, and 1/10000th that of the plasmid-free strain. In spite of the lack of a strong statistical correlation between bacterial loads and vegetation weights, it is noteworthy that the mean vegetation weight

Figure 6. Vegetations on rabbit aortic valves. **(A)** Aortic valve of a rabbit infected with the central aggregation domain insertion mutant (OG1SSp [pCF10-1]). The aortic valve is composed of three cup-shaped leaflets, as indicated by the blue box. Bacterial load of the vegetation removed was 1.50×10^1 CFU. The majority of the vegetation is found on the right-hand leaflet (as indicated by the arrow). **(B)** Infected with N-terminal single RGDS mutant (OG1SSp [pCF10-3]), where the valves exhibit no apparent vegetations. Vegetation bacterial load: 5.30×10^3 CFU. **(C)** Infected with Asc10$^-$ plasmid-free strain (OG1SSp), with one vegetation in the center leaflet (arrow). Vegetation bacterial load: 2.40×10^7 CFU.

Figure 6.

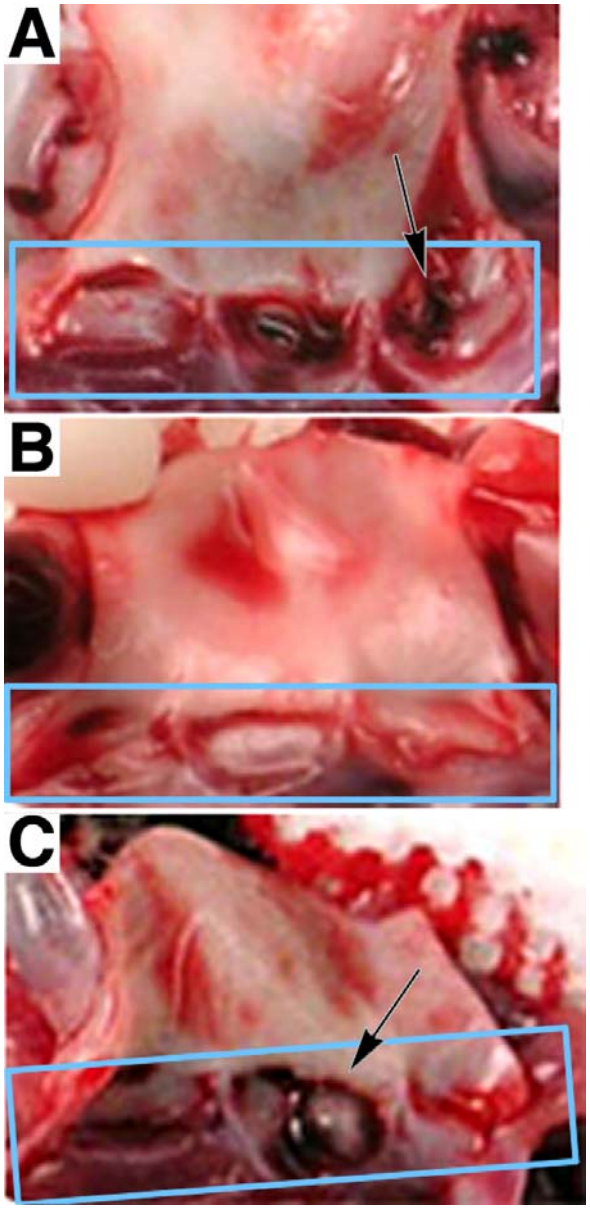

Figure 7. Log_{10} vegetation bacterial load (total CFU) versus vegetation weight in a rabbit endocarditis model. *E. faecalis* cells expressing Asc10 mutant derivatives were injected intravenously at 2×10^9 CFU after catheter placement in the carotid artery for 2 h; the catheter was removed prior to microbe injection. All vegetations on the aortic valve of each rabbit were pooled to obtain the vegetation weight and bacterial loads. When no vegetations were found, the valves were removed and plated to determine valve bacterial load. The low R^2 value of 0.27 indicates there is no correlation between these sets of values.

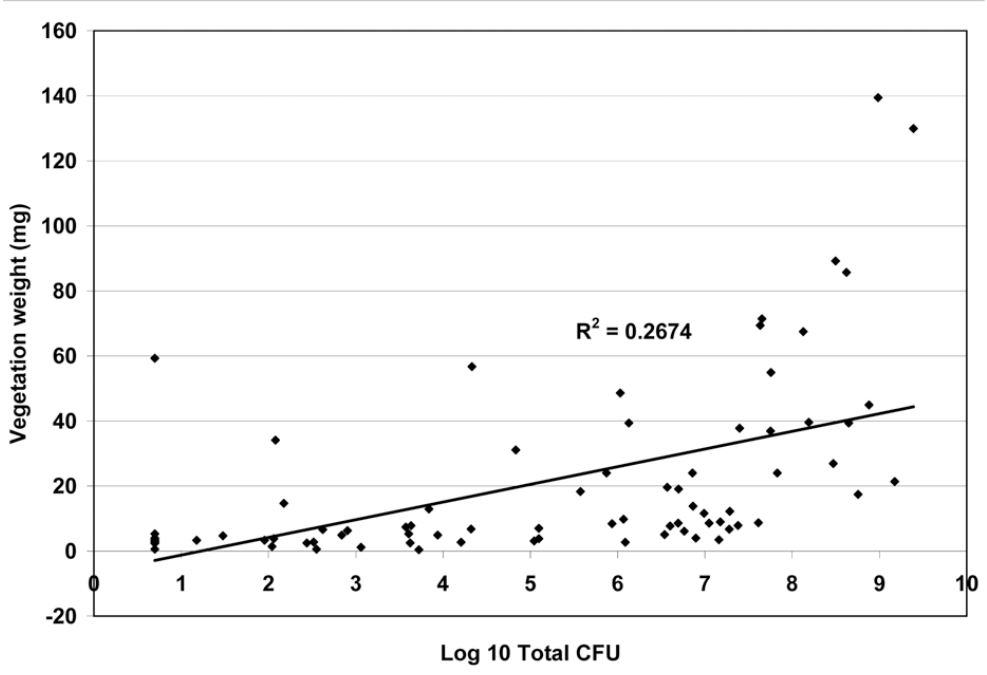

Figure 8. Arithmetic and geometric mean vegetation bacterial loads in the rabbit endocarditis model, expressed as $\log_{10}$ values (total CFU). *E. faecalis* cells expressing Asc10 mutant derivatives were injected intravenously at 2×10^9 CFU after catheter placement in the carotid artery for 2 h; the catheter was removed prior to microbe injection. All vegetations on the aortic valve of each rabbit were pooled to obtain the vegetation weight and bacterial loads. When no vegetations were found, the valves were removed and plated to determine valve bacterial load. Dashed line indicates minimum level of detection at 0.70. * denotes $p \leq 0.01$, as compared to $Asc10^+$ OG1SSp (pCF10).

Figure 8.

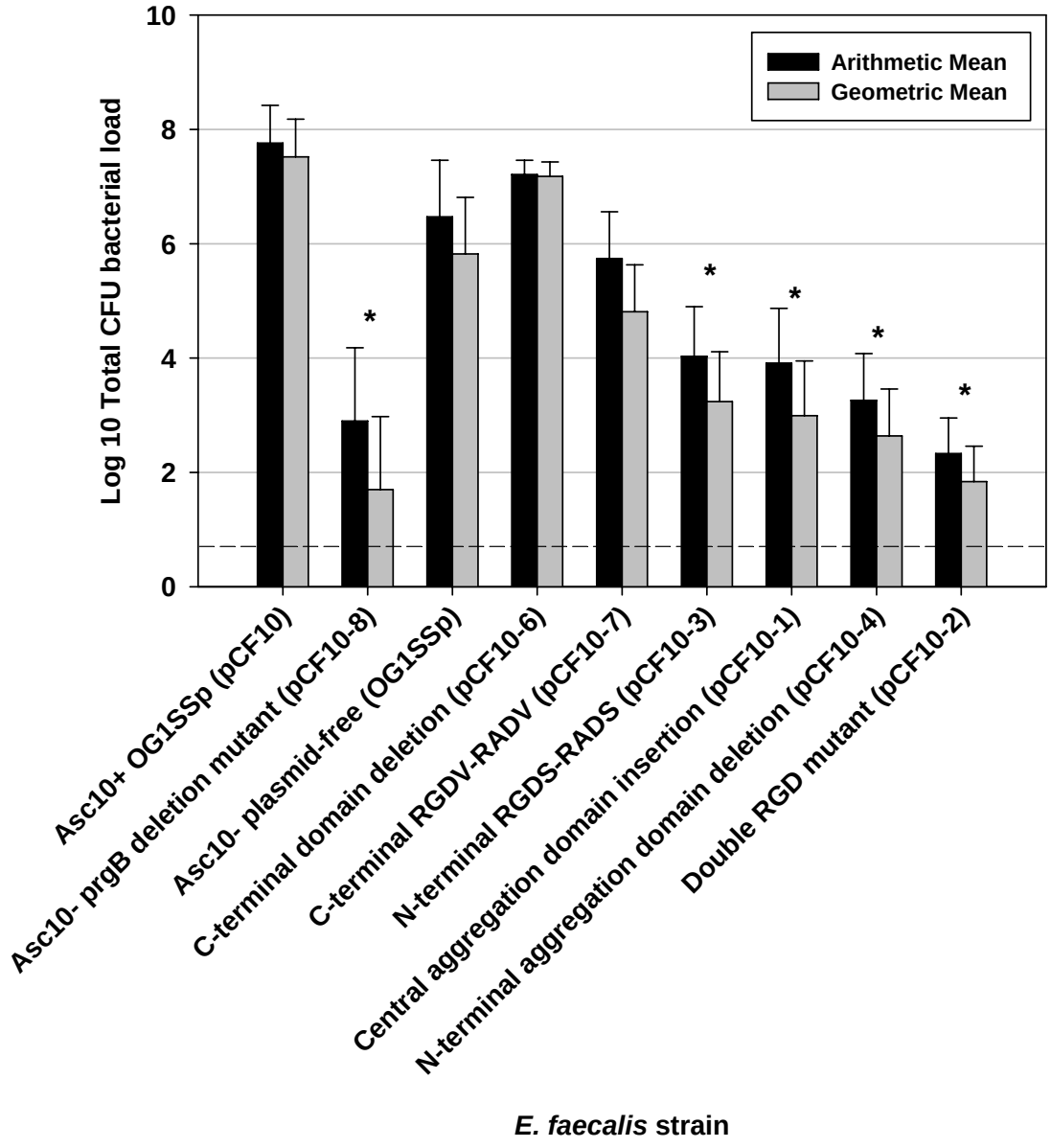
Log 10 Total CFU bacterial load
10
8
6
4
2
0
Arithmetic Mean
Geometric Mean
*
*
*
*
*
Asc10+ OG1SSp (pCF10)
Asc10- prgB deletion mutant (pCF10-8)
Asc10- plasmid-free (OG1SSp)
C-terminal domain deletion (pCF10-6)
C-terminal RGDV-RADV (pCF10-7)
N-terminal RGDS-RADS (pCF10-3)
Central aggregation domain insertion (pCF10-1)
N-terminal aggregation domain deletion (pCF10-4)
Double RGD mutant (pCF10-2)
E. faecalis strain

Figure 9. (a) Mean vegetation bacterial loads in the rabbit endocarditis model, expressed as $\log_{10}$ values (CFU/g). Dashed line indicates minimal level of detection at 1.93, and * denotes $p \leq 0.01$, as compared to the Asc10$^+$ OG1SSp (pCF10) strain. **(b)** Bacterial counts (CFU/g) obtained from vegetations in a rabbit endocarditis model. *E. faecalis* cells expressing Asc10-mutant derivatives were injected intravenously at 2×10^9 CFU after catheter placement in the carotid artery for two hours, with subsequent removal. All vegetations on the aortic valve of each rabbit were pooled to obtain each data point. In some cases, no vegetations were found; however, the valves were then removed and plated to determine valve bacterial load. The horizontal bar denotes the average $\log_{10}$ CFU/g for each group of data points; the dotted line represents the minimum level of detection at 1.30×10^3 CFU/g.

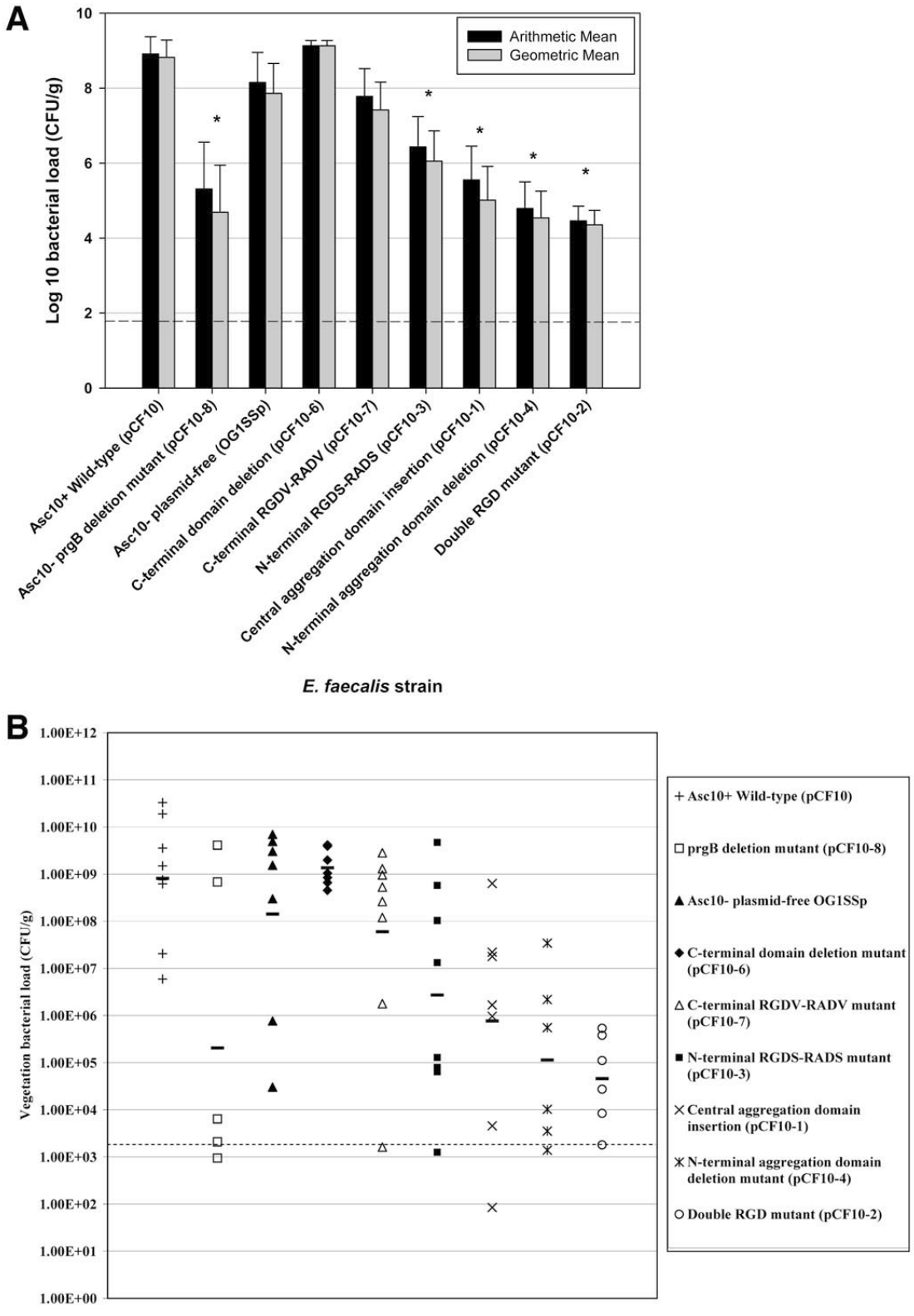
A
Arithmetic Mean
Geometric Mean
Log 10 bacterial load (CFU/g)
10
8
6
4
2
0
*
Asc10+ Wild-type (pCF10)
Asc10- prgB deletion mutant (pCF10-8)
Asc10- plasmid-free (OG1SSp)
C-terminal domain deletion (pCF10-6)
C-terminal RGDV-RADV (pCF10-7)
N-terminal RGDS-RADS (pCF10-3)
Central aggregation domain insertion (pCF10-1)
N-terminal aggregation domain deletion (pCF10-4)
Double RGD mutant (pCF10-2)
E. faecalis strain
B
Vegetation bacterial load (CFU/g)
1.00E+12
1.00E+11
1.00E+10
1.00E+09
1.00E+08
1.00E+07
1.00E+06
1.00E+05
1.00E+04
1.00E+03
1.00E+02
1.00E+01
1.00E+00
Asc10+ Wild-type (pCF10)
prgB deletion mutant (pCF10-8)
Asc10- plasmid-free OG1SSp
C-terminal domain deletion mutant (pCF10-6)
C-terminal RGDV-RADV mutant (pCF10-7)
N-terminal RGDS-RADS mutant (pCF10-3)
Central aggregation domain insertion (pCF10-1)
N-terminal aggregation domain deletion mutant (pCF10-4)
Double RGD mutant (pCF10-2)

Figure 9.

for the *prgB* deletion strain was 5.35 mg, which was the lowest weight recorded among the Asc10 mutant strains (in comparison to 49.2 mg for wild type pCF10).

A strain carrying an in-frame deletion (OG1SSp [pCF10-6]) resulting in the loss of a 450 amino acid region of Asc10 proximal to the wall anchoring C-terminal domain exhibited virulence that was indistinguishable from the strain carrying wild-type pCF10, while other less drastic changes in Asc10 had much greater effects on virulence. This indicates that amino acid residues 688-1138 of Asc10 play a minimal role in the pathogenic effects of the protein.

The mutant exhibiting the lowest virulence in the endocarditis model was the double RGD variant (OG1SSp [pCF10-2]). This result was striking because the *prgB* point mutations resulting in the single amino acid substitutions changing RGD to RAD represent the most subtle changes we made in the protein (the other variants all had significant insertions or deletions in the protein). The aggregation domain variants (OG1SSp [pCF10-1] and [pCF10-4]) were less virulent than strains expressing the wild-type protein, but they retained a higher level of virulence than the double RGD mutant. Moreover, cells expressing the double RGD mutation were still able to clump, which also indicates that bacterial aggregation itself is not the sole determinant of Asc10-mediated virulence. The N-terminal single RGDS mutation (OG1SSp [pCF10-3]) resulted in bacterial loads approximately $1/10000^{th}$ those observed in infections with a strain expressing wild-type pCF10, whereas the double RGD mutant (OG1SSp [pCF10-2]) was less than $1/100000^{th}$ that of the $Asc10^{+}$ OG1SSp (pCF10) strain and essentially

equivalent to the virulence of the strain carrying the *prgB* null allele. Mutation of the C-terminal RGDV domain had a more modest, but still significant effect on virulence, producing bacterial loads about $1/100^{th}$ those associated with wild-type Asc10. This suggests that both the RGD motifs contribute to virulence, but that the N-terminal motif may be more important. Since the predicted topology of the protein is with the N-terminus projecting away from the cell and the C-terminus being more buried in the thick cell envelope, this observation is not surprising. Possible explanations for the fact that several mutant alleles of *prgB* were less virulent than the plasmid-free strain are considered in the Discussion.

Immunization with Fab fragments of anti-Asc10 antibodies diminishes *Enterococcus faecalis* endocarditis

Microarray studies demonstrate that Asc10 reduces inflammatory responses against *E. faecalis* during endocarditis infection. To characterize the host response against $Asc10^+$ and $Asc10^-$ *E. faecalis* during endocarditis, 3 rabbits per group were challenged with $Asc10^+$ OG1SSp (pINY1801) and $Asc10^-$ OG1SSp (pWM401) after catheterization across the aortic valve for 2 h. After 4 days, vegetations were extracted, and RNA was isolated for hybridization to the Affymetrix GeneChip Human Genome U133A array. Vegetations from $Asc10^+$-infected rabbits were larger than $Asc10^-$, but vegetations were still present in $Asc10^-$-infected animals (data not shown). RNA was also extracted from aortic valve tissue of rabbits that were uninfected, but had undergone the catheterization procedure.

Analysis by the Affymetrix MAS 5.0 algorithm revealed that 5,264 transcripts were present. Since the rabbit genome is not sequenced and there is no rabbit genomic

microarray available, we had to rely on the similarity between the rabbit and human for this analysis. However, cross-hybridization did occur, as 24% of the total transcripts found on the array were represented.

Expression values from altered genes were averaged, and then compared to the values from the uninfected, catheterized rabbits. We found 202 genes with altered mRNA expression in vegetations from Asc10$^+$-infected rabbits (OG1SSp [pINY1801]), and 241 for the Asc10$^-$-infected rabbits (OG1SSp [pWM401]) as compared to the negative uninfected control. Using the Ingenuity Pathways analysis, 27 pathways had changed for Asc10$^+$-infected rabbits, and 35 pathways for Asc10$^-$; 14 pathways were shared between the two strains. We noted that several genes involved in the adaptive immune response were altered when Asc10$^+$- (OG1SSp [pINY1801]) and Asc10$^-$-infected rabbits (OG1SSp [pWM401]) were compared. Class II major histocompatibility molecules (MHC class II; HLA-D) were observed to be more upregulated in Asc10$^-$-infected animals than Asc10$^+$. In addition, mRNA expression of T-cell receptor α and tumor necrosis factor (TNF)-α induced proteins 3 and 6 were increased in Asc10$^-$ vs. Asc10$^+$ (**Table 3**). These data suggest that the adaptive immune response is dampened in the Asc10$^+$-infected rabbits, and that in the absence of Asc10, this response is allowed to run more rampant.

Histological examination of immune response in vegetations. To determine whether an influx of immune cells could account for the heightened immune response in rabbits infected with Asc10$^-$ (OG1SSp [pWM401]) as seen in the microarray analysis, we examined vegetations histologically for the presence of CD4$^+$ and CD8$^+$ T cells. We

Table 3. Human microarray anaylsis of host response in a rabbit endocarditis model. Adaptive immune system genes are up-regulated more often by Asc10$^-$ enterococci compared to untreated controls than by isogenic Asc10$^-$ organisms compared to untreated controls.

Gene Affected	Fold Increase in Gene Level of Asc10$^-$ Versus Control	Fold Increase in Gene Level of Asc10$^+$ Versus Control
HLA DRβ4	1.6	NS[a]
HLA DRβ5	1.9	NS
HLA DRβ1	2.2	1.5
HLA DQβ1	2.0	NS
Immunoglobulin Light Chain	2.1	NS
T Cell Receptor-α	5.2	3.8
TNF-α Induced Protein 3	1.5	NS
TNF-α Induced Protein 6	20.9	8.8

[a]NS, No Significant Up-regulation

attempted to stain for B cells and phagocytes, but these antibodies were not able to stain effectively. As shown in **Figure 10A and B**, a large number $CD4^+$ T cells were recruited into the $Asc10^-$-infected vegetation; the influx of $CD8^+$ T cells into the $Asc10^-$-infected vegetation is seen in **Figure 10D and E**. This is in contrast to **Figure 10C and F,** where a few $CD4^+$ and $CD8^+$ T cells are shown by arrows in the $Asc10^+$-infected vegetation. In the $Asc10^-$-infected animal, the significant recruitment of $CD4^+$ T cells is indicative of a T helper cell response, resulting in antigen presentation and production of antibody. The $CD8^+$ T cell presence points to a cytotoxic T cell response. These data corroborate our results from the microarray, where the $Asc10^-$ OG1SSp (pWM401) organism elicits a stronger immune response than $Asc10^+$ OG1SSp (pINY1801).

Active immunization against $Asc10^+$ *E. faecalis* is ineffective against reducing severity of endocarditis. Previous studies have demonstrated that immunization with antibodies against an N-terminal fragment of Asc10 (amino acids 44-331) has been ineffective at protecting against $Asc10^+$ *E. faecalis* endocarditis (37). In addition, we have used heat- and gentamicin-killed $Asc10^+$ OG1SSp (pINY1801) and $Asc10^-$ (pWM401) to actively immunize rabbits, with subsequent challenge by $Asc10^+$ bacteria in endocarditis infection. Most of the rabbits that we immunized with $Asc10^+$ OG1SSp (pINY1801) bacteria succumbed to the infection before the end of the experiment; only one rabbit survived the time period (**Table 4**). All of the rabbits had severe vegetations that blocked the aortic vessel opening, which likely lead to their death. In $Asc10^-$-immunized rabbits, only 2 animals died before the end of the experiment, and vegetations were not as large in size or as numerous as in the $Asc10^+$-immunized

Figure 10. Asc10$^-$ *E. faecalis* induce larger infiltration of CD4$^+$ (A, B) and CD8$^+$ (D, E) T cells into the vegetation tissue than Asc10$^+$ *E. faecalis* (C, F). Panels A, C, D, and F 10x magnification; B, E 50x magnification. The arrows in C and F denote the sparse CD4$^+$ and CD8$^+$ T cells found in the Asc10$^+$ *E. faecalis*-infected vegetations.

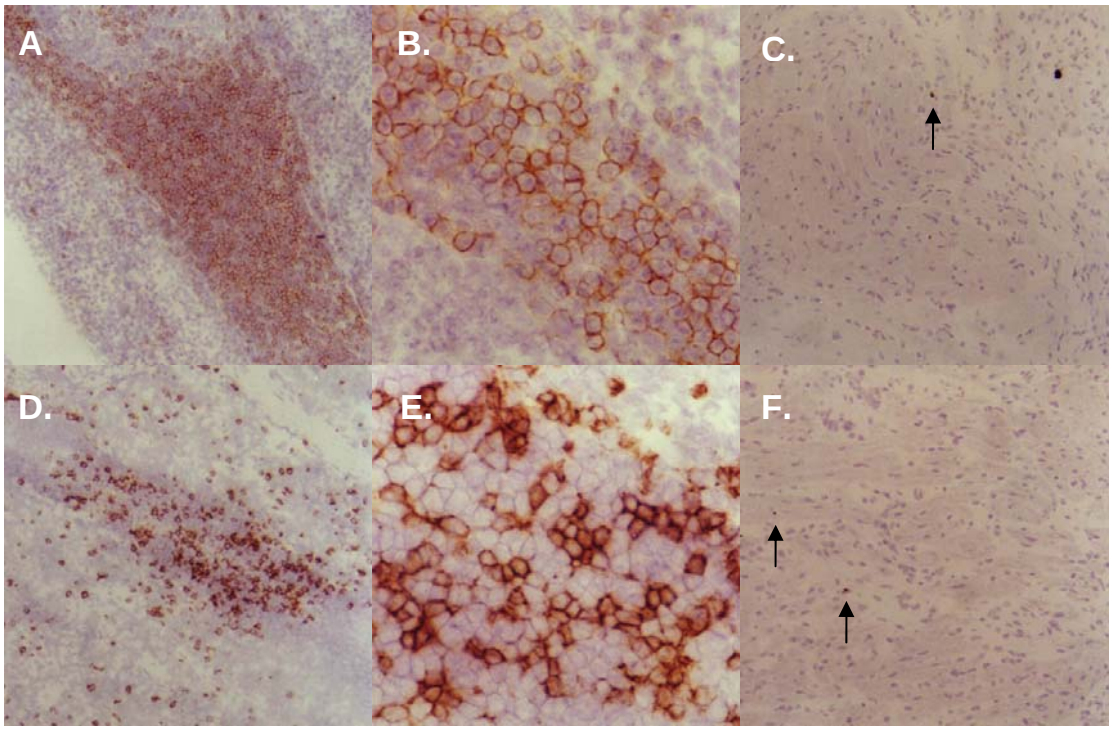

Table 4. Active immunization against *E. faecalis* exacerbates infectious endocarditis in rabbits.

Rabbits Immunized Against:	**Alive /Total Tested**	***P*-Value compared to Asc10$^+$ *E. faecalis* Immunized Animals[a]**	**Vegetations[b]**	**Respiratory Condition**
Asc10$^+$ *E. faecalis*	1/10		3+	pneumonia
None	5/5	0.002	2+	Normal
Asc10$^-$ *E. faecalis*	7/9	0.005	2+	pneumonia

[a] Determined with use of Fishers Exact Test.

[b] 1+ vegetations were small in size and number (approximately 10 mg); 2+ vegetations were moderate in size and number (approximately 50 mg); and 3+ vegetations were large in size and numbers, often obstructing the aorta (> 75 mg).

rabbits. There was pneumonia present in both groups; however, Asc10$^+$-immunized rabbits exhibited more severe pneumonia. It is likely that anti-Asc10 antibodies caused the Asc10$^+$ OG1SSp (pINY1801) bacteria to aggregate more readily, and that these large clumps were easily trapped in the small capillaries of the lungs. None of the non-immunized animals succumbed prior to the end of the experiment, and the vegetations were similar in size and number to Asc10$^-$ OG1SSp (pWM401)-immunized rabbits.

Immunization with Fab fragments of anti-Asc10 antibodies reduces severity of *E. faecalis* endocarditis. Because we hypothesized that increased aggregation of Asc10$^+$ *E. faecalis* was mediated by anti-Asc10 antibodies, we decided to cleave the antibodies into Fab fragments. Removing the Fc portion of the antibody would allow the Fab fragments to bind separately to Asc10$^+$ *E. faecalis* cells without enhancing aggregation as might occur following administration of intact antibodies. Passive immunization with Fab fragments specific for Asc10 prior to infection with Asc10$^+$ OG1SSp (pINY1801) decreased the size and bacterial loads of vegetations in comparison to the control group that received no immunization treatment (**Table 5**). Control rabbits had a mean vegetation weight of 39.5 mg, while Fab fragment immunized-animals had a mean weight of 10.5 mg. Also, Fab-treated rabbits had a mean total log CFU vegetation bacterial load that was more than 2 logs below the control rabbit vegetation loads. No lung congestion was observed in Fab-treated animals, though mild congestion was seen in two of six rabbits in the control group. None of the animals died before the end of the experimental period.

Table 5. Ability of IgG Fabs against aggregation substance to reduce the severity of enterococcal endocarditis in rabbits.

Treatment Group	Number of Rabbits	Mean Vegetation Weight (mg)	*P*-Value	Mean Log CFU Total in Vegetations	*P*-Value
Untreated control	6	39.5		6.9	
Fab Treated	6	10.5	0.06	4.3	0.02

Fab fragments against Asc10 reduce *in vitro* aggregation between Asc10$^+$ *E. faecalis* cells. To demonstrate that whole antibodies against Asc10 do indeed intensify aggregation between Asc10$^+$ *E. faecalis* cells, we added whole polyclonal IgG antibodies against Asc10 to a stationary phase culture of Asc10$^+$ *E. faecalis* OG1SSp (pINY1801). We observed that these polyclonal anti-Asc10 antibodies further increased aggregation between *E. faecalis* cells, as shown in **Fig. 11** (middle culture as compared to left-hand untreated control). In contrast, the Fab anti-Asc10 fragments were able to almost completely eliminate aggregation.

Figure 11. Whole polyclonal antibodies against Asc10 further increase aggregation between Asc10^{+} *E. faecalis* OG1SSp (pINY1801), while Fab fragments against Asc10 almost completely abolish this aggregation. IgG-treated = full-length anti-Asc10 antibody-treated.

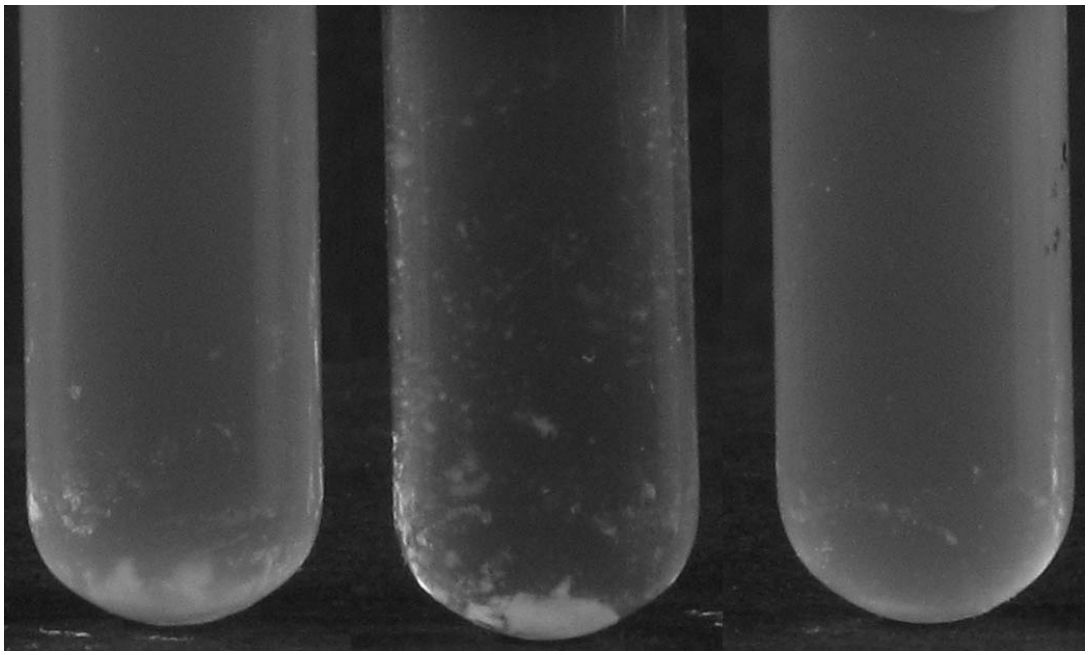

Untreated Control IgG-treated Fab-treated

Use of porcine cardiac valve tissue in an *ex vivo* study of Asc10-mediated adherence of *Enterococcus faecalis* and biofilm formation

Development of porcine valve bacterial adherence assay. Initial experiments performed to assess the ability of Asc10$^+$ OG1SSp (pCF10) and mutant Asc10-expressing *E. faecalis* to adhere to porcine valve tissue were done with freshly dissected valve sections that were incubated for 1 to 1.5 h in erythromycin (10 μg/ml). Once we inoculated the valve tissue with bacteria, this was done in the absence of antibiotics. However, we had difficulties with growth of contaminating organisms, and thus we incubated the valve tissue in endothelial cell medium with gentamicin overnight before inoculating with *E. faecalis*, to ensure the absence of contamination. No significant differences between the two procedures were observed, and data from any valve adherence experiments with contaminated valve tissue was eliminated from our analysis.

In-frame deletion of the *prgB* gene has minor effects on Asc10$^+$ *E. faecalis* valve tissue adherence. We observed a dramatic decrease in vegetation bacterial load for the *prgB* deletion mutant (OG1SSp [pCF10-8]) in our rabbit endocarditis study results (7), where its loads were less than 1/100000th the Asc10$^+$ OG1SSp (pCF10) bacterial load. To determine whether decreased valve adherence might account for this lowered virulence, we utilized the *ex vivo* porcine heart valve tissue model. Adherence of this mutant to valve tissue was not impaired at 0.5, 1, and 2 h, as compared to Asc10$^+$ OG1SSp (pCF10) (**Fig. 12**). At 4 h, the numbers of *prgB* deletion mutant bacteria adherent to valve tissue was approximately 40% of the Asc10$^+$ OG1SSp (pCF10) valve

Figure 12. *prgB* deletion mutant (OG1SSp [pCF10-8]) is not impaired in porcine valve adherence. Porcine aortic, tricuspid, and mitral valves were infected with *E. faecalis* strains carrying wild-type pCF10 and the *prgB* deletion derivative pCF10-8 for 0.5, 1.0, 2.0 and 4.0 h. Valves were washed and homogenized, and adherent bacteria were quantified by plating onto agar. The data shown are a compilation of at least three experiments.

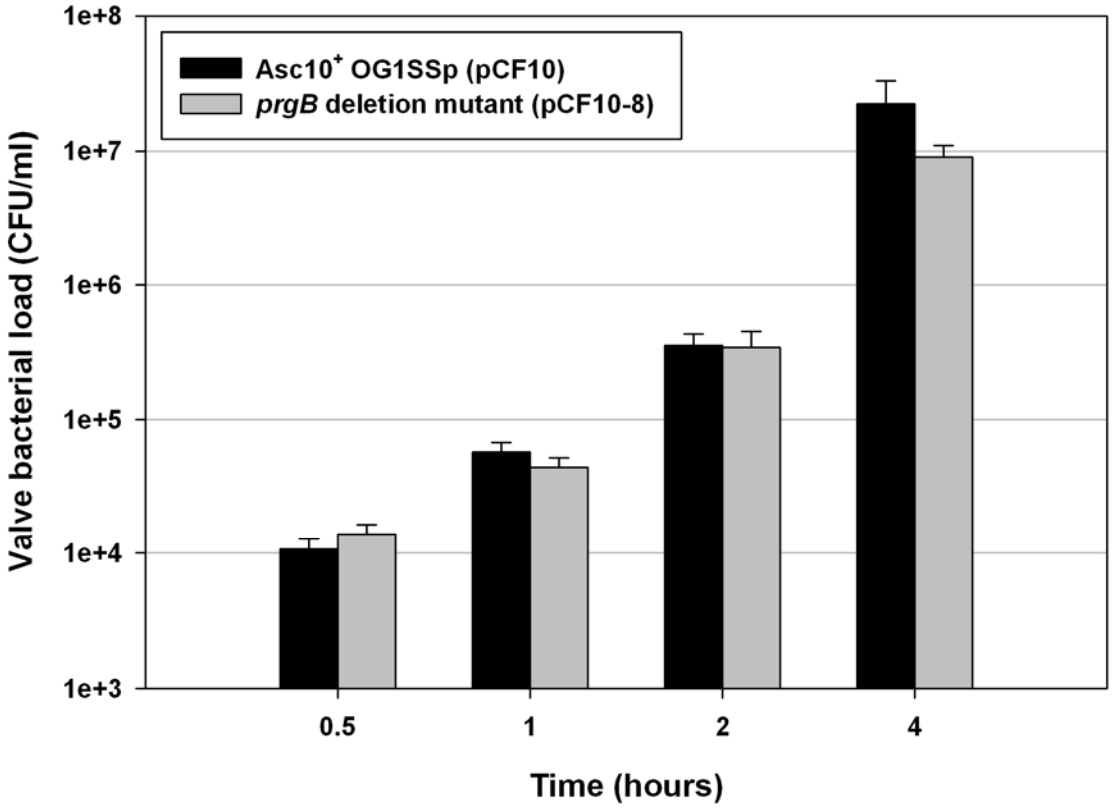

bacterial load. This modest decrease at 4 h of the mutant valve loads suggests that Asc10 is not crucial in initial adherence of *E. faecalis* to valve tissue, though expression of Asc10 could contribute to an increased adherent population of bacteria at longer time points.

Mutations in the aggregation domains of *prgB* diminish binding to porcine heart valves. Our studies in the rabbit endocarditis model (7) demonstrated that the aggregation domains of Asc10 contribute to *E. faecalis* endocarditis virulence. Strains expressing an Asc10 variant with singly mutated aggregation domains were at most $1/10000^{th}$ the $Asc10^{+}$ OG1SSp (pCF10) vegetation bacterial load. To further investigate a potential mechanism for this decreased virulence, adherence of the double aggregation domain mutant (OG1SSp [pCF10-5]; see **Fig. 4**) to porcine aortic and tricuspid valve tissue was examined. The double aggregation domain mutant was slow during the first hour to bind the valve tissue, but between 1 and 2 h there was a sharper increase in cells binding. This was followed by another slow increase at 4.0 h, whereas the $Asc10^{+}$ OG1SSp (pCF10) strain maintained a steady increase throughout the 4 h experiment. At 1 h, we found that the mutant adhered at 18% of the $Asc10^{+}$ OG1SSp (pCF10) bacterial loads, and at 4 h the gap increased, where the mutant's loads were 19% of the $Asc10^{+}$ OG1SSp (pCF10) loads (**Fig. 13A**). The single aggregation domain mutants (OG1SSp [pCF10-1] and [pCF10-4]) bound valve tissue as well as the $Asc10^{+}$ OG1SSp (pCF10) strain initially, but as time passed, they seemed to be at a disadvantage (**Fig. 13B**). Both aggregation domains appear to contribute to binding of $Asc10^{+}$ *E. faecalis* to heart valves.

Figure 13. Alteration of the aggregation domain mutants in Asc10 lowers the ability of *E. faecalis* to bind to valve tissue**. (A)** Double aggregation domain mutant (OG1SSp [pCF10-5]) with N-terminal aggregation domain deletion and central aggregation 31-aa insertion. The mutant is unable to bind as well as $Asc10^{+}$ OG1SSp (pCF10). **(B)** Single aggregation domain mutants bind as well as $Asc10^{+}$ OG1SSp (pCF10) initially, but over time the gap between the $Asc10^{+}$ OG1SSp (pCF10) and mutant grows increasingly. The data shown are a compilation of at least three experiments. * denotes $p \leq 0.05$, with respect to $Asc10^{+}$ OG1SSp (pCF10) valve bacterial loads.

Figure 13.

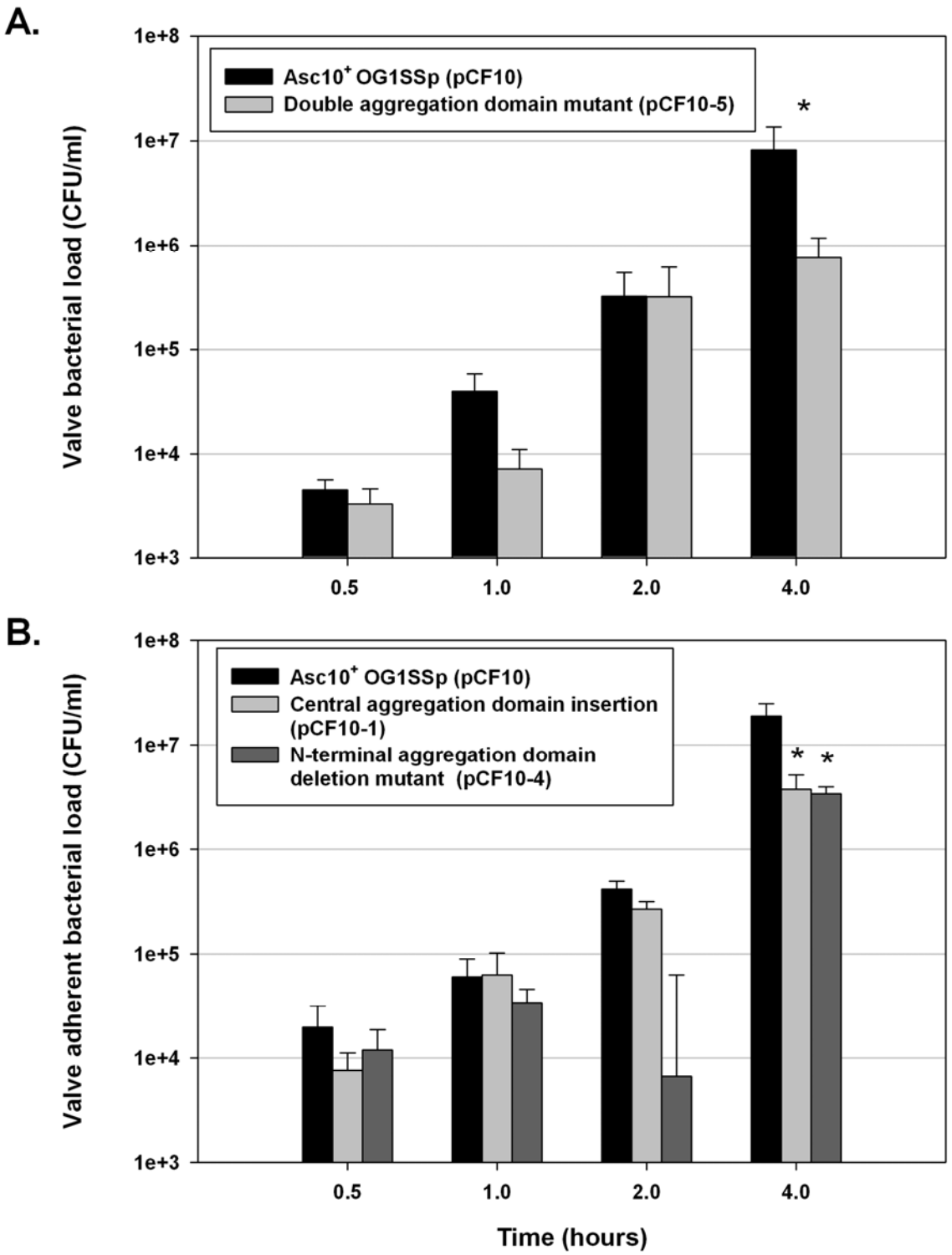
A.
Asc10+ OG1SSp (pCF10)
Double aggregation domain mutant (pCF10-5)
Valve bacterial load (CFU/ml)
1e+8
1e+7
1e+6
1e+5
1e+4
1e+3
*
0.5
1.0
2.0
4.0
B.
Asc10+ OG1SSp (pCF10)
Central aggregation domain insertion (pCF10-1)
N-terminal aggregation domain deletion mutant (pCF10-4)
Valve adherent bacterial load (CFU/ml)
1e+8
1e+7
1e+6
1e+5
1e+4
1e+3
* *
0.5
1.0
2.0
4.0
Time (hours)

The RGD motifs of Asc10 are a factor in persistence of *E. faecalis* in binding to valve tissue. We observed in our previous study that rabbits infected with the double RGD mutant (OG1SSp [pCF10-2]) had vegetation bacterial loads $1/1000000^{th}$ of wild-type, the lowest of all the *prgB* mutants tested (7). In line with our hypothesis that the RGD motifs contribute to persistence of *E. faecalis* during endocarditis (7) binding by the double RGD mutant to porcine valve tissue was lower compared to $Asc10^{+}$ OG1SSp (pCF10) at 4 h (**Fig. 14A**). In contrast, at 0.5, 1 and 2 h, the double RGD mutant shows no defect in binding, and at 0.5 and 1.0 h the double RGD mutant bound better than the $Asc10^{+}$ OG1SSp (pCF10) strain. These results demonstrate that though the RGD motifs do not contribute to early colonization of $Asc10^{+}$ *E. faecalis* on valve tissue, its ability to persist is affected by the RGD motifs.

The C-terminal domain of Asc10 has minimal involvement in the initial binding to valve tissue. The C-terminal domain deletion mutant (OG1SSp [pCF10-6]) colonized the endocarditis vegetations at levels similar to $Asc10^{+}$ OG1SSp (pCF10) (7). Similarly, the C-terminal domain mutant bound the valve tissue at numbers comparable to $Asc10^{+}$ OG1SSp (pCF10), though at the 4 h timepoint the mutant adhered at 25% of the $Asc10^{+}$ OG1SSp (pCF10) valve bacterial load (**Fig. 14B**). Considering the endocarditis and valve adherence assay results, the C-terminal domain could serve as a scaffolding support to display the other domains, such as the aggregation domains. However, this will need to be confirmed by structural studies. In the initial adherence of Asc10-expressing *E. faecalis* cells to valve tissue, however, the C-terminal domain is not an important factor.

Figure 14. RGD to RAD amino acid substitutions in the RGD motifs and deletion of the C-terminal domain do not decrease *E. faecalis* binding below Asc10$^+$ OG1SSp (pCF10) levels. (A) The double RGD mutant (OG1SSp [pCF10-2]) binds as well or better than Asc10$^+$ OG1SSp (pCF10); no deficiency in binding to porcine valve tissue was detected until 4 h. **(B)** Deletion of the C-terminal domain of Asc10 does not significantly affect the ability of *E. faecalis* to bind to valve tissue. The data shown are a compilation of at least three experiments.

Figure 14.

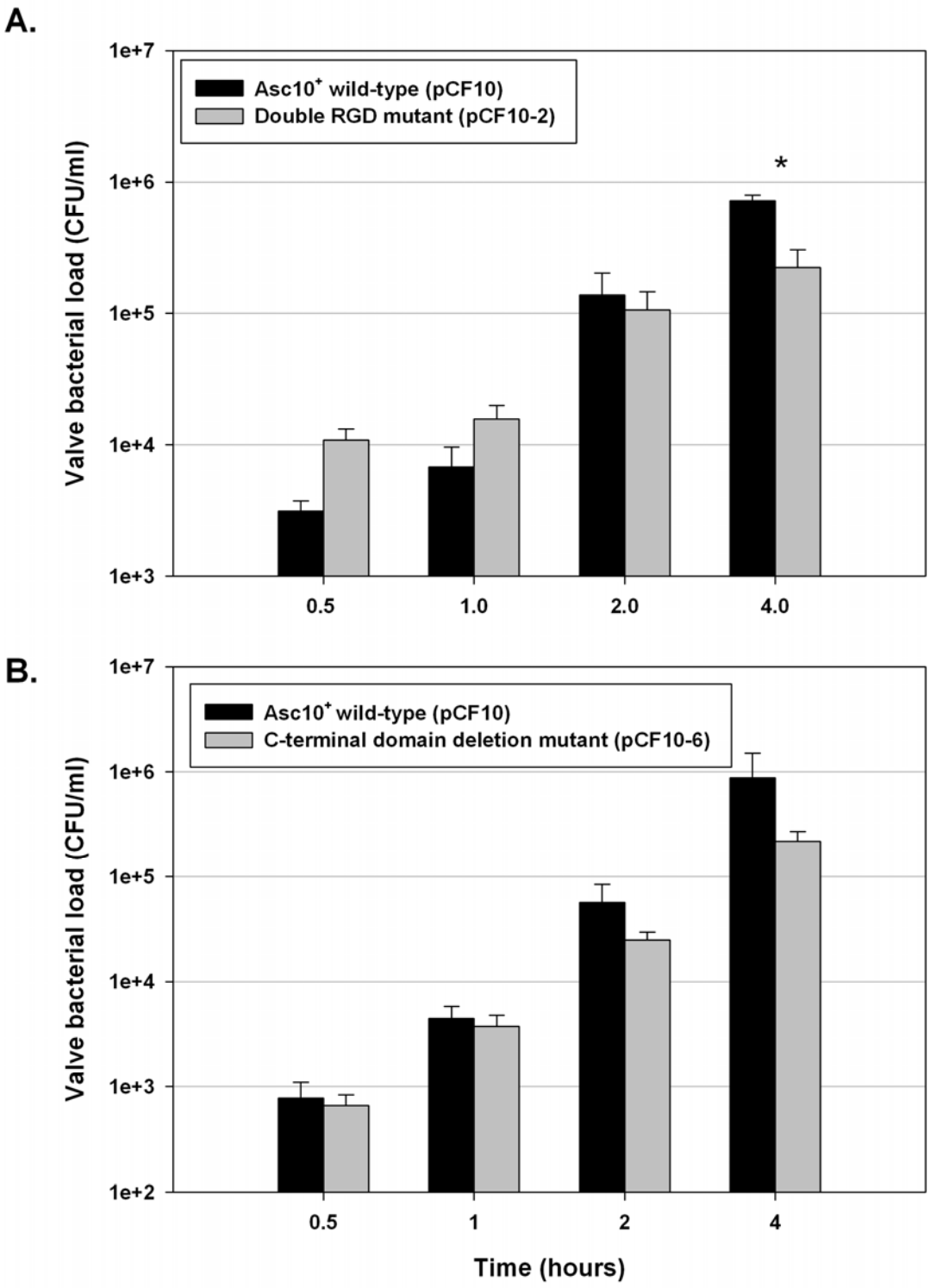
A.
Asc10+ wild-type (pCF10)
Double RGD mutant (pCF10-2)
Valve bacterial load (CFU/ml)
1e+7
1e+6
1e+5
1e+4
1e+3
*
0.5
1.0
2.0
4.0
B.
Asc10+ wild-type (pCF10)
C-terminal domain deletion mutant (pCF10-6)
Valve bacterial load (CFU/ml)
1e+7
1e+6
1e+5
1e+4
1e+3
1e+2
0.5
1
2
4
Time (hours)

Biofilm formation on porcine heart valves as examined by scanning electron microscopy. This *ex vivo* valve adherence model has served well in examining biofilm formation, for we now have a more physiologically relevant surface than plastic or glass for bacterial adherence. We used high resolution SEM to assess binding of $Asc10^+$ OG1SSp (pCF10) to porcine heart valves at 0.5, 1, 2, and 4 h timepoints. In **Fig. 15**, $Asc10^+$ OG1SSp (pCF10) *E. faecalis* were shown to bind at increasing numbers over time, with aggregates that grew in size over the 4 h time period. It also appeared that a component of the valve tissue might be accelerating growth of the *E. faecalis* cells, because we observed increased growth during the 4 h time period of the experiment, as compared to growth in broth cultures (data not shown).

We noted that the *E. faecalis* cells appeared to preferentially bind damaged tissue, as seen in **Fig. 15A** (note lower right-hand corner where tissue appears intact and contrast with the rest of the tissue surface). The smooth intact layer of endothelial cells seemed to be denuded, and the underlying matrix from the interior of the valve tissue was exposed; the *E. faecalis* cells were found to bind this denuded tissue. It is not clear whether the damage was induced by the *E. faecalis* cells, or if this damage was caused by the deterioration of the tissue once it had been excised from the porcine host. **Figs. 15B and 15C** display the growing aggregates of bacterial cells, in contrast to the sparsely distributed chains and individual $Asc10^+$ *E. faecalis* cells that were seen bound to the surface after 0.5 h in **Fig. 15A**. At 2 h, groups of *E. faecalis* aggregates were

Figure 15. Scanning electron micrographs of *E. faecalis* Asc10^{+} OG1SSp (pCF10) incubated with heart valve segments for 0.5 h (A), 2 h (B), and 4 h (C), showing noticeable enlargement of bacterial aggregates over time, an observation compatible with biofilm formation. Part A also highlights preferential adherence of *E. faecalis* to areas of noticeable tissue damage, as opposed to areas where the tissue appears more intact (lower right of photograph). Scale bars: A, 1 μ; B, 2 μ; C, 4 μ.

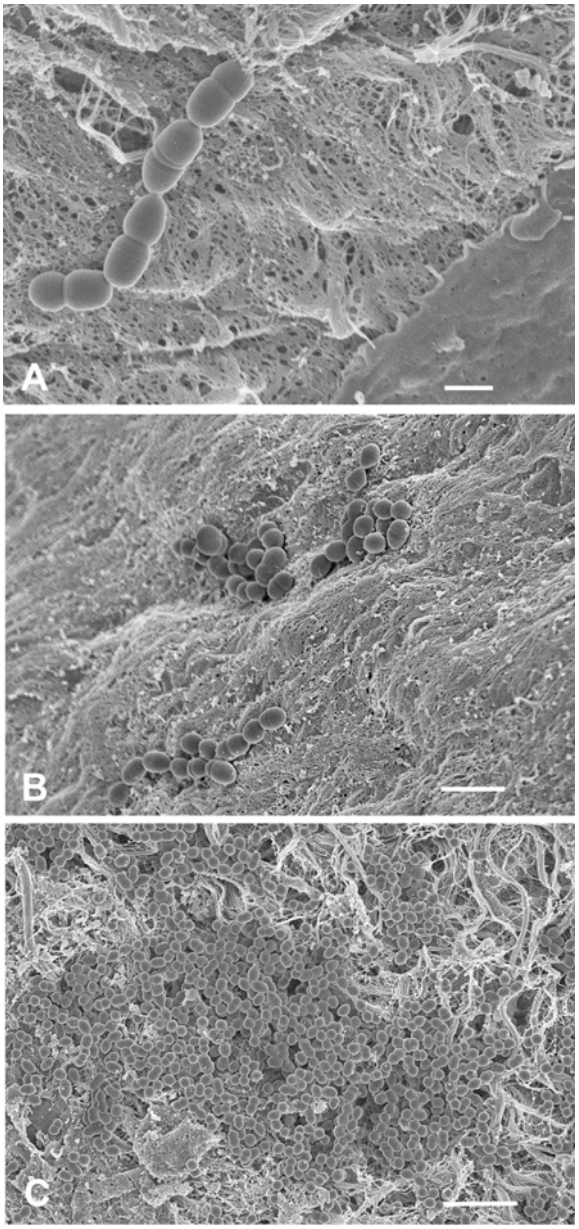

observed more readily across the surface of the valve (**Fig. 15B**), and after 4 h, large microcolonies were found easily on the valve surface (**Fig. 15C**). **Fig. 16** demonstrates the presence of an exopolymeric matrix that appears to form over time; the 0.5 h image (**Fig. 16A**) shows bacterial cells that are relatively smooth, while the cells in the 2 h image (**Fig. 16B**) seem to be connected by stringy material. The formation of large aggregates and exopolymeric material over time is evidence that this *ex vivo* porcine heart valve model will allow for study of biofilm formation and development.

To visualize differences that might be present between the Asc10$^+$ OG1SSp (pCF10) and *prgB* deletion mutant strains, we used SEM analysis to image valve tissue that was infected with either Asc10$^+$ OG1SSp (pCF10) or Asc10$^-$ *prgB* deletion mutant (OG1SSp [pCF10-8]) for 0.5, 1, 2, and 4 h. At 0.5, 1, and 2 h, both the Asc10$^+$ OG1SSp (pCF10) and *prgB* deletion mutant adhered at low numbers, but at fairly similar levels. This was consistent with our valve bacterial adherence results (**Fig. 12**), where we saw comparable levels of adherence between the Asc10$^+$ OG1SSp (pCF10) and mutant at these time points. However, at 4 h, there was a marked difference between the two strains, which again was consistent with the adherence data; the Asc10$^+$ OG1SSp (pCF10) visibly bound at higher numbers than the *prgB* deletion mutant (**Fig. 17**). The WT strain was found in large aggregates spread across large sections of the valve tissue, whereas the *prgB* deletion mutant bound in short chains or single cells sparsely across the surface of the valve. The difference between valve-bound cells of Asc10$^+$ OG1SSp (pCF10) and *prgB* deletion mutant seemed much larger when we imaged the valves than in the adherence assays, but this is due to the large numbers of adherent bacteria at this timepoint in the adherence assays: 2.22×10^7

Figure 16. Scanning electron micrographs of *E. faecalis* Asc10^{+} OG1SSp (pCF10) incubated 0.5 h (A) and 2 h (B) showing typical comparatively smooth appearance of the bacterial surface at early incubation times (A) compared to the fibrillar strands that became more evident over time and appeared to mediate bacterial aggregation (B). Scale bars: A, 0.3 μ; B, 0.5 μ.

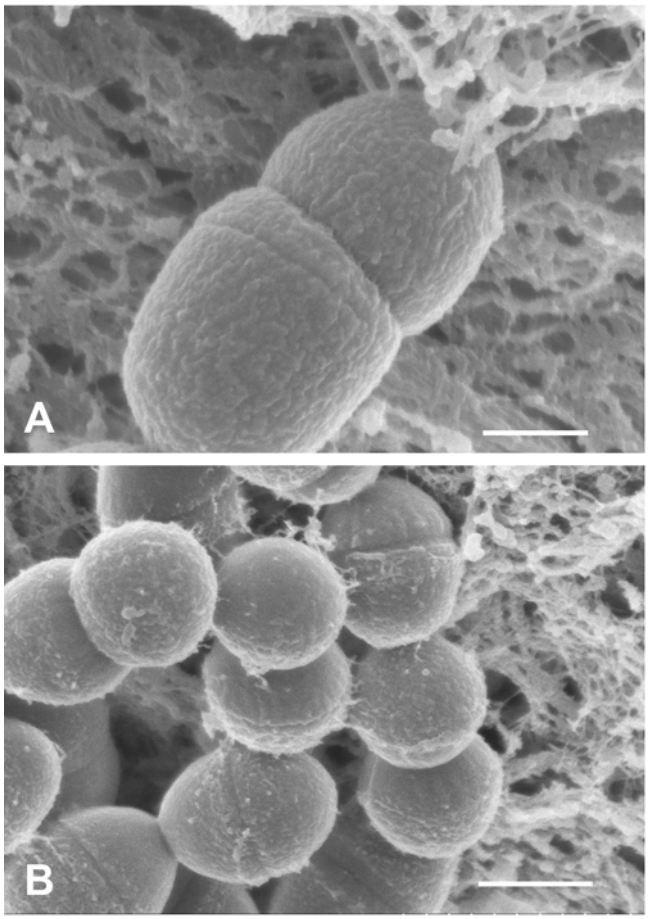

Figure 17. Valve tissue infected with Asc10$^+$ OG1SSp (pCF10) (part A) and Asc10$^-$ *prgB* deletion mutant strains (OG1SSp [pCF10-8]; B), as analyzed by scanning electron microscopy. Note the density of Asc10$^+$ OG1SSp (pCF10) cells colonizing the valve, whereas the *prgB* deletion mutant bound in single cells or short chains; both images were taken at 4 h post-infection. Scale bar: A and B, 3 μ.

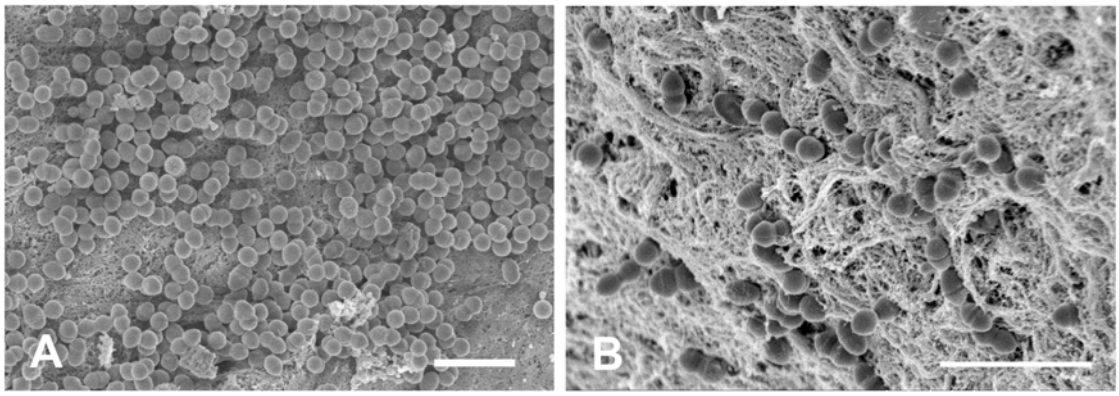

CFU/ml for the Asc10$^+$ OG1SSp (pCF10), and 9.09×10^6 CFU/ml, yielding a difference of 1.31×10^7 CFU/ml. This would be easily seen by SEM.

Because we observed a difference at 4 h in adherent bacteria by SEM between the Asc10$^+$ OG1SSp (pCF10) and Asc10$^-$ *prgB* deletion mutant (OG1SSp [pCF10-8]), we hypothesized that the *prgB* deletion mutant could be defective in biofilm formation. We also observed exopolymeric material (more apparent for Asc10$^+$ OG1SSp (pCF10) strain, **Fig. 16B**), a mark of biofilm formation. This exopolymeric matrix warrants further study with cationic dyes like alcian blue for stabilization, enabling us to better preserve and observe this matrix.

Full-length Asc10 does not mediate adherence to extracellular matrix (ECM) proteins. ECM proteins and glycosaminoglycans (GAGs) are significant components of the valve tissue; they are found in the inner layers between single sheets of endothelial cells. Thus, it is possible that upon infliction of valvular damage, ECM proteins and GAGs could be exposed to serve as a binding substrate for infecting *E. faecalis* cells. Since it was previously shown that Asa1 mediated *E. faecalis* binding to the ECM proteins fibronectin, vitronectin, thrombospondin, and collagen type I (54), Asc10 interactions with these ECM proteins were investigated in this study. Fibrinogen, fibronectin, vitronectin, and von Willebrand factor binding were tested in an ELISA assay, to investigate potential interactions between purified Asc10 protein and these ECM proteins (**Fig. 18**). Asc10 binding above background levels was not observed with the wild-type protein. However, some Asc10 variants such as the N-

Figure 18. Adherence of mutant Asc10 purified proteins to ECM proteins. Bound Asc10 proteins were measured by ELISA, where increasing absorbance represents greater amounts of Asc10 protein adhering to the ECM substrate. **(A)** Asc10 binding to fibrinogen. The N-terminal aggregation domain deletion variant protein (encoded by pCF10-4), but not the wild-type protein, is shown to bind fibrinogen. **(B)** The N-terminal aggregation domain deletion (encoded by pCF10-4) and double aggregation domain variant proteins (encoded by pCF10-5), but not the wild type protein, are able to bind vitronectin. **(C)** The central aggregation domain insertion variant protein (encoded by pCF10-1), but not the wild-type protein, binds von Willebrand factor. Each graph is representative of at least 3 experiments.

Figure 18.

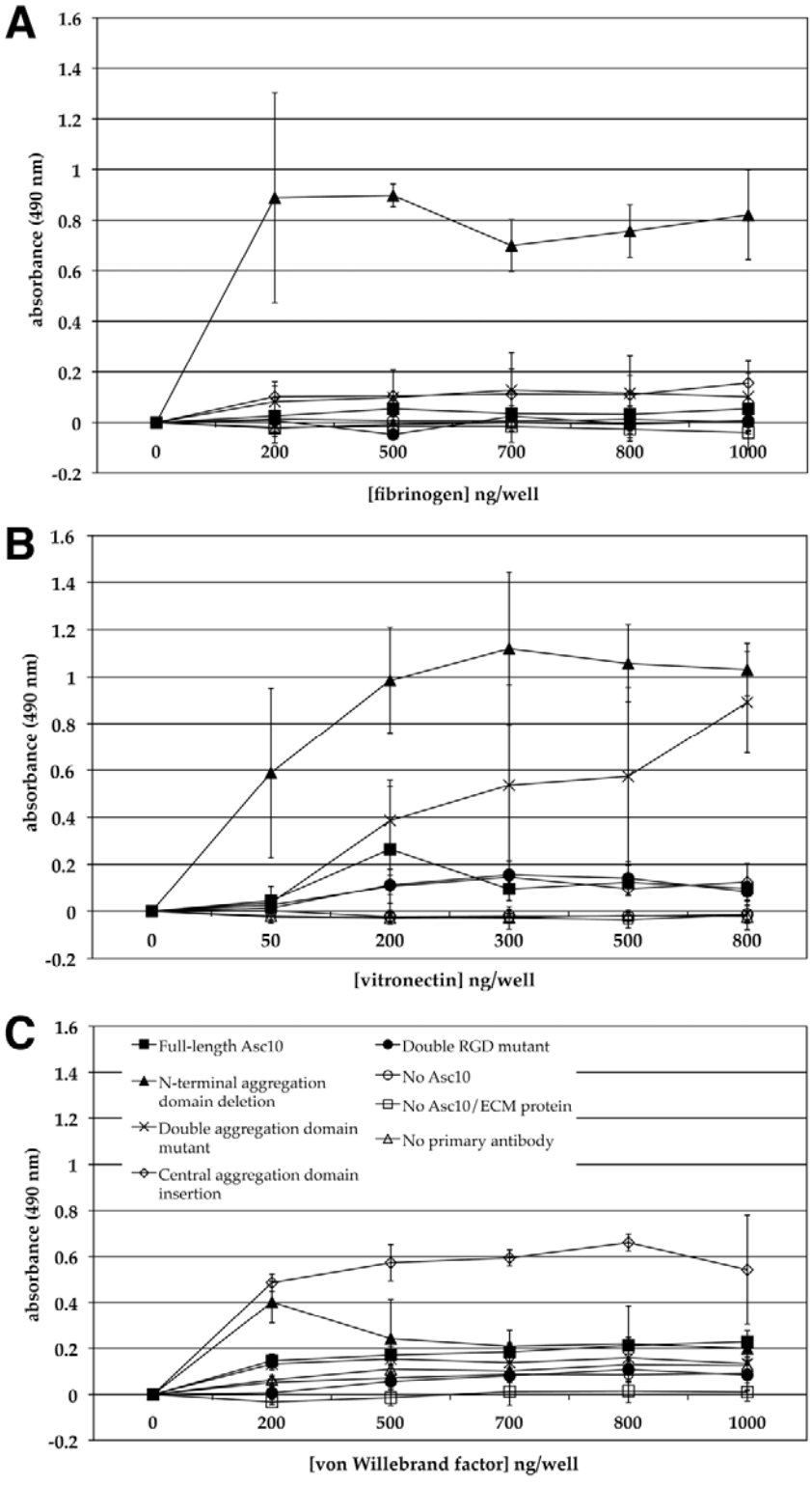
A
absorbance (490 nm)
1.6
1.4
1.2
1
0.8
0.6
0.4
0.2
0
-0.2
0
200
500
700
800
1000
[fibrinogen] ng/well
B
absorbance (490 nm)
0
50
200
300
500
800
[vitronectin] ng/well
C
Full-length Asc10
N-terminal aggregation domain deletion
Double aggregation domain mutant
Central aggregation domain insertion
Double RGD mutant
No Asc10
No Asc10/ECM protein
No primary antibody
absorbance (490 nm)
[von Willebrand factor] ng/well

terminal aggregation domain deletion (shown in **Fig. 2**) were shown to bind at much higher levels than the WT protein to immobilized ECM proteins (**Fig. 18**).

It is possible that the changes in protein structure of the Asc10 variants allowed for binding via a domain masked in the wild-type protein, but it is not known whether such variants could be produced from the full-length protein during *in vivo* growth. Adherence was further tested with *E. faecalis* cells expressing the mutant derivatives of Asc10, and no binding attributable to Asc10 was demonstrated with any of the strains. These cumulative data do not suggest strongly that Asc10 mediates bacterial binding to these ECM proteins *in vivo*.

The GAGs heparan sulfate (HS) and chondroitin sulfate (CS) were investigated for binding to *E. faecalis* cells; CHO cells expressing differing levels of HS and CS were used in uptake assays of $Asc10^{+}$ and $Asc10^{-}$ *E. faecalis* (**Table 2**). **Figure 19 (a) and (b)** illustrate the results from CHO cell uptake of induced and uninduced TX5128 (pMSP7517). We had hypothesized that if Asc10 was mediating binding to GAGs, then an $Asc10^{+}$ strain would show a large decrease in uptake by CHO cells lacking expression of both HS and CSA or by CHO cells that are impaired in sulfate transport, in comparison to the wild-type CHO cell line. In contrast, the uninduced $Asc10^{-}$ strain would be taken up by these three CHO cell lines at similar levels. However, we observed that both uninduced ($Asc10^{-}$) and induced ($Asc10^{+}$) were taken up at lower levels by CHO cells lacking HS and CSA and those without sulfate transport, when compared to the wild-type CHO cell line. Similar results were observed for induced and uninduced OG1SSp (pCF10), where Asc10 is expressed from its native context, on

Figure 19. CHO cell uptake of Asc10$^+$ and Asc10$^-$ *E. faecalis*. **(a)** CHO cell internalization of induced TX5128 (pMSP7517) Asc10$^+$, which expresses *prgB* from a nisin-inducible promoter. CHO cell lines are detailed in **Table 2**; wild-type 70% HS + 30% CS = K1, no HS or CS = CRL-2242, 3x CS, no HS = CRL-2244, no sulfate transport = CRL-2245. HS = heparan sulfate, CS = chondroitin-4-sulfate. **(b)** Same strain as (a), but the *E. faecalis* strain is uninduced, and thus does not express Asc10. **(c)** Wild-type Asc10 is expressed in its native context on the pCF10 plasmid of OG1SSp, with addition of exogenous pheromone. **(d)** Uninduced OG1SSp (pCF10), Asc10$^-$. * denotes a p-value ≤ 0.01 with respect to bacterial uptake by the wild-type CHO cell line (~70% HS + ~30% CS; K1).

Figure 19.

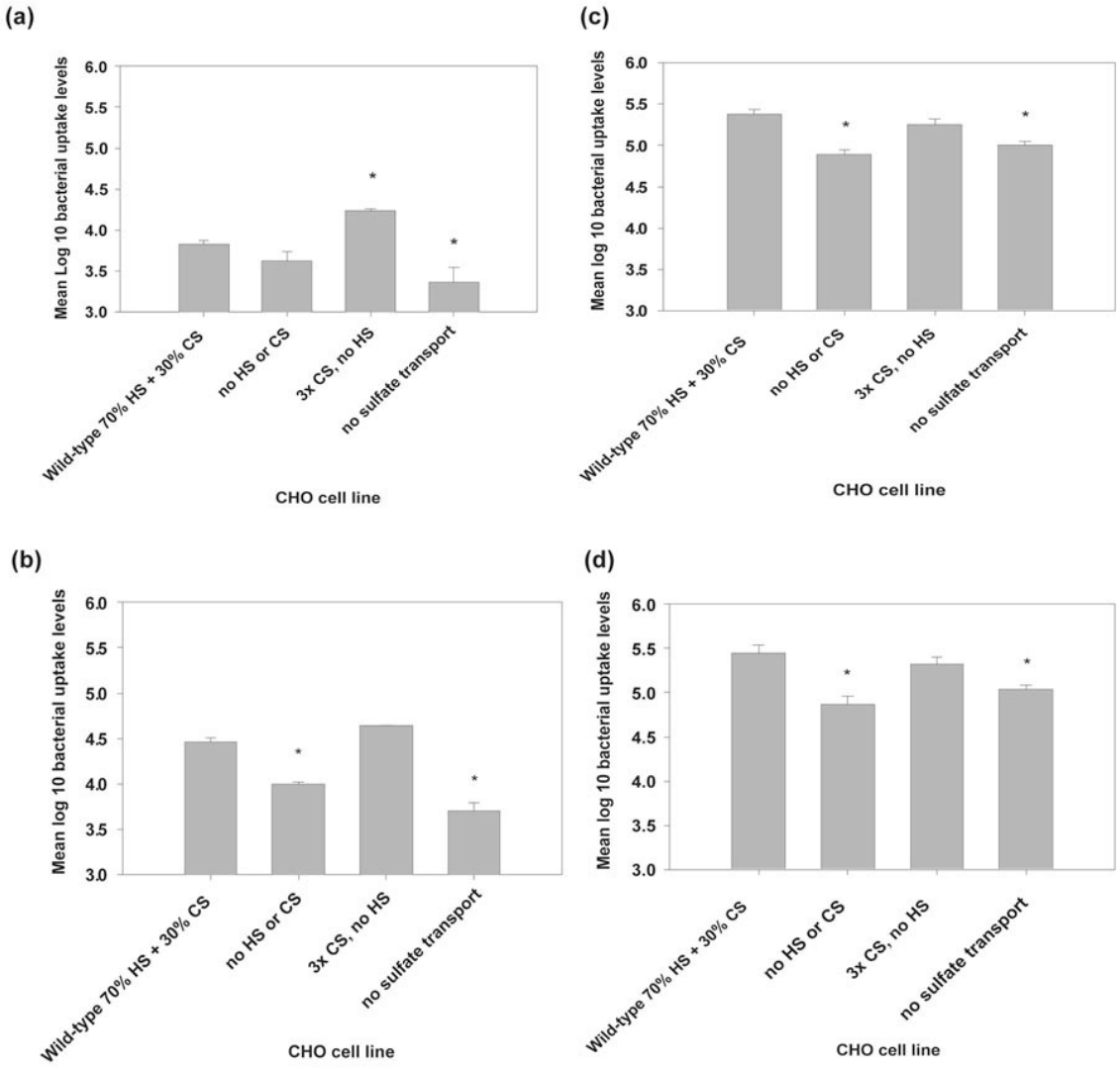
(a)
Mean Log 10 bacterial uptake levels
6.0
5.5
5.0
4.5
4.0
3.5
3.0
*
*
Wild-type 70% HS + 30% CS
no HS or CS
3x CS, no HS
no sulfate transport
CHO cell line
(c)
Mean log 10 bacterial uptake levels
6.0
5.5
5.0
4.5
4.0
3.5
3.0
*
*
Wild-type 70% HS + 30% CS
no HS or CS
3x CS, no HS
no sulfate transport
CHO cell line
(b)
Mean log 10 bacterial uptake levels
6.0
5.5
5.0
4.5
4.0
3.5
3.0
*
*
Wild-type 70% HS + 30% CS
no HS or CS
3x CS, no HS
no sulfate transport
CHO cell line
(d)
Mean log 10 bacterial uptake levels
6.0
5.5
5.0
4.5
4.0
3.5
3.0
*
*
Wild-type 70% HS + 30% CS
no HS or CS
3x CS, no HS
no sulfate transport
CHO cell line

the pCF10 plasmid (**Figure 19 [c] and [d]**). CHO cells expressing three times the amount of CSA, but no HS appeared to take up equal or greater numbers of bacteria in comparison to the wild-type CHO cell line. This could suggest that either the increased expression of CSA compensates for the lack of HS, or that *E. faecalis* does not bind well to HS. In preliminary studies, exogenous CSA added to CHO cells was able to disrupt uptake of Asc10^{+} *E. faecalis* (OG1SSp [pCF10]) in a dose-dependent manner (data not shown). Altogether, these data suggest that an adhesin on the surface of *E. faecalis* is able to mediate binding with HS and CSA, but that this interaction does not involve Asc10. Asc10-independent binding of *E. faecalis* to GAGs could play a role in vegetation formation by Asc10^{-} strains.

Characterization of Asc10 Tn*917* insertion *E. faecalis* mutants

Tn*917* mutants OG1SSp (pCF121) and OG1SSp (pCF175) secrete N-terminal fragments of Asc10. In a previous study (6), a Tn*917* transposon screen was conducted to characterize different antigens expressed from the pCF10 plasmid. pCF121 and pCF175 are two pCF10 derivatives from this study, each carrying a Tn*917* transposon insertion at a different position in the *prgB* gene. Since these insertions had been previously localized only by restriction enzyme digestion, we sequenced the Tn*917*-*prgB* gene junctions. This revealed that the transposon inserted at nucleotide 1409 in pCF121, and nucleotide 1784 in pCF175. As shown in **Figure 20A**, these two strains are unable to clump with addition of pheromone, unlike the wild-type pCF10. s3599 (TX5128 [pCWΩ3599]) is a strain that secretes a variant of Asc10 that encompasses amino acids from the end of the signal sequence to just prior to the LPXTG cell wall anchor motif. This nearly full-length protein is secreted because of the absence of the cell wall anchor, and thus is also unable to clump. As seen in **Fig. 4**, if one of the aggregation domains is deleted or disrupted, the strain is unable to clump. Thus, since OG1SSp (pCF10-6) and (pCF10-7) have deletions or substitutions in other areas than the aggregation domains, these strains maintain clumping ability (**Fig. 20A**). We observed by Western blot (**Fig. 20B)** that both of the Tn*917* insertion mutants (OG1SSp [pCF121] and [pCF175]) are deficient in surface-expressed Asc10 (last 2 lanes of cell wall fraction). However, when we examined the supernatant fractions, we found that both mutants secrete fragments of Asc10. As shown by sequencing, these fragments are from the N-terminal portion of Asc10, and since the Tn*917* transposon inserts upstream of the cell wall anchor, these fragments are secreted. The N-terminal Asc10 fragment

Figure 20. Tn*917* strain characterization by clumping visualization and Western blot analysis. (A) Clumping of Tn*917* (OG1SSp [pCF121] and OG1SSp [pCF175]) strains as compared to Asc10^{+} *E. faecalis* OG1SSp (pCF10). The Tn*917* insertions in OG1SSp (pCF121) and OG1SSp (pCF175) impair the strains' ability to aggregate. In contrast, both the C-terminal domain deletion (OG1SSp [pCF10-6]) and C-terminal RGDV → RADV mutation (OG1SSp [pCF10-7)]) do not affect aggregation. **(B)** Western blot analysis of purified cell wall and supernatant fractions. All strains used in the clumping and Western blot analyses were of an OG1SSp background, except for Ω3599 (also known as pCWΩ3599), which is expressed in TX5128. As previously shown, the bulk of Asc10 produced by Ω3599 is secreted because the Asc10 expressed lacks the cell wall anchor (69). OG1SSp (pCF10) produced mainly a ~175-kDa band, which is larger than the predicted 137-kDa size for Asc10. This may be due to glycosylation or association of LTA with Asc10. The ~98-kDa band produced by OG1SSp (pCF10) corresponds to an N-terminal 78-kDa cleavage product that has been observed previously (26). Arrows indicate the size of the proteins secreted by the Tn*917* insertion mutants.

Figure 20.

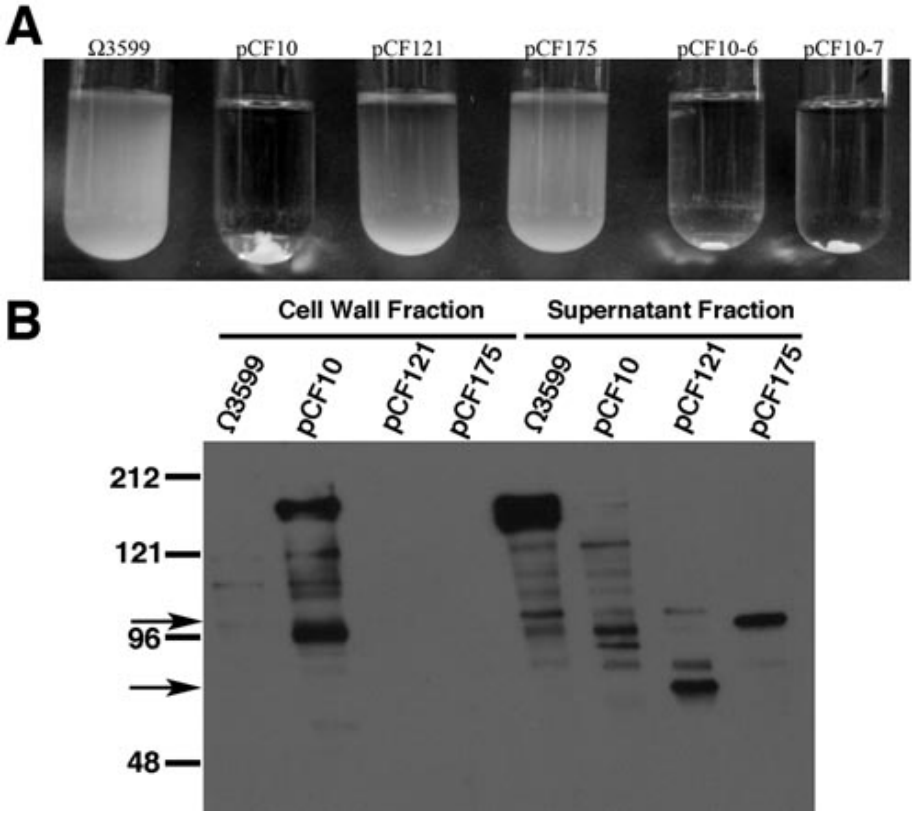
A
Ω3599
pCF10
pCF121
pCF175
pCF10-6
pCF10-7
B
Cell Wall Fraction
Supernatant Fraction
Ω3599
pCF10
pCF121
pCF175
Ω3599
pCF10
pCF121
pCF175
212
121
96
48

secreted from OG1SSp (pCF121) includes the N-terminal LTA-binding aggregation domain (**Figure 4**; ~75 kDa, 469 aa from Asc10 expressed), but most of the remainder of the protein is no longer expressed. From OG1SSp (pCF175), a larger N-terminal fragment is secreted (~100 kDa, 569 aa from Asc10 expressed), encompassing the N-terminal aggregation domain, and a portion of the central aggregation domain. However, neither strain produced an Asc10 fragment that contains the RGD motifs.

Genes downstream of *prgB* are not affected by the Tn*917* transposon insertions. To ensure that no polar effects on genes downstream of *prgB* due to the transposon insertions, we performed both filter and broth matings. Many of the downstream genes on pCF10 encode for the conjugation machinery necessary for transfer of plasmids between donor and recipient cells. We mated the strains listed in **Table 6** with OG1RF, which served as the recipient. The table displays the frequency of plasmid transfer of pCF10, pCF121, and pCF175 plasmids into OG1RF, expressed as transconjugants per donor. We observed low frequencies of transfer for the Tn*917* insertion mutants OG1SSp (pCF121) and (pCF175) as compared to OG1SSp (pCF10) in the broth mating, but higher frequencies for the Tn*917* insertion mutants in the filter mating. This indicates that since the Tn*917* insertion mutants are not able to express surface Asc10, in broth they cannot mediate aggregation with the recipient OG1RF cells, and thus conjugation frequencies are low. However, in the filter matings, the donor and recipient cells are placed in direct contact with one another, and surface expression of Asc10 is not necessary to bring the donor and recipients together for formation of the mating

Table 6. Tn*917* strain filter and broth mating frequencies.

***E. faecalis* Strain**	**Filter Mating transconjugants/donor (frequency)**	**Broth Mating transconjugants/donor (frequency)**
OG1SSp (pCF10)	9.29×10^{-2}	9.86×10^{-6}
Tn*917* insertion OG1SSp (pCF121)	1.25×10^{-2}	3.57×10^{-8} [a]
Tn*917* insertion OG1SSp (pCF175)	3.38×10^{-3}	2.50×10^{-7}

[a] Minimum level of detection for assay; there were no transconjugants that were observed on the agar plates.

channel. Since plasmid transfer is still able to take place in the filter matings, this suggests that the remainder of the conjugation machinery is still expressed. In addition, these results strongly imply that the only pCF10-encoded protein whose expression was altered by the transposon insertion was Asc10.

Characterization of Tn*917* insertion mutants in the rabbit endocarditis model. We also tested these Tn*917* insertion mutants in the rabbit endocarditis model to determine the role of the secreted N-terminal fragments of Asc10 in the disease progression. Interestingly, vegetation bacterial loads for the Tn*917* insertion mutant OG1SSp (pCF175) remained at the same level as the plasmid-free OG1SSp strain, but about one log ($1/10^{th}$) below $Asc10^{+}$ OG1SSp (pCF10) (**Figure 21**). The Tn*917* insertion mutant OG1SSp (pCF121) had vegetation bacterial loads that were $1/100^{th}$ of the plasmid-free OG1SSp strain, but $1/1000^{th}$ $Asc10^{+}$ OG1SSp (pCF10). These results suggest that the Asc10 fragments expressed from pCF121 and pCF175 still are able to enhance *E. faecalis* virulence in endocarditis, as both of these strains induced bacterial loads higher than the *prgB* deletion mutant. However, the pCF175-expressed Asc10 fragment includes a portion of the central aggregation domain that is absent in the pCF121 fragment. Because the vegetation loads are higher for OG1SSp (pCF175), this central aggregation domain fragment appears to aid *E. faecalis* in better colonizing the vegetation.

Colonization of porcine heart valves is not impaired for the Tn*917* insertion mutant OG1SSp (pCF175) at early timepoints. As shown in **Figure 22**, the Tn*917* insertion mutant OG1SSp (pCF175) binds as well as $Asc10^{+}$ OG1SSp (pCF10) to

Figure 21. Vegetation bacterial loads of Tn*917* insertion mutants OG1SSp (pCF121) and OG1SSp (pCF175) in the rabbit endocarditis model, expressed as log-transformed total CFUs values. Dashed line indicates minimal level of detection at 0.70, and * denotes $p \leq 0.01$, as compared to the Asc10$^+$ OG1SSp (pCF10) strain.

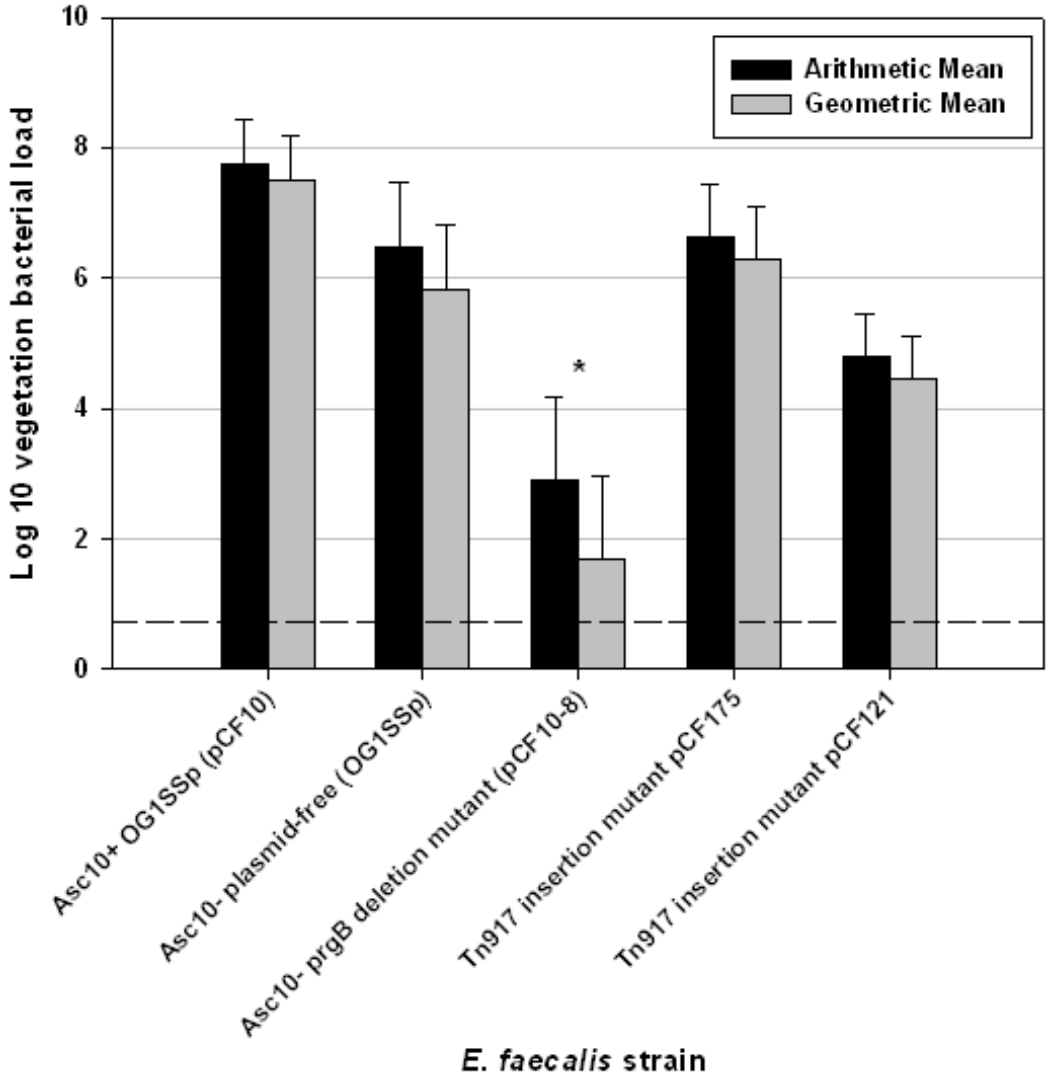

Figure 22. Adherence of Tn*917* insertion mutant OG1SSp (pCF175) to porcine heart valve tissue as compared to Asc10^{+} OG1SSp (pCF10). The data shown are a compilation of at least nine experiments.

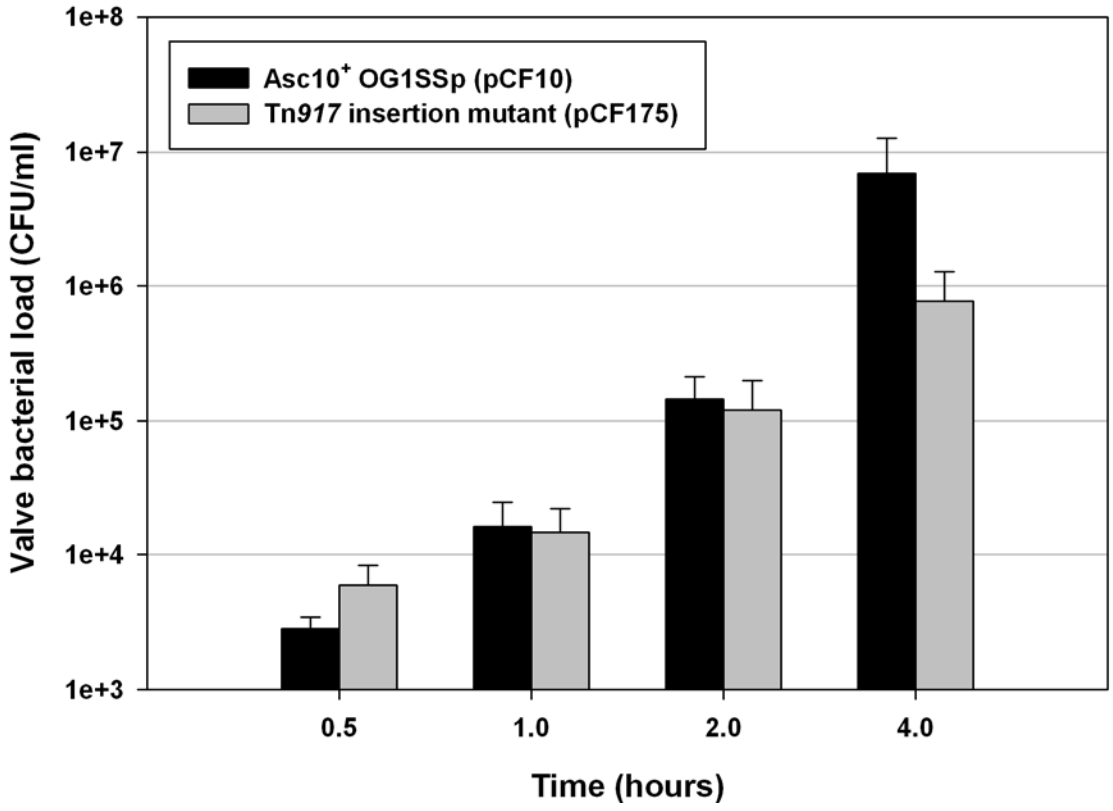

porcine heart valves at 0.5, 1, and 2 h. At 4 h, however, fewer OG1SSp (pCF175) cells adhere to the valve tissue than Asc10^{+} OG1SSp (pCF10), or the Asc10^{+} OG1SSp (pCF10) could be adhering at a much higher rate than OG1SSp (pCF175) between 2 and 4 h. These results suggest that the Asc10 fragment expressed from pCF175 mediates binding to the valve tissue, though the interaction may not be as strong as with full-length Asc10.

DISCUSSION

Role of multiple Asc10 functional domains in *E. faecalis* endocarditis virulence

Asc10 domains involved in the endocarditis disease process have not been previously characterized, which served as the main motivation for this study. Past studies have indicated that Asc10$^+$ *E. faecalis* is able to induce large vegetations in New Zealand white rabbits (25), although smaller vegetations were still found in Asc10$^-$ plasmid-free (OG1SSp) *E. faecalis*-infected animals. Hirt *et al.* (25) observed a larger difference in vegetation weights produced from infection with a strain carrying pCF10 versus a plasmid-free strain than in this study. These workers also examined isogenic strains carrying pCF10, pCF121, or no plasmid, and used vegetation weights as the indicator of virulence, but did not find significant differences in vegetation bacterial loads (25). In the current study we examined a larger number of strains, including those tested previously (25) and a *prgB* deletion mutant. Although the infected hearts in this study with larger vegetations generally contained higher bacterial loads (**Fig. 7**), there was not a quantitative correlation between vegetation weights and bacterial loads. Nevertheless, our present data is in general agreement with the previous report (25), as the pCF10-containing strain in both studies induced larger vegetations and bacterial loads than the Asc10$^-$ strains. In the case of the pCF10-containing strain, all the infected hearts contained bacterial loads greater than 10^6 CFU/g, while numerous rabbits infected with the *prgB* deletion mutant and several other *prgB* mutants contained $< 10^4$ CFU/g (**Fig. 9B**). The smaller vegetations observed by Hirt *et al.* (25) in rabbits infected with a plasmid-free strain could result from the fact that the animals in the present study were younger and smaller, or that we used outbred rabbits, which might

show variability in susceptibility to these infections. Furthermore, these experiments only examined a single endpoint in assessing virulence, and it is possible that some of the animals with high bacterial counts but small or no vegetations might have developed vegetations if examined after longer periods of time.

This is the first time a complete in-frame *prgB* deletion mutant has been employed in the rabbit endocarditis model, and this mutant was dramatically decreased in vegetation weight and bacterial load in comparison to the strain carrying pCF10. The fact that a pCF10 derivative carrying a *prgB* null allele was much less virulent than a plasmid-free strain suggests that the carriage of the pCF10 plasmid may suppress expression of other chromosomally-encoded adhesins, or that abundant expression of Asc10 or other surface proteins encoded by pCF10, such as Sec10 (encoded by *prgA* on the pCF10 plasmid; involved in preventing donor cell aggregation), could mask the exposure of surface adhesins encoded by the chromosome or other proteins that could contribute to vegetation formation and share functional redundancy with Asc10. In view of the fact that abundant expression of Asc10 and Sec10 can essentially coat the entire cell surface (44), it is quite conceivable that cells carrying pCF10 variants expressing either no Asc10 or defective Asc10 could be less virulent than plasmid-free cells. This was confirmed by cryo-SEM evaluation of $Asc10^{+}$ $Sec10^{+}$ OG1SSp (pINY1801), a technique that better preserves the bacterial cell for microscopic analysis. These images revealed widespread expression of Asc10 and Sec10 on the *E. faecalis* surface, compared to the relatively smooth appearance of $Asc10^{-}$ $Sec10^{-}$ OG1SSp (pWM401) (**Fig. 23**). Further experimentation is required to evaluate this possibility.

Figure 23. Abundant expression of Asc10 (larger globular mass; green arrow) and Sec10 (smaller helical shape; red arrow) on the surface of OG1SSp (pINY1801), as visualized by field-emission SEM of cryofixed and partially dried *E. faecalis* cells. The right-hand panel demonstrates this abundant expression by the white-colored knobby material on the *E. faecalis* cell. The left-hand panel is an Asc10$^-$ Sec10$^-$ OG1SSp (pWM401) cell, displaying a relatively smooth surface, and the absence of Asc10 expression. Scale bars: A and B, 100 nm. Images taken and prepared by Stanley Erlandsen.

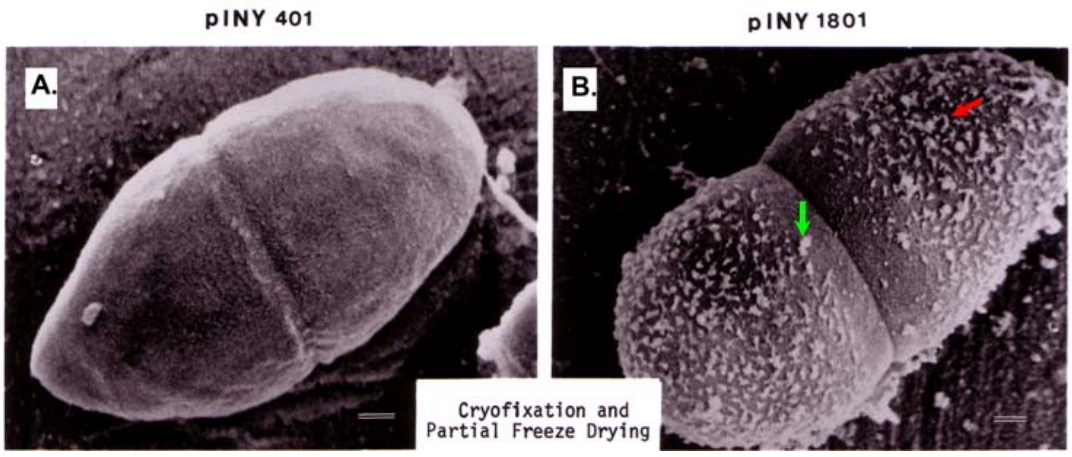

In a previous functional analysis of Asc10, the protein was expressed from cloned *prgB* alleles using a nisin-inducible expression system (69). Preliminary unpublished experiments suggested that the plasmid vector used previously might be unstable during experimental infections, so in this study we used a recently developed allelic exchange system (32) to move mutant alleles back into the native context within pCF10, where strong *in vivo* induction of *prgB* expression during *in vivo* growth has been demonstrated (3, 25). Western blot analysis of the strains used for these studies indicated that all of the Asc10 variants used in these experiments were expressed at similar levels and retained significant stability to be detected readily (**Fig. 5**); also, all of the mutations outside of the previously identified aggregation domains retained bacterial aggregation functions, suggesting that the overall structure of the protein was intact in most cases. We cannot completely rule out that some of the phenotypic effects of the mutations tested could result from reduced protein stability *in vivo*. However, we note that the large deletion associated with pCF10-6 had no effects on virulence, whereas point mutations resulting in RGD → RAD changes, which could be considered the most subtle changes made in the protein, had the greatest effects on virulence. Therefore we believe that most of the phenotypic changes observed result from disruption of specific functional domains rather than gross, nonspecific alterations in protein stability.

The simplest explanation for the cumulative results of this study is that two different functional domains of Asc10 affect the virulence of the *E. faecalis* bacterium in the host during experimental endocarditis (**Fig. 24**). Disruption of the previously identified N-

Figure 24. Proposed functions of Asc10 protein domains.

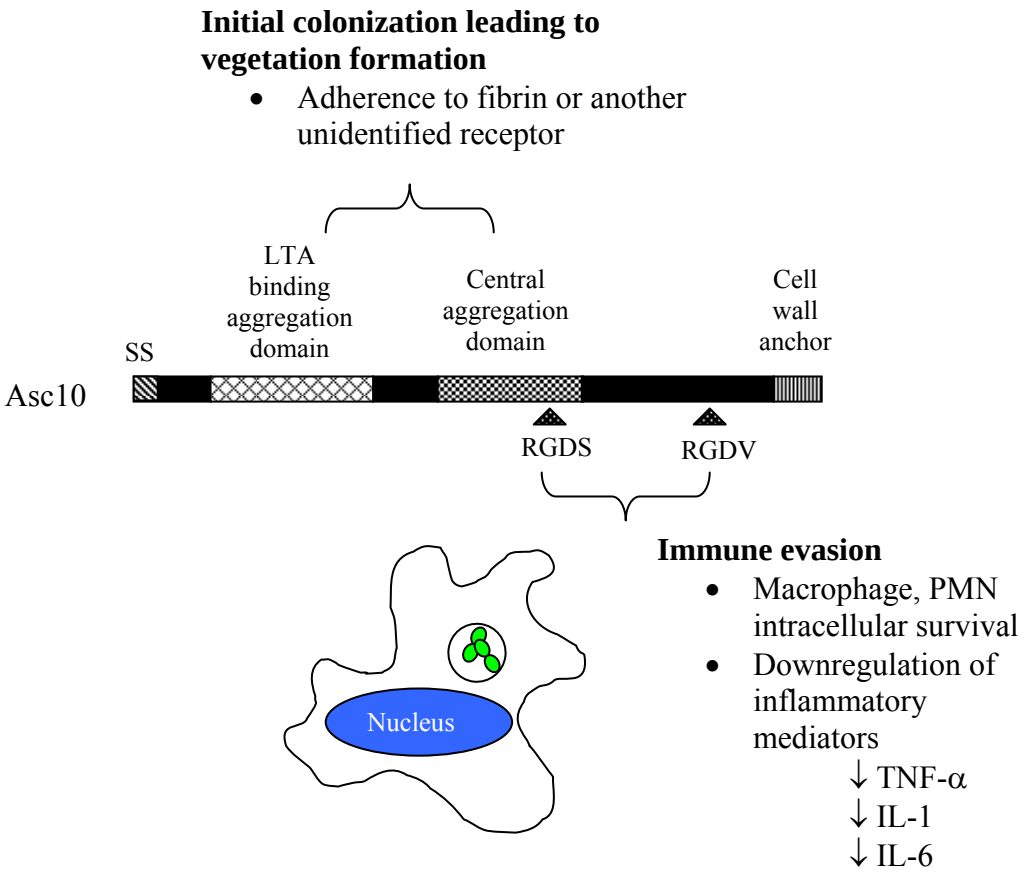

terminal and central domains involved in bacterial aggregation and cell wall LTA binding had a significant effect on virulence in these studies. Previous results suggested that Asc10 mediates binding to fibrin, and our attempts to identify Asc10-mediated binding activities to other host receptors (ECM proteins and GAGs) (**Figs. 18 and 19**) did not reveal any additional ligands for Asc10 binding. The porcine cardiac valve *ex vivo* studies suggest the involvement of the aggregation domains in attachment to endocardiac tissue, presumably using either fibrin or a thus-far unidentified receptor. Thus it appears that the contribution of the aggregation domains to virulence in experimental endocarditis involves initial attachment to host tissues.

We think that the RGD motifs are involved in a second, independent function that enhances virulence. The mechanistic nature of this function is currently unknown, though our group has previously shown that these motifs are not involved in adherence and internalization of $Asc10^{+}$ *E. faecalis* by intestinal epithelial cells (70, 71). However, there is previous evidence that the RGD motifs have a role in Asc10-mediated resistance to killing following ingestion of bacteria by PMNs, even though Asc10-expressing bacteria may attach more efficiently to the PMN surface (50). Vanek *et al.* (65) demonstrated that Asc10 mediated *E. faecalis* binding through CR3 expressed on the surface of PMNs, in cooperation with an $\alpha_5\beta_3$/IAP complex. CR3-mediated binding by bacteria has been shown to be an opsonin-independent pathway that blocks release of respiratory burst molecules (75). It is possible that the Asc10 protein RGD motifs are used to bind the CR3 receptor on phagocytes to evade the respiratory burst response.

From our studies regarding the host response to infection, we have found an Asc10-mediated suppression of expression of host immune function genes in experimental endocarditis, and it may be speculated that the effects of the RGD mutations observed in the present study relate to a role of these motifs in suppression of the initial host response to infection of the cardiac tissue. These motifs may also somehow promote the anti-inflammatory environment that is seen in Asc10$^+$ *E. faecalis*-infected rabbits (**Table 3, Fig. 10**). As these motifs mediate binding to PMNs or other professional phagocytes, it is possible that by increasing opportunities for Asc10$^+$ *E. faecalis* to become enclosed in phagosomes, the bacteria are better able to interfere with the phagocyte's normal ability to kill the invading organisms. Once intracellular, Asc10$^+$ *E. faecalis* may block expression of inflammatory cytokines such as TNF-α, IL-1β, and IL-6.

The possibility of Asc10 possessing immunomodulatory properties was also suggested in a previous study by Schlievert *et al.* (58). The dual-function model for Asc10 in virulence could account for the fact that some of the mutants were less virulent than a plasmid-free strain. If a mutant retained the ability to attach to phagocytes, but lost the ability to protect the bacterium from phagocytic killing, the mutant would be less virulent than a strain not expressing Asc10. Alternatively, expression of an Asc10 variant could reduce or mask surface expression of another chromosomally-encoded surface virulence factor such as the Ace protein (52), without providing a positive contribution to virulence (**Fig. 23**).

Anti-Asc10 Fab fragments lessen severity of Asc10$^+$ *E. faecalis* endocarditis

A previous study (37) demonstrated that immunization with whole antibodies against the N-terminal domain of Asc10 did not protect rabbits against endocarditis disease. Several explanations were given to explain why this immunization approach was not successful (as discussed in the Introduction); our data demonstrate that it was most likely that the antibodies against this N-terminal fragment of Asc10 were increasing aggregation events between the Asc10$^+$ *E. faecalis* cells. As shown in **Fig. 11**, antibodies against full-length Asc10 exacerbated aggregation of cells, and large clumps were found in the Asc10$^+$ *E. faecalis* OG1SSp (pINY1801) culture. A dominant epitope recognized by these antibodies should be in the N-terminal region of Asc10, as other studies have shown that antibodies directed against the N-terminal region of Asc10 are able to recognize surface-expressed Asc10 (26, 37). Increased aggregation of Asc10$^+$ *E. faecalis* would lead to more severe pneumonia and larger vegetations, as observed in rabbits that were actively immunized with Asc10$^+$ *E. faecalis* (OG1SSp [pINY1801]). Thus, since the antigen binding arms are not linked in Fab fragments, the increased aggregation between *E. faecalis* cells can be abolished. From **Fig. 11**, it appeared that the Fab fragments were able to neutralize the majority of Asc10 expressed on the *E. faecalis* cells, because most of the visible aggregation was eliminated.

Our results from the host response microarray studies indicate that the presence of Asc10 appears to dampen the inflammatory response that would normally take place against *E. faecalis*. When rabbits were infected with Asc10$^-$ *E. faecalis* (OG1SSp [pWM401]), a more robust immune response was mounted, with significant mRNA up-

regulation of inflammatory molecules. MHC class II molecules and T cell receptor-α are known to increase in expression during inflammatory responses. The TNF-α induced protein 3 is an anti-apoptotic zinc finger protein; TNF-α induced protein 6 binds glycosaminoglycans such as hyaluronan, and is expressed abundantly under inflammatory conditions (40, 67). These data provide more evidence that Asc10 is involved in immune modulatory functions, as has been observed Vanek and Rakita *et al.* (50, 65). It is possible that as the RGD motifs of Asc10 mediate increased interactions with phagocytes, more Asc10-expressing *E. faecalis* enter phagosomes and can alter the phagosomal compartment, and also interfere with the phagocyte's signaling pathways. A 78-kDa N-terminal cleavage fragment of Asc10 has been found to be released from the surface of *E. faecalis* (26), and this fragment could be interacting with phagocyte cell factors, resulting in downregulation of inflammatory responses. Ultimately, recruitment of other immune mediators such as $CD4^+$ and $CD8^+$ T cells would be impeded, and cytokine release decreased. In addition, the microarray data support a model of vegetation formation that involves two pathways; the first in the absence of Asc10, where an extensive inflammatory response arises, and smaller vegetations result. The second pathway takes place with the presence of Asc10, and the inflammatory response seen in the first pathway is now reduced, and the vegetations are significantly larger. It is possible that the smaller vegetations observed in rabbits infected with $Asc10^-$ *E. faecalis* (OG1SSp [pWM401]) are a result of a more severe immune response; however, this will require further experimentation.

Our studies suggest that Fab fragment immunization is an effective method of controlling $Asc10^+$ *E. faecalis* infectious endocarditis. It is plausible that this technique

could be applied to other surface adhesins that induce aggregation, in bacteria that also cause endocarditis. In *S. aureus*, a family of adhesins known as microbial surface components recognizing adhesive matrix molecules (MSCRAMMs) can mediate aggregation (47), and could be targeted with the use of Fab fragments or drugs that block activity of the adhesins.

Ex vivo porcine cardiac valve model: Implications for Asc10 functional domains and use as a biofilm formation model

We have utilized the porcine heart valve model as a means to examine development of endocarditis, focused mainly on initial bacterial adherence to valve tissue. Additionally, we have been able to observe the formation of Asc10$^+$ *E. faecalis* biofilms on this surface, which will shed light on development of the vegetation, a biofilm in itself. The porcine heart valve *ex vivo* model is less complex than the rabbit model of endocarditis that we have long utilized in our laboratory (7, 25, 37, 38, 58). The simplicity of the porcine model allows us to isolate the initial stages of vegetation formation that would not be as easily done in the rabbit model; one porcine heart is used per experiment, with the different *E. faecalis* strains infecting valves from the same animal. However, in the rabbit model, each strain infects a different rabbit, which could produce more variation due to differences in each rabbit's health. More experiments can also be performed in a shorter amount of time, since the rabbit model requires a large amount of surgical work and precision for isolation of the carotid artery and catheter placement. It is likely that the porcine valve model could be testing the alternative model of endocarditis pathogenesis, where an undamaged native valve becomes diseased. However, this is difficult to determine, because in our SEM studies of *E. faecalis* adherence to valve

tissue, the bacteria preferred to bind damaged tissue. It is possible though that the *E. faecalis* cells could inflict damage on the valve tissue before binding. The porcine valve model does have its disadvantages though; the intense shear forces of blood being pumped through the valves of the heart *in vivo* cannot be imitated with a rocker. Also, the porcine heart valve model lacks access to an extensive immune response, aside from the endothelial and interstitial cells that are present in the valve tissue.

Despite these advantages and disadvantages of the porcine heart valve model, this model still tests the ability of *E. faecalis* to bind valve tissue, an event that occurs during endocarditis vegetation formation. The results that we obtained support our hypothesis that Asc10 contributes mainly to persistence of Asc10$^+$ *E. faecalis,* which could be due to its role in host immune evasion. We observed that most of the strains expressing Asc10 variants were unable to colonize the heart valves as well as the Asc10$^+$ OG1SSp (pCF10) strain during later timepoints (4 h). However, the aggregation domains of Asc10 appear to play the largest role in mediating *E. faecalis* valve adherence, as the aggregation domain mutants were impaired at more than one timepoint. These data suggest that another adhesin(s) could be mediating the initial binding to valve tissue, and Asc10 plays its main role in persistence by strengthening the binding between the *E. faecalis* cells and valve tissue later in the colonization process. The aggregation domains still contribute to initial Asc10-mediated *E. faecalis* binding, but Asc10 may cooperate with other adhesins during first contact with the valve tissue. The RGD motifs have more importance in promoting persistence of *E. faecalis*, consistent with our endocarditis results (7).

Interestingly, though several of our Asc10 mutant strains displayed deficiencies in valve binding, the *prgB* deletion mutant bound at levels comparable to Asc10$^+$ OG1SSp (pCF10) at most timepoints, except at 4 h. At 4 h, there was a decrease in the *prgB* deletion mutant's ability to bind to the valve tissue, though this difference between the mutant and Asc10$^+$ OG1SSp (pCF10) was not as large as the other mutants. To explain the apparent inconsistency between the greater deficiency of strains expressing Asc10 variants (aggregation domains and RGD motifs) than the strain without Asc10 (*prgB* deletion mutant), we propose two potential pathways of biofilm formation (**Fig. 24**).

In the first pathway shown in **Fig. 24A**, biofilm formation can occur independent of Asc10, as we have observed that Asc10$^-$ plasmid-free OG1SSp is able to induce formation of vegetations in endocarditis, though the vegetation bacterial load was still less than the Asc10$^+$ OG1SSp (pCF10) strain. Adhesins such as Ebp, Esp, and Ace are able to mediate *E. faecalis* binding to the valve surface, where increased adherence of bacteria to the valve surface, replication of valve-attached bacteria, and exopolymeric matrix formation contribute to biofilm formation. Additionally, the absence of Asc10 in the *prgB* deletion mutant could allow for increased expression of other adhesins such as enterococcal surface protein (Esp), adhesin of collagen from *E. faecalis* (Ace), endocarditis and biofilm-associated pili (Ebp), and others. These adhesins would be able to compensate for the loss of Asc10 and mediate binding to valve tissue, since we observed comparable valve binding for the *prgB* deletion mutant (OG1SSp [pCF10-8]) as compared to Asc10$^+$ OG1SSp (pCF10) at most timepoints.

Figure 25. Asc10-independent and -dependent biofilm formation models.

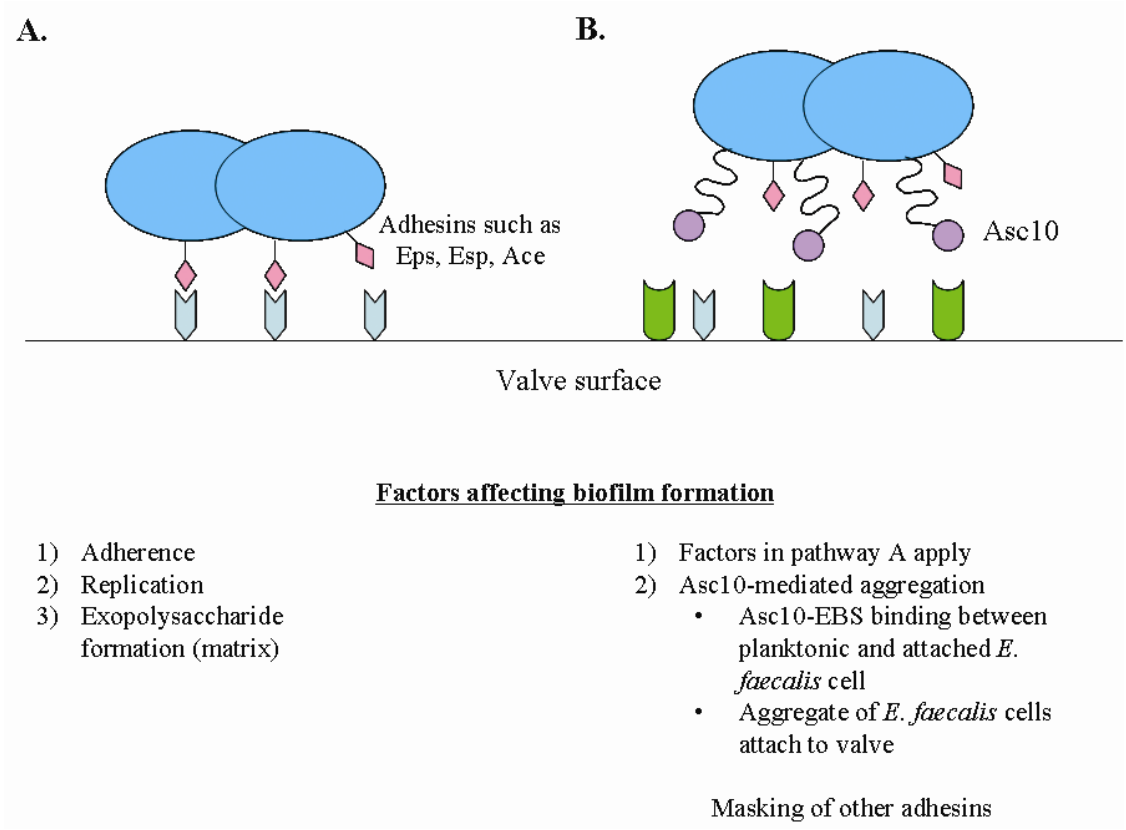

In an Asc10-dependent pathway of biofilm formation, **Fig. 24B** illustrates that Asc10 expression could mask the presence of other adhesins, preventing them from binding their ligand on the valve surface. All of the factors contributing to the Asc10-independent pathway of biofilm formation apply in this case. Additionally, Asc10-mediated aggregation further accelerates formation of the biofilm through two ways: (1) Asc10-EBS binding between cells attached to the valve and planktonic cells, and (2) attachment of Asc10-expressing *E. faecalis* cell aggregates to the valve tissue. The presence of an altered Asc10 protein could more severely impair the ability of *E. faecalis* to bind valve tissue, where the altered Asc10 protein might not be able to mediate binding to the valve tissue ligand, or the binding interaction is weak. Because the other adhesins are still masked by this variant Asc10, they are still not able to interact with the valve surface. We have observed abundant expression of Asc10 on the *E. faecalis* cell surface, supporting our hypothesis that Asc10 (variant or wild-type) could mask other adhesins (44). Alternately, Asc10 could be acting in cooperation with other adhesins, strengthening the binding interaction between the *E. faecalis* cell and valve surface.

The results from our ECM protein studies appear to conflict with data from another study examining the interaction of ECM proteins and Aggregation Substance protein. Their study found that Aggregation Substance was able to mediate interactions with ECM proteins (54). However, a different background strain was used (OG1X instead of OG1RF), and the Aggregation Substance protein examined was Asa1. Asa1 shares 90% identity with Asc10, excluding a variable region where the identity is only 30-40%; it is possible that the variable domain of Asa1 mediates interaction with the

ECM. In our studies, we utilized a background strain (TX5128), which does not express the gelatinase or serine proteases and which facilitates purification of full-length protein; these proteases in a wild-type strain may process the Asc10 protein, resulting in exposure of ECM-binding domains. These issues remain unresolved, but merit further study.

As a model for biofilm formation, the porcine heart valve tissue served as a physiologically relevant scaffold. We observed growing microcolonies of bacteria over time, and the presence of exopolymeric matrix that increased with passing time as well. In the future, we will be able to use this valve tissue model as a way to examine the ultrastructure of biofilms through SEM, in addition to determining whether other genes might be involved in biofilm formation. Our results appear to support the hypothesis that *E. faecalis* could bind native, undamaged valves to initiate vegetation formation, as seen in some clinical cases. However, it is difficult to know whether the damage that we observed on the porcine heart valves was inflicted by the Asc10-expressing *E. faecalis* cells, or simply from the tissue deteriorating over time. In addition, the valves could be damaged from valve aberrancies present in the pig before sacrifice. Future studies will need to be conducted to examine the ability of Asc10$^+$ *E. faecalis* to interact with endothelial cells. If Asc10 can promote *E. faecalis* uptake by endothelial cells, it is possible that this is the mechanism by which *E. faecalis* could stimulate vegetation formation in patients without past histories of valve abnormalities.

The mechanisms detailed in **Fig. 24B** detailing how Asc10 accelerates biofilm formation could complicate the porcine valve adherence assay. This is due to the difficulty in determining whether the increase in Asc10$^+$ OG1SSp (pCF10) cells

adherent to the valve tissue is because of an increasing number of individual cells that are adhering to the tissue, or if several cells bind and other cells bind those through Asc10 interactions. However, this Asc10-mediated binding between bacterial cells could serve as a mechanism to more quickly increase the biomass of the biofilm. In addition, once more cells are in the microcolony, this could stimulate production of exopolymeric matrix, a major marker of biofilm formation. Thus, blocking Asc10 function could decrease the rate of biofilm formation, and in combination with other antimicrobial treatments, increase the likelihood that the infection could be cleared from the patient.

Asc10 fragment secreted from Tn*917* mutants functional during endocarditis

The Tn*917* mutants were originally thought to be null mutants of *prgB,* unable to express Asc10. OG1SSp (pCF121) was used in the Hirt *et al.* endocarditis study as an Asc10$^-$ mutant (25), and though the vegetation weight of this Tn*917* insertion mutant was as low as the plasmid-free strain OG1SSp (contrary to the high vegetation bacterial loads we observed for the Tn*917* insertion mutants), we found in our current endocarditis studies that vegetation weight does not necessarily correlate with vegetation bacterial load (**Fig. 7**). Also, as explained in the endocarditis discussion section, outbred rabbits were used in the previous and in our current study, which could show variation in susceptibility to endocarditis. However, in further characterization of the Tn*917* mutants OG1SSp (pCF121) and (pCF175), we confirmed that surface-expressed Asc10 was absent as seen before (6), but discovered that an N-terminal fragment was secreted from both strains. Interestingly, the Asc10 fragments appear to mediate functions in both the rabbit endocarditis and *ex vivo* porcine cardiac valve

models, as the Tn*917* insertion strains maintained higher bacterial loads in vegetations than the other Asc10 variant strains (**Figs. 8 and 21**). OG1SSp (pCF175) in particular was more effective in colonizing the vegetation than OG1SSp (pCF121) (**Fig. 21**), presumably due to secretion of a larger N-terminal Asc10 fragment, as displayed in **Figures 4 and 20B**. From these data, we speculate that the segment of the central aggregation domain that is included in the pCF175-expressed Asc10 fragment and not in the fragment from pCF121 is important in promoting higher colonization levels of *E. faecalis* in the vegetation. Because these fragments are secreted, it is possible that the N-terminal Asc10 fragment binds to the damaged tissue through interactions with fibrin or another ECM protein, and that through cell-surface LTA, the *E. faecalis* cells are able to bind these free-binding Asc10 fragments via the N-terminal LTA-binding aggregation domain. However, perhaps both the N-terminal and central aggregation domains are needed to interact with fibrin or other ECM protein, and this is why there is higher colonization for the pCF175-carrying strain. The vegetation bacterial loads for both Tn*917* insertion mutants are still lower than Asc10$^+$ OG1SSp (pCF10), which might be due to the absence of the RGD motifs in both Tn*917* secreted N-terminal Asc10 fragments. Without the RGD motifs, the N-terminal Asc10 fragments are not able to mediate CR3 opsonin-independent binding to phagocytes, and thus these Tn*917* insertion mutants are killed more easily by these immune cells.

The N-terminal Asc10 fragments that are secreted by the Tn*917* insertion mutants may bear some resemblance to the 78-kDa N-terminal Asc10 cleavage product (26), especially the Asc10 fragment expressed from the pCF175. The 78-kDa cleavage

product includes the N-terminus of the protein to amino acid 550 (69); nucleotide 1650), while the pCF175 Asc10 fragment encompasses just slightly more of the Asc10 protein, extending to amino acid 594 (nucleotide 1784). Thus, the results observed from our studies could be transferred to the function of the 78-kDa cleavage fragment, which might also be able to mediate long-range functions of the N-terminal portion of Asc10 on host cells. However, further study is necessary to determine the function of the 78-kDa Asc10 cleavage fragment during endocarditis disease.

CONCLUSION

Enterococcus faecalis aggregation substance (Asc10) is one of several characterized virulence factors that this bacterium possesses to establish its presence in the endocarditic vegetation. Due to the natural antibiotic resistance and increasing prevalence of vancomycin-resistant enterococci, it is imperative that we develop new treatments to combat this hardy and persistent pathogen. Our current studies show that Asc10 is a worthy target in reducing the severity of *E. faecalis* endocarditis, because of its ability to mediate interactions valve tissue and promote persistence of *E. faecalis* through downplay of the host immune response, all of which allow this bacterium to survive amidst high shear forces in blood flow that surround the valve.

Characterization of Asc10 functional domains in the endocarditis disease process was a central focus of this work to better understand the mechanisms by which this surface protein mediates *E. faecalis*-host interactions. We utilized two models in characterizing these domains: the *in vivo* rabbit endocarditis and *ex vivo* porcine cardiac valve bacterial adherence models. In summary, both the aggregation domains and RGD motifs play a consequential role in a rabbit endocarditis model, where point mutations in the RGD motifs had a more prominent impact on Asc10-mediated *E. faecalis* virulence than large deletions and insertions in the aggregation domains. Through our work, the mechanism by which the RGD motifs increase $Asc10^{+}$ *E. faecalis* endocarditis virulence is not clear. However, Vanek and Rakita *et al.* (50, 65) suggest that the RGD motifs contribute to immune evasion. They demonstrated that these motifs potentially allow *E. faecalis* to enter phagocytes via an opsonin-independent pathway, avoiding the respiratory burst response. Further studies into this RGD motif-

mediated immune evasion mechanism are needed. Through the *ex vivo* porcine cardiac valve model we demonstrated the importance of the aggregation domains in attachment of *E. faecalis* to valve tissue. The C-terminal domain, in contrast, plays a minor role in endocarditis pathogenesis, though it may serve a structural role in supporting the N-terminal portion of Asc10 that is more surface-exposed. Further studies investigating the structure of Asc10 will be needed to confirm this.

In the course of our work we have also developed an *ex vivo* porcine cardiac valve system as a model to explore the process of biofilm formation. Accumulation of exopolymeric matrix and growing aggregates of bacterial microcolonies were observed, providing evidence confirming the development of *E. faecalis* biofilms on the valve tissue. This model will serve as a valuable tool for studying the dynamics of a biofilm on explanted tissue.

Finally, our Fab fragment immunization studies demonstrate the importance of preventing increased aggregation between bacteria expressing multiple adhesins. This approach could be applied to other pathogens such as *S. aureus*, to prevent interaction between their adhesins and host tissues, in addition to impeding formation of large aggregates of bacteria that could cause pneumonia and become trapped in other small spaces. Ideally, a group of adhesins and virulence factors will need to be targeted in immunization strategies to be effective, since bacteria like *E. faecalis* ensure their persistence in the host by modulating expression of multiple surface factors. Continued research into virulence factors like aggregation substance will enable us to develop more efficient treatments against *Enterococcus faecalis* and other bacterial pathogens.

1. **Bensing, B. A., and G. M. Dunny.** 1993. Cloning and molecular analysis of genes affecting expression of binding substance, the recipient-encoded receptor(s) mediating mating aggregate formation in *Enterococcus faecalis*. J. Bacteriol. **175:**7421-7429.

2. **Bryan, E. M., T. Bae, M. Kleerebezem, and G. M. Dunny.** 2000. Improved vectors for nisin-controlled expression in gram-positive bacteria. Plasmid **44:**183-190.
3. **Chandler, J. R., H. Hirt, and G. M. Dunny.** 2005. A paracrine peptide sex pheromone also acts as an autocrine signal to induce plasmid transfer and virulence factor expression *in vivo*. Proc. Natl. Acad. Sci. USA **102:**15617-15622.
4. **Chow, J. W., L. A. Thal, M. B. Perri, J. A. Vazquez, S. M. Donabedian, D. B. Clewell, and M. J. Zervos.** 1993. Plasmid-associated hemolysin and aggregation substance production contribute to virulence in experimental enterococcal endocarditis. Antimicrob Agents Chemother **37:**2474-2477.
5. **Christie, P. J., and G. M. Dunny.** 1986. Identification of regions of the *Streptococcus faecalis* plasmid pCF-10 that encode antibiotic resistance and pheromone response functions. Plasmid **15:**230-241.
6. **Christie, P. J., S. M. Kao, J. C. Adsit, and G. M. Dunny.** 1988. Cloning and expression of genes encoding pheromone-inducible antigens of *Enterococcus (Streptococcus) faecalis*. J. Bacteriol. **170:**5161-5168.
7. **Chuang, O. N., P. M. Schlievert, C. L. Wells, D. A. Manias, T. J. Tripp, and G. M. Dunny.** 2009. Multiple functional domains of *Enterococcus faecalis* aggregation substance Asc10 contribute to endocarditis virulence. Infect Immun **77:**539-548.
8. **Cleary, P. P.** 2009. Personal communication.
9. **Cremieux, A. C., B. Maziere, J. M. Vallois, M. Ottaviani, A. Azancot, H. Raffoul, A. Bouvet, J. J. Pocidalo, and C. Carbon.** 1989. Evaluation of antibiotic diffusion into cardiac vegetations by quantitative autoradiography. J Infect Dis **159:**938-944.
10. **DeMaster, E., N. Schnitzler, Q. Cheng, and P. Cleary.** 2002. M(+) group a streptococci are phagocytized and killed in whole blood by C5a-activated polymorphonuclear leukocytes. Infect Immun **70:**350-359.
11. **Dombek, P. E., D. Cue, J. Sedgewick, H. Lam, S. Ruschkowski, B. B. Finlay, and P. P. Cleary.** 1999. High-frequency intracellular invasion of epithelial cells by serotype M1 group A streptococci: M1 protein-mediated invasion and cytoskeletal rearrangements. Mol Microbiol **31:**859-870.
12. **Dunny, G., M. Yuhasz, and E. Ehrenfeld.** 1982. Genetic and physiological analysis of conjugation in *Streptococcus faecalis*. J. Bacteriol. **151:**855-859.

13. **Dunny, G. M., B. L. Brown, and D. B. Clewell.** 1978. Induced cell aggregation and mating in *Streptococcus faecalis*: evidence for a bacterial sex pheromone. Proc. Natl. Acad. Sci. USA **75:**3479-3483.
14. **Dunny, G. M., R. A. Craig, R. L. Carron, and D. B. Clewell.** 1979. Plasmid transfer in *Streptococcus faecalis*: production of multiple sex pheromones by recipients. Plasmid **2:**454-465.
15. **Durack, D. T.** 1975. Experimental bacterial endocarditis. IV. Structure and evolution of very early lesions. J. Pathol. **115:**81-89.
16. **Durack, D. T., and P. B. Beeson.** 1972. Experimental bacterial endocarditis. I. Colonization of a sterile vegetation. Br. J. Exp. Pathol. **53:**44-49.
17. **Ed. Gorbach, S. L., J. G. Bartlett, and N. R. Blacklow.** 2004. Infectious Diseases. Chapter 62: Infective Endocarditis., p. 569-581. 3rd ed. Lippincott Williams and Wilkins, Philadelphia.
18. **Esko, J. D., A. Elgavish, T. Prasthofer, W. H. Taylor, and J. L. Weinke.** 1986. Sulfate transport-deficient mutants of Chinese hamster ovary cells. Sulfation of glycosaminoglycans dependent on cysteine. J Biol Chem **261:**15725-15733.
19. **Esko, J. D., T. E. Stewart, and W. H. Taylor.** 1985. Animal cell mutants defective in glycosaminoglycan biosynthesis. Proc Natl Acad Sci U S A **82:**3197-3201.
20. **Galli, D., A. Friesenegger, and R. Wirth.** 1992. Transcriptional control of sex-pheromone-inducible genes on plasmid pAD1 of *Enterococcus faecalis* and sequence analysis of a third structural gene for (pPD1-encoded) aggregation substance. Mol Microbiol **6:**1297-1308.
21. **Galli, D., F. Lottspeich, and R. Wirth.** 1990. Sequence analysis of *Enterococcus faecalis* aggregation substance encoded by the sex pheromone plasmid pAD1. Mol Microbiol **4:**895-904.
22. **Hayden, M. K.** 2000. Insights into the epidemiology and control of infection with vancomycin-resistant enterococci. Clin Infect Dis **31:**1058-1065.
23. **Hess, D. J., M. J. Henry-Stanley, S. L. Erlandsen, and C. L. Wells.** 2006. Heparan sulfate proteoglycans mediate *Staphylococcus aureus* interactions with intestinal epithelium. Med. Microbiol. Immunol. **195:**133-141.
24. **Hirt, H., S. L. Erlandsen, and G. M. Dunny.** 2000. Heterologous inducible expression of *Enterococcus faecalis* pCF10 aggregation substance asc10 in *Lactococcus lactis* and *Streptococcus gordonii* contributes to cell hydrophobicity and adhesion to fibrin. J. Bacteriol. **182:**2299-2306.
25. **Hirt, H., P. M. Schlievert, and G. M. Dunny.** 2002. *In vivo* induction of virulence and antibiotic resistance transfer in *Enterococcus faecalis* mediated by the sex pheromone-sensing system of pCF10. Infect. Immun. **70:**716-723.
26. **Hirt, H., G. Wanner, D. Galli, and R. Wirth.** 1993. Biochemical, immunological and ultrastructural characterization of aggregation substances encoded by *Enterococcus faecalis* sex-pheromone plasmids. Eur. J. Biochem. **211:**711-716.

27. **Horstmann, R. D., H. J. Sievertsen, J. Knobloch, and V. A. Fischetti.** 1988. Antiphagocytic activity of streptococcal M protein: selective binding of complement control protein factor H. Proc Natl Acad Sci U S A **85:**1657-1661.
28. **Isenmann, R., M. Schwarz, E. Rozdzinski, R. Marre, and H. G. Beger.** 2000. Aggregation substance promotes colonic mucosal invasion of *Enterococcus faecalis* in an *ex vivo* model. J. Surg. Res. **89:**132-138.
29. **Kao, S. M., S. B. Olmsted, A. S. Viksnins, J. C. Gallo, and G. M. Dunny.** 1991. Molecular and genetic analysis of a region of plasmid pCF10 containing positive control genes and structural genes encoding surface proteins involved in pheromone-inducible conjugation in *Enterococcus faecalis*. J. Bacteriol. **173:**7650-7664.
30. **Kreft, B., R. Marre, U. Schramm, and R. Wirth.** 1992. Aggregation substance of *Enterococcus faecalis* mediates adhesion to cultured renal tubular cells. Infect. Immun. **60:**25-30.
31. **Kristich, C. J., J. R. Chandler, and G. M. Dunny.** 2007. Development of a host-genotype-independent counterselectable marker and a high-frequency conjugative delivery system and their use in genetic analysis of *Enterococcus faecalis*. Plasmid **57:**131-144.
32. **Kristich, C. J., D. A. Manias, and G. M. Dunny.** 2005. Development of a method for markerless genetic exchange in *Enterococcus faecalis* and its use in construction of a *srtA* mutant. Appl. Environ. Microbiol. **71:**5837-5849.
33. **Lancefield, R. C.** 1962. Current knowledge of type-specific M antigens of group A streptococci. J Immunol **89:**307-313.
34. **Lidholt, K., J. L. Weinke, C. S. Kiser, F. N. Lugemwa, K. J. Bame, S. Cheifetz, J. Massague, U. Lindahl, and J. D. Esko.** 1992. A single mutation affects both N-acetylglucosaminyltransferase and glucuronosyltransferase activities in a Chinese hamster ovary cell mutant defective in heparan sulfate biosynthesis. Proc Natl Acad Sci U S A **89:**2267-2271.
35. **Mazmanian, S. K., H. Ton-That, and O. Schneewind.** 2001. Sortase-catalysed anchoring of surface proteins to the cell wall of *Staphylococcus aureus*. Mol. Microbiol. **40:**1049-1057.
36. **McCormick, J. K., H. Hirt, G. M. Dunny, and P. M. Schlievert.** 2000. Pathogenic mechanisms of enterococcal endocarditis. Curr. Infect. Dis. Rep. **2:**315-321.
37. **McCormick, J. K., H. Hirt, C. M. Waters, T. J. Tripp, G. M. Dunny, and P. M. Schlievert.** 2001. Antibodies to a surface-exposed, N-terminal domain of aggregation substance are not protective in the rabbit model of *Enterococcus faecalis* infective endocarditis. Infect. Immun. **69:**3305-3314.
38. **McCormick, J. K., T. J. Tripp, G. M. Dunny, and P. M. Schlievert.** 2002. Formation of vegetations during infective endocarditis excludes binding of bacterial-specific host antibodies to *Enterococcus faecalis*. J Infect Dis **185:**994-997.
39. **Megran, D. W.** 1992. Enterococcal endocarditis. Clin. Infect. Dis. **15:**63-71.
40. **Milner, C. M., and A. J. Day.** 2003. TSG-6: a multifunctional protein associated with inflammation. J Cell Sci **116:**1863-1873.

41. **Moellering, R. C., Jr.** 1992. Emergence of Enterococcus as a significant pathogen. Clin. Infect. Dis. **14:**1173-1176.
42. **Moreillon, P., and Y. A. Que.** 2004. Infective endocarditis. Lancet **363:**139-149.
43. **Olmsted, S. B., G. M. Dunny, S. L. Erlandsen, and C. L. Wells.** 1994. A plasmid-encoded surface protein on *Enterococcus faecalis* augments its internalization by cultured intestinal epithelial cells. J. Infect. Dis. **170:**1549-1556.
44. **Olmsted, S. B., S. L. Erlandsen, G. M. Dunny, and C. L. Wells.** 1993. High-resolution visualization by field emission scanning electron microscopy of *Enterococcus faecalis* surface proteins encoded by the pheromone-inducible conjugative plasmid pCF10. J Bacteriol **175:**6229-6237.
45. **Olmsted, S. B., S. M. Kao, L. J. van Putte, J. C. Gallo, and G. M. Dunny.** 1991. Role of the pheromone-inducible surface protein Asc10 in mating aggregate formation and conjugal transfer of the *Enterococcus faecalis* plasmid pCF10. J. Bacteriol. **173:**7665-7672.
46. **Parsek, M. R., and P. K. Singh.** 2003. Bacterial biofilms: an emerging link to disease pathogenesis. Annu Rev Microbiol **57:**677-701.
47. **Patti, J. M., B. L. Allen, M. J. McGavin, and M. Hook.** 1994. MSCRAMM-mediated adherence of microorganisms to host tissues. Annu. Rev. Microbiol. **48:**585-617.
48. **Peacock, S. J., N. P. Day, M. G. Thomas, A. R. Berendt, and T. J. Foster.** 2000. Clinical isolates of *Staphylococcus aureus* exhibit diversity in *fnb* genes and adhesion to human fibronectin. J. Infect. **41:**23-31.
49. **Perkins, S., E. J. Walsh, C. C. Deivanayagam, S. V. Narayana, T. J. Foster, and M. Hook.** 2001. Structural organization of the fibrinogen-binding region of the clumping factor B MSCRAMM of *Staphylococcus aureus*. J. Biol. Chem. **276:**44721-44728.
50. **Rakita, R. M., N. N. Vanek, K. Jacques-Palaz, M. Mee, M. M. Mariscalco, G. M. Dunny, M. Snuggs, W. B. Van Winkle, and S. I. Simon.** 1999. *Enterococcus faecalis* bearing aggregation substance is resistant to killing by human neutrophils despite phagocytosis and neutrophil activation. Infect. Immun. **67:**6067-6075.
51. **Rantz, L. A. a. W. M. M. K.** 1943. Enterococcic infections. An evaluation of the importance of fecal streptococci and related organisms in the causation of human disease. Arch. Intern. Med. **71:**516-528.
52. **Rich, R. L., B. Kreikemeyer, R. T. Owens, S. LaBrenz, S. V. Narayana, G. M. Weinstock, B. E. Murray, and M. Hook.** 1999. Ace is a collagen-binding MSCRAMM from *Enterococcus faecalis*. J. Biol. Chem. **274:**26939-26945.
53. **Rostand, K. S., and J. D. Esko.** 1997. Microbial adherence to and invasion through proteoglycans. Infect. Immun. **65:**1-8.
54. **Rozdzinski, E., R. Marre, M. Susa, R. Wirth, and A. Muscholl-Silberhorn.** 2001. Aggregation substance-mediated adherence of *Enterococcus faecalis* to immobilized extracellular matrix proteins. Microb. Pathog. **30:**211-220.

55. **Ruoslahti, E.** 1996. RGD and other recognition sequences for integrins. Annu Rev Cell Dev Biol **12:**697-715.
56. **Sartingen, S., E. Rozdzinski, A. Muscholl-Silberhorn, and R. Marre.** 2000. Aggregation substance increases adherence and internalization, but not translocation, of *Enterococcus faecalis* through different intestinal epithelial cells *in vitro*. Infect Immun **68:**6044-6047.
57. **Schaberg, D. R., D. H. Culver, and R. P. Gaynes.** 1991. Major trends in the microbial etiology of nosocomial infection. Am. J. Med. **91:**72S-75S.
58. **Schlievert, P. M., P. J. Gahr, A. P. Assimacopoulos, M. M. Dinges, J. A. Stoehr, J. W. Harmala, H. Hirt, and G. M. Dunny.** 1998. Aggregation and binding substances enhance pathogenicity in rabbit models of *Enterococcus faecalis* endocarditis. Infect. Immun. **66:**218-223.
59. **Singh, K. V., X. Qin, G. M. Weinstock, and B. E. Murray.** 1998. Generation and testing of mutants of *Enterococcus faecalis* in a mouse peritonitis model. J. Infect. Dis. **178:**1416-1420.
60. **Styriak, I., A. Laukova, C. Fallgren, and T. Wadstrom.** 1999. Binding of selected extracellular matrix proteins to enterococci and *Streptococcus bovis* of animal origin. Curr. Microbiol. **39:**327-0335.
61. **Sussmuth, S. D., A. Muscholl-Silberhorn, R. Wirth, M. Susa, R. Marre, and E. Rozdzinski.** 2000. Aggregation substance promotes adherence, phagocytosis, and intracellular survival of *Enterococcus faecalis* within human macrophages and suppresses respiratory burst. Infect. Immun. **68:**4900-4906.
62. **Taylor, P. M., S. P. Allen, and M. H. Yacoub.** 2000. Phenotypic and functional characterization of interstitial cells from human heart valves, pericardium and skin. J Heart Valve Dis **9:**150-158.
63. **Taylor, P. M., P. Batten, N. J. Brand, P. S. Thomas, and M. H. Yacoub.** 2003. The cardiac valve interstitial cell. Int J Biochem Cell Biol **35:**113-118.
64. **Trotter, K. M., and G. M. Dunny.** 1990. Mutants of *Enterococcus faecalis* deficient as recipients in mating with donors carrying pheromone-inducible plasmids. Plasmid **24:**57-67.
65. **Vanek, N. N., S. I. Simon, K. Jacques-Palaz, M. M. Mariscalco, G. M. Dunny, and R. M. Rakita.** 1999. *Enterococcus faecalis* aggregation substance promotes opsonin-independent binding to human neutrophils via a complement receptor type 3-mediated mechanism. FEMS Immunol. Med. Microbiol. **26:**49-60.
66. **Veltrop, M. H., H. Beekhuizen, and J. Thompson.** 1999. Bacterial species- and strain-dependent induction of tissue factor in human vascular endothelial cells. Infect Immun **67:**6130-6138.
67. **Vendrell, J. A., S. Ghayad, S. Ben-Larbi, C. Dumontet, N. Mechti, and P. A. Cohen.** 2007. A20/TNFAIP3, a new estrogen-regulated gene that confers tamoxifen resistance in breast cancer cells. Oncogene **26:**4656-4667.
68. **Voyich, J. M., and F. R. DeLeo.** 2002. Host-pathogen interactions: leukocyte phagocytosis and associated sequelae. Methods Cell Sci **24:**79-90.

69. **Waters, C. M., and G. M. Dunny.** 2001. Analysis of functional domains of the *Enterococcus faecalis* pheromone-induced surface protein aggregation substance. J. Bacteriol. **183:**5659-5667.
70. **Waters, C. M., H. Hirt, J. K. McCormick, P. M. Schlievert, C. L. Wells, and G. M. Dunny.** 2004. An amino-terminal domain of *Enterococcus faecalis* aggregation substance is required for aggregation, bacterial internalization by epithelial cells and binding to lipoteichoic acid. Mol. Microbiol. **52:**1159-1171.
71. **Waters, C. M., C. L. Wells, and G. M. Dunny.** 2003. The aggregation domain of aggregation substance, not the RGD motifs, is critical for efficient internalization by HT-29 enterocytes. Infect. Immun. **71:**5682-5689.
72. **Weigel, L. M., D. B. Clewell, S. R. Gill, N. C. Clark, L. K. McDougal, S. E. Flannagan, J. F. Kolonay, J. Shetty, G. E. Killgore, and F. C. Tenover.** 2003. Genetic analysis of a high-level vancomycin-resistant isolate of *Staphylococcus aureus*. Science **302:**1569-1571.
73. **Wells, C. L., E. A. Moore, J. A. Hoag, H. Hirt, G. M. Dunny, and S. L. Erlandsen.** 2000. Inducible expression of *Enterococcus faecalis* aggregation substance surface protein facilitates bacterial internalization by cultured enterocytes. Infect. Immun. **68:**7190-7194.
74. **Wirth, R., F. Y. An, and D. B. Clewell.** 1986. Highly efficient protoplast transformation system for Streptococcus faecalis and a new Escherichia coli-S. faecalis shuttle vector. J Bacteriol **165:**831-836.
75. **Wright, S. D., and S. C. Silverstein.** 1983. Receptors for C3b and C3bi promote phagocytosis but not the release of toxic oxygen from human phagocytes. J. Exp. Med. **158:**2016-2023.
76. **Zhang, L., G. David, and J. D. Esko.** 1995. Repetitive Ser-Gly sequences enhance heparan sulfate assembly in proteoglycans. J Biol Chem **270:**27127-27135.
77. **Zimmerlein, B., H. S. Park, S. Li, A. Podbielski, and P. P. Cleary.** 2005. The M protein is dispensable for maturation of streptococcal cysteine protease SpeB. Infect Immun **73:**859-864.

APPENDIX: Survival of Asc10$^+$ *E. faecalis* in blood and in a rabbit abscess model

Materials and Methods

Whole blood bacterial survival assay

E. faecalis overnight cultures were grown for 12-15 h without aeration, with subsequent 1:10 dilution in fresh medium. Diluted cultures were grown for another 2-3 h, and in the last half hour of incubation, 10 ng/ml pheromone (cCF10) was added to induce Asc10 expression. Diluted cultures were washed twice with fresh TH broth, then brought to an OD_{600} of 1.0. *S. pyogenes* overnight cultures were grown for 12-15 h in 7% CO_2 and then diluted 1:20. Incubation in 7% CO_2 was continued for 2.5-3 h or until the OD_{600} reached 0.3. *S. pyogenes* cultures were washed twice with fresh TH-Y medium and kept at an OD_{600} of 0.3.

As described previously (10, 33), blood was collected from healthy human volunteers using 10-ml Vacutainer blood collection tubes (Becton-Dickinson). One hundred microliters of approximately 10^3 to 10^4 CFU of *E. faecalis* and 10^3 CFU *S. pyogenes* were added to 900 µl human blood for a total volume of 1 ml. Tubes were incubated at 37°C with end-to-end rotation for 3 h; at each half hour timepoint, 90 µl of the blood-bacterial mixture was removed for aliquoting and plating onto agar for quantification. *S. pyogenes* 90-226 wild-type served as a positive control, as this strain is known to resist phagocytosis; *S. pyogenes* 90-226 *emm*$^-$ was the negative control because it is more easily phagocytosed than the *S. pyogenes* 90-226 wild-type strain (27, 33).

RESULTS

Asc10-expressing *E. faecalis* survive in whole human blood

Deletion of *prgB* gene and glycine-to-alanine substitutions in the RGD motifs do not affect survival of Asc10-expressing *E. faecalis* in whole blood. In preliminary studies, we compared survival of Asc10$^+$ *E. faecalis* OG1SSp (pCF10) to the double RGD mutant OG1SSp (pCF10-2) in whole human blood. Blood contains phagocytes, in particular PMNs, complement factors, B and T cells, and peripheral blood mononuclear cells (PBMCs). However, since the B and T cells require a specific receptor to recognize the *E. faecalis* cells, the bulk of the antibacterial response will most likely be by phagocytes, specifically PMNs. PMNs comprise 60-70% of all white blood cells in blood (68). The double RGD mutant was of particular interest because we knew of the possible role of the RGD motifs in mediating interactions with PMNs, and that immune evasion might be a reason for its low virulence in the rabbit endocarditis model (**Fig. 8**).

We found that over a 3 h period, survival abilities of Asc10$^+$ *E. faecalis* OG1SSp (pCF10), *prgB* deletion mutant (OG1SSp [pCF10-8]), and double RGD mutant (OG1SSp [pCF10-2]) were mostly comparable in preliminary studies performed (**Fig. 26**). Two different starting inocula for the *E. faecalis* strains were used in the studies—either 10^3 or 10^4 CFU/ml, and general trends indicated that bacterial loads in blood were similar between the three strains. However, in one study shown in **Fig. 26B**, the double RGD mutant bacterial loads decreased 0.5 logs below the Asc10$^+$ OG1SSp (pCF10) and *prgB* deletion mutant loads at 2.5 and 3 h. In half of the studies performed, the bacterial loads of the *E. faecalis* strains increased slightly over time (as

Figure 26. Survival of Asc10-variant expressing *E. faecalis* in whole human blood. Whole human blood was inoculated with *E. faecalis* and *S. pyogenes* bacteria, and bacterial survival was assessed over a 3-h period. Two representative experiments are shown; trends were similar between several experiments. **(A)** Starting inoculum for this panel was at approximately 10^3 CFU/ml for the *E. faecalis* strains. Dashed line denotes the minimum detection level of this assay, at 1.7. **(B)** Starting inoculum at approximately 10^4 CFU/ml for *E. faecalis* strains.

Figure 26.

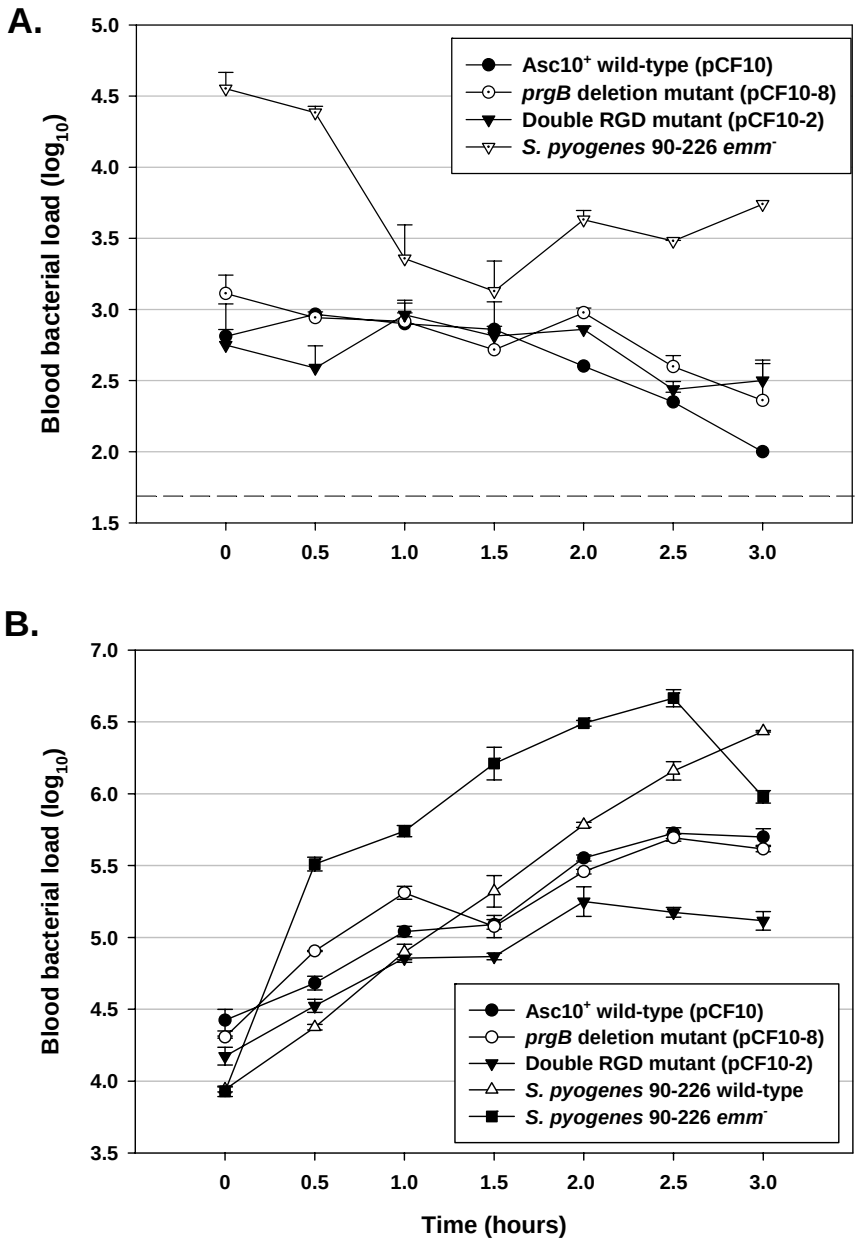
A.
Blood bacterial load (log10)
5.0
4.5
4.0
3.5
3.0
2.5
2.0
1.5
0
0.5
1.0
1.5
2.0
2.5
3.0
Asc10+ wild-type (pCF10)
prgB deletion mutant (pCF10-8)
Double RGD mutant (pCF10-2)
S. pyogenes 90-226 emm-
B.
Blood bacterial load (log10)
7.0
6.5
6.0
5.5
5.0
4.5
4.0
3.5
0
0.5
1.0
1.5
2.0
2.5
3.0
Time (hours)
Asc10+ wild-type (pCF10)
prgB deletion mutant (pCF10-8)
Double RGD mutant (pCF10-2)
S. pyogenes 90-226 wild-type
S. pyogenes 90-226 emm-

represented by **Fig. 26B**), whereas in the remainder the loads were decreasing over time (**Fig. 26A**). From these results, it appears that Asc10 does not affect the ability of *E. faecalis* to resist killing by phagocytes, complement, and other immune mediators in whole blood. However, further studies with the use of an antiserum against whole *E. faecalis* cells will need to be done to ensure that the *E. faecalis* cells are opsonized for more efficient phagocytosis by phagocytes. It is possible that antibodies against Asc10 were present in the human volunteers' blood, and that these were preventing Asc10 from mediating interaction between the *E. faecalis* cells and PMNs.

DISCUSSION

Persistence of Asc10$^+$ *E. faecalis* in whole human blood

Since previous studies (50, 65) have established that Asc10 has a role in immune evasion, we were interested to test the double RGD mutant (OG1SSp [pCF10-2]) against phagocytic attack. We hypothesized that the double RGD mutant and the *prgB* deletion mutant would be more susceptible to phagocytosis and killing in whole blood due to the absence of the RGD motifs. However, in our preliminary studies, the double RGD mutant was killed at approximately the same rate as the Asc10$^+$ OG1SSp (pCF10) strain in the whole blood bacterial killing assays (**Fig. 25**), with the exception of the 2.5 and 3.0 h timepoints in **Fig. 25B**. In reality, this assay is a competition between the ability of the bacteria to grow in the blood and the rate at which the PMNs and other immune mediators in the blood can kill the bacteria (8). To address this issue, studies with the use of purified PMNs should be conducted; this assay is done only in the presence of Hanks' balanced salt solution, a poor growth medium. The presence of anti-Asc10 antibodies might have also interfered with the whole blood bacterial killing assay, since we observed that all of the strains dropped at about the same rate. This could be due to the anti-Asc10 antibodies, which would be able to opsonize the Asc10$^+$ OG1SSp (pCF10) and double RGD mutant strains, but not the *prgB* deletion mutant. Thus, the Asc10$^+$ OG1SSp (pCF10) and double RGD mutant bacteria would be killed more readily, and the levels of the *prgB* deletion mutant would be artificially high without efficient opsonization.

Further studies should be conducted using fluorescence microscopy to determine whether differences are observed between numbers of Asc10^{+} OG1SSp (pCF10), *prgB* deletion mutant, and double RGD mutant *E. faecalis* cells that are contained inside phagosomes. It is possible that we would observe similar trends as Rakita and Vanek *et al.* (50, 65), where more Asc10^{+} OG1SSp (pINY1801) bacteria were found associated with PMNs, and greater numbers of cells were seen inside phagosomes than for Asc10^{-} OG1SSp (pWM401) bacteria.